



**WATER RESOURCE EVALUATION AND MODELLING OF MOTLOUTSE
ALLUVIAL WATER COURSE - A case study of Tobane River reach**

By

EDWIN O. KEAITSE

A Thesis Submitted in Partial Fulfillment of the Requirements for the Degree of Master of
Science in Hydrogeology

Department of Geology

Faculty of Science

University of Botswana

April 2016

Supervisor: Professor B.F Alemaw

Co- Supervisor: Dr K Laletsang and Prof. Tafesse

DECLARATION

I declare that this work has been done at my prior knowledge and in my own capacity in the Department of Geology at the University of Botswana and it has not been previously submitted to any institution.

Name:

Signed: Date:

DEDICATION

To my mother, brothers and sister for all the moral support.

ABSTRACT

Surface water is generally not available for irrigation as rain fed agriculture is hindered by the harsh climatic conditions in Botswana. In order to suite their agricultural needs communities in the Motloutse River catchment depend on Motloutse River. However, the river is ephemeral resulting in lack of surface water therefore groundwater potential of the Motloutse alluvial aquifer had to be studied to support irrigation development and improve the livelihoods of the communal farmers in these areas. The government of Botswana has also decided to undertake irrigation along the Motloutse using groundwater resources from the sand river beds and also to incorporate groundwater resources in the NSWCP to augment surface water resources.

Alluvial aquifers are unconfined, groundwater systems hosted in sand river channels or flood plain presenting a potentially large resource for agriculture as they can store and supply water throughout the dry season. The study area lies in eastern Botswana along the Motloutse River, downstream of the Letsibogo dam in the Motloutse catchment, a sub catchment of the Limpopo basin near Tobane and Bobonong villages.

Groundwater evaluation of Motloutse was carried out through integration of geological, hydrogeological and groundwater modelling tools. Geophysical profiling was carried out to obtain information on the thickness and lithology of river alluvium using GPR to help in aquifer volume estimation. An average depth of 6 metres for the gravelly sand was resolved successfully and laboratory analysis of aquifer material was done to estimate aquifer parameters.

The hydrochemistry of the Motloutse alluvial aquifer was assessed and the water deemed suitable for irrigation with a potential pollution from the BCL Mine. It was also found that 3 water types exist in the Motloutse alluvial aquifer dominated by Ca-Na-SO₄-Cl water class

that have to be monitored on regular basis due to contamination from the mine. Consequently, a simple steady state groundwater model was developed to simulate and plot groundwater flow to improve the understanding of ground-water flow in the Motloutse sand river aquifer. Model yielded calibrated K values of 145 and 11m/day for the riverbed and riverbank respectively, calibrated recharge and evaporation of 172mm/yr and 120mm respectively. A sustainable groundwater yield of 120m³/day with the potential to irrigate an area of 2.4 hectares was determined. The model is associated with a number of uncertainties resulting from the simplification and assumptions made regarding complex field conditions and data quality. Thus limitations of the model should be taken into consideration prior to applying the model for groundwater resource management.

ACKNOWLEDGEMENTS

I wish to express my sincere gratitude and acknowledge the following:

- ❖ All Glory and honour goes to the Almighty King, my living God for having seen me through and keeping me safe.
- ❖ My supervisors; Professor B.F Alemaw, Dr K. Laletsang and Prof. N. Tafesse have been of great motivation throughout my studies.
- ❖ My family especially my mother for all the countless sacrifices she made for me to be the man I am today.
- ❖ My fellow colleagues Edmore and Kgotlafela, you are also acknowledged for your motivation and pieces of academic advice in the hard times that I have gone through.
- ❖ The University of Botswana for financial assistance through Office of Research and Development (ORD), and The Department of Geology staff for their contribution.

TABLE OF CONTENTS

ABSTRACT.....	I
ACKNOWLEDGEMENTS	III
1.0 INTRODUCTION.....	1
1.1 BACKGROUND OF STUDY	1
1.2 STATEMENT OF THE PROBLEM	2
1.3 JUSTIFICATION OF STUDY	2
1.4 OBJECTIVES OF THE STUDY	4
1.5 RESEARCH QUESTIONS.....	4
1.7 SIGNIFICANCE OF STUDY AND ORGANIZATION OF THE THESIS.....	5
2.0 DESCRIPTION OF STUDY AREA	6
2.1 GEOGRAPHICAL LOCATION AND CATCHMENT DIVISION	6
2.2 TOPOGRAPHY AND CLIMATE	8
2.3 LANDUSE, VEGETATION AND SOILS	11
2.4 GEOLOGY OF THE AREA.....	13
2.4.1 Precambrian Basement Complex	13
2.4.2 Karoo Supergroup	17
2.4.3 Structural Geology.....	18
2.4.4 Hydrogeology.....	18
2.5 SOCIO-ECONOMIC CONDITIONS	21
2.6 WATER USES AND DEMAND	22
3.0 LITERATURE REVIEW	24
3.1 PREVIOUS WORK.....	24
3.2 DESCRIPTION OF ALLUVIAL AQUIFERS.....	28
3.3 GEOMETRY AND PHYSICAL PROPERTIES OF ALLUVIAL AQUIFERS ...	29
3.4 HYDRAULIC CONDUCTIVITY	32
3.5 COMPARISON OF DEPTH ESTIMATION METHODS	34
3.5.1 Overview of Ground Penetrating Radar	36
3.6 WATER BALANCE OF AN ALLUVIAL AQUIFER SYSTEM	38
3.7 GROUNDWATER RESOURCE EVALUATION	39
4.0 METHODOLOGY	41

4.1 GEOPHYSICS INVESTIGATION	41
4.1.1 Site Selection.....	41
4.1.4 GPR Method Fieldwork	41
4.1.5 Data Processing	43
4.1.6 Interpretation	45
4.1.7 Ground truthing excursion	45
4.2 AQUIFER MATERIAL PROPERTIES ANALYSIS.....	48
4.2.1 General.....	48
4.2.2 Sample Collection.....	48
4.2.3 Porosity	49
4.2.4 Specific Yield	52
4.2.5 Hydraulic Conductivity	54
4.3 HYDROCHEMISTRY.....	63
4.3.1 General.....	63
4.3.2 Water Sampling and Analysis	65
4.3.3 Unstable Chemical and Physical Parameters.....	66
4.3.4 Water type Classification	68
4.3.5 Metal Concentrations	70
4.3.6 Water Quality.....	70
4.4 GROUNDWATER MODELLING	74
4.4.1 General.....	74
4.4.2 Previous Modelling	75
5.0 RESULTS AND DISCUSSION	77
5.1 GEOPHYSICS RESULTS	77
5.1.1 Interpretation	77
5.2 AQUIFER MATERIAL PROPERTIES ANALYSIS.....	87
5.2.1 Porosity	87
5.2.2 Specific Yield	88
5.2.3 Hydraulic Conductivity	89
5.3 HYDROCHEMISTRY RESULTS.....	94
5.3.1 Unstable Chemical and Physical Parameters.....	94
5.3.2 Water type Classification	94
5.3.4 Water Quality.....	100
5.4 GROUNDWATER MODELLING RESULTS	104
5.4.1 Model Development	104
5.4.2 Calibration.....	114
5.4.3 Water balance.....	119
5.4.4 Sensitivity Analysis	120
5.4.5 Scenario Simulations	123
5.4.6 Model Limitations.....	126
5.5 RESOURCE QUANTIFICATION	127
6.0 CONCLUSIONS AND RECOMMEDATIONS	129

6.1 CONCLUSIONS	129
6.2 RECOMMENDATIONS	130
7.0 REFERENCES	132
APPENDICES	147

LIST OF TABLES

TABLE 1: STRATIGRAPHY OF THE STUDY AREA	13
TABLE 2: HYDRODYNAMIC PROPERTIES OF AQUIFERS OF BOTSWANA MAJOR AND INTERMEDIATE RIVERS. (MODIFIED FROM BWNMPR, 2006)	19
TABLE 3: PERCENTAGES OF POPULATION IN LIMPOPO BY COUNTRY (OWEN, 2012).	22
TABLE 4: SAND RIVER CLASSIFICATION OF BOTSWANA RIVERS AFTER NORD (1985).....	25
TABLE 5: COMPARISON OF GEOPHYSICAL METHODS IN SAND RIVER STUDY.	35
TABLE 6: GPR REFLECTION DATA COLLECTION PARAMETERS.....	44
TABLE 7: CLASSIFICATION OF WATER BASED ON TDS (FREEZE AND CHERRY, 1979).....	68
TABLE 8: HARDNESS CLASSIFICATION OF WATER (AFTER SAWYER AND McCARTY, 1967)	69
TABLE 9: WATER QUALITY CLASSIFICATION FOR IRRIGATION.	73
TABLE 10: METHOD 1 OF DETERMINING POROSITY	87
TABLE 11: METHOD 2 OF DETERMINING POROSITY.....	87
TABLE 12: CALCULATION OF SPECIFIC YIELD.....	88
TABLE 13: USCS CLASSIFICATION OF AQUIFER MATERIAL SAMPLES.	91
TABLE 14: HYDRAULIC CONDUCTIVITY DETERMINED BY DIFFERENT EMPIRICAL FORMULAE....	91
TABLE 15: HYDRAULIC CONDUCTIVITY FROM CONSTANT HEAD PERMEABILITY TEST.	92
TABLE 16: HYDRAULIC CONDUCTIVITY FROM SLUG TEST.	93
TABLE 17: pH VALUES OF THE MOTLOUTSE WATER SAMPLES.....	94
TABLE 18: TDS AND EC VALUES OF MOTLOUTSE WATER SAMPLES AND CLASSIFICATION.	95
TABLE 19: WATER TYPE CLASSIFICATIONS OF MOTLOUTSE BASED ON HARDNESS.....	96
TABLE 20: WATER TYPE OF MOTLOUTSE SAMPLES.....	98
TABLE 21: WATER QUALITY OF MOTLOUTSE AQUIFER COMPARED TO DIFFERENT WATER QUALITY STANDARDS.....	101
TABLE 22: MOTLOUTSE ALLUVIAL WATER QUALITY SUITABILITY FOR IRRIGATION.	102
TABLE 23: MONTHLY OPEN WATER EVAPORATION ESTIMATES (MACDONALD, 1990) *ALL FIGURES IN MM.	112
TABLE 24: ERRORS OF THE CALIBRATED MODEL.....	117
TABLE 25: WET SEASON WATER BUDGET.....	120
TABLE 26: DRY SEASON WATER BUDGET.	124
TABLE 27: SUMMARY OF WELL OPTIMISATION PARAMETERS.....	126

LIST OF FIGURES

FIGURE 1: LOCATION MAP OF STUDY AREA WITHIN SOUTHERN AFRICA AND LIMPOPO BASIN. ...	7
FIGURE 2: MEAN MONTHLY RAINFALL FOR MOTLOUTSE CATCHMENT MAJOR TOWN AND VILLAGES WITH SUPERIMPOSED PLOT OF POTENTIAL EVAPOTRANSPIRATION.....	9
FIGURE 3: BOBONONG ANNUAL RAINFALL VS AVERAGE ANNUAL RAINFALL.	10
FIGURE 4: MOTLOUTSE CATCHMENT TEMPERATURES AND OPEN WATER EVAPORATION.....	10
FIGURE 5: IRRIGATION BLOCKS RECOGNISED BY McDONALD (1990).....	12
FIGURE 6: BANDED GNEISS NEAR MMADINARE.....	14
FIGURE 7: GEOLOGICAL MAP OF STUDY AREA (MODIFIED FROM WSB, 2007).	16
FIGURE 8: HYDROGRAPH SHOWING WATER AND SAND LEVELS FOR 1979-1982 PERIOD (BNWMP, 1991).....	20
FIGURE 9: HYDROGRAPH SHOWING SAND AND WATER LEVELS FOR JUNE 1990 TO JUNE 1995 PERIOD (ANDERSON,1997).....	21
FIGURE 10: RIVER CHANNEL CUTS THROUGH A HARD ROCK DOWNSTREAM OF GEOLOGICAL BOUNDARY AND DUE TO THE RESISTANT LITHOLOGY DOWNSTREAM COUPLED WITH THE SOFT ROCK ERODIBILITY, MEANDERS FORM UPSTREAM OF CONTACT.	30
FIGURE 11: METHODS FOR DETERMINING HYDRAULIC CONDUCTIVITY (MODIFIED FROM OOSTERBAAN AND NIJLAND, 1994)	33
FIGURE 12: RAW RADARGRAM SHOWING TIME IN NANOSECONDS, DEPTH IN METRES ON VERTICAL SCALES AND DISTANCE IN METRES ON HORIZONTAL SCALE AFTER BURVAL WORKING GROUP,(2006)	36
FIGURE 13: LOCATION OF GPR PROFILES AND SIMPLIFIED PLAN VIEW OF THE GPR SURVEY...	42
FIGURE 14: DISPLAY MONITOR, STORAGE AND CONTROL UNITS AND THE ANTENNAE USED FOR THE SURVEY	43
FIGURE 15: MEASURING DEPTH TO WATER LEVEL	46
FIGURE 16: A 1M HOLE DUG IN THE RIVERBED BEFORE AUGER INSTALLATION	47
FIGURE 17: LOCATION OF AQUIFER MATERIAL SAMPLING SITE IN RELATION TO GPR PROFILES	49
FIGURE 18: EQUIPMENT USED FOR GRADATION	58
FIGURE 19: CONSTANT HEAD PARAMETER TEST EQUIPMENT	60
FIGURE 20: LOCATIONS OF WATER SAMPLING POINTS.....	64
FIGURE 21: REFLEX 2D SOFTWARE PROCESSED RADARGRAM FOR FIRST PROFILE.	77
FIGURE 22: REFLEX 2D SOFTWARE PROCESSED RADARGRAM FOR SECOND PROFILE.	78
FIGURE 23: REFLEX 2D PROCESSED RADARGRAM FOR THIRD PROFILE.	78
FIGURE 24: REFLEX 2D PROCESSED RADARGRAM FOR FOURTH PROFILE.	79
FIGURE 25: REFLEX 2D PROCESSED RADARGRAM FOR THE FIFTH PROFILE	80
FIGURE 26: SUNT PROCESSED AND INTERPRETED RADARGRAM IN WIGGLE FORM SHOWING THE AQUIFER STRATIGRAPHY.	81
FIGURE 27: A SINGLE TRACE WAVELET ALONGSIDE A RADARGRAM SHOWING THE AMPLITUDE OF THE WAVELET IN RESPONSE TO THE HETEROGENEITY OF THE AQUIFER.	82
FIGURE 28: BEDROCK REFLECTOR IN THE FIRST PROFILE LINE.	83
FIGURE 29: RADARGRAM DEPICTING RIVERBANK BOUNDING SURFACES COMMON IN MOST RADAR RECORDS.	84

FIGURE 30: MOTLOUTSE SAND DEPTH TO BEDROCK CONTOUR MAP.....	85
FIGURE 31: SCHEMATIC CROSS SECTION OF MOTLOUTSE ALLUVIAL AQUIFER.	86
FIGURE 32: GRAIN SIZE DISTRIBUTION CURVE OF THE MOTLOUTSE	90
FIGURE 33: TDS AND EC OF MOTLOUTSE SAMPLES.	95
FIGURE 34: HARDNESS VALUES OF MOTLOUTSE WATER SAMPLES.....	97
FIGURE 35: DUROV PLOT OF MOTLOUTSE WATER SAMPLES.....	97
FIGURE 36: CONCENTRATIONS OF CATIONS IN THE WATER SAMPLES.	99
FIGURE 37: CONCENTRATIONS OF ANIONS OF WATER SAMPLES.	99
FIGURE 38: COMPARISON OF METAL CONCENTRATIONS OF MOTLOUTSE SAMPLING POINTS. ..	100
FIGURE 39: MODEL AREA FOR MOTLOUTSE.....	105
FIGURE 40: PICTORIAL REPRESENTATION OF THE HYDROLOGIC SYSTEM OF MOTLOUTSE RIVER BASIN.	106
FIGURE 41: CONCEPTUAL MODEL OF MOTLOUTSE ALLUVIAL AQUIFER CROSS SECTION.....	107
FIGURE 42: CONCEPTUAL MODEL-PLAN VIEW	107
FIGURE 43: MODEL BOUNDARY CONDITIONS	109
FIGURE 44: SPATIAL DISTRIBUTION OF HYDRAULIC CONDUCTIVITY ON MODEL DOMAIN	113
FIGURE 45: COMPARISON OF OBSERVED VS SIMULATED HEADS (AT 9 OBSERVATION WELLS).	116
FIGURE 46: SIMULATED HEAD DISTRIBUTION AND FLOW DIRECTION AND PATHS.....	118
FIGURE 47: LOCATION OF OBSERVATION WELLS.	119
FIGURE 48: SENSITIVITY PLOT OF CALIBRATED MODEL WITH RESPECT TO K ZONE 1.....	121
FIGURE 49: MODEL SENSITIVITY TO K ZONE 2	122
FIGURE 50 : PLOT OF MODEL SENSITIVITY TO RECHARGE.....	122
FIGURE 51: SENSITIVITY PLOT OF EVAPORATION	123
FIGURE 52: SSD SCENARIO CONTOURS	125

LIST OF ACRONYMS

ASTM	American Society for Testing and Materials
BCL	Bamangwato Concession Limited
BNWMPR	Botswana National Water Master Plan Review (2006)
BOBS	Botswana Bureau of Standards
CHB	Constant Head Boundary
DGS	Department of Geological Surveys
DWA	Department of Water Affairs
EC	Electrical Conductivity
EM	Electro-Magnetic method
ET	Evapotranspiration
FAO	Food and Agriculture Foundation
GHB	General Head Boundary
GPR	Ground Penetrating Radar
GPS	Global Positioning System
ITCZ	Inter Tropical Convergence Zone
K	Hydraulic conductivity
LIMCOM	Limpopo water course Commission
m/d	metres per day
m ³ /d	cubic metres per day
MAE	Mean Absolute Error
mamsl	metres above mean sea level
MAP	Mean Annual Precipitation
mbgl	metres below ground level
MCM	Million Cubic Metres
ME	Mean Error
mm/yr	millimetres per year
MOA	Ministry of Agriculture
MSZ	Magogaphate Shear Zone

NAMPAAD	National Agricultural Master Plan for Agricultural Development
NSWC	North South Water Carrier
RMSE	Root Mean Square Error
SAR	Sodium Absorption Ratio
SSD	Sand Storage Dam
TDS	Total Dissolved Solids
UNDP	United Nations Development Programme
USCS	Unified Soil Classification System
VES	Vertical Electrical Sounding
WHO	World Health Organisation
WS1	Water sampling point 1
WSB	Water Surveys Botswana

LIST OF APPENDICES

APPENDIX A	147
APPENDIX B	156
APPENDIX C	169
APPENDIX D	170
APPENDIX E	176

Chapter 1

1.0 INTRODUCTION

1.1 BACKGROUND OF STUDY

Botswana is a semi-arid country in Southern Africa with flat topography culminating in low rates of surface runoff and low rates of groundwater recharge (BNWMMPR, 2006). Rural communities of Botswana rely on agriculture as the principle source of income, food and employment. The agricultural practices require water and because of the aforementioned low rates of surface runoff and groundwater recharge, surface water is generally not available for irrigation as rain fed agriculture is hindered by the harsh climatic condition. Ephemeral rivers in eastern part of Botswana constitute the main sources of under-utilised groundwater (BNWMMPR 2006; Herbert et al, 1997). Alluvial aquifers are potentially large resource for agriculture as they can store and supply water throughout the dry season, thus in this dissertation, Motloutse alluvial aquifer is studied.

Motloutse River is one of the major tributaries of the perennial Limpopo River and 90% of the rainfall over Motloutse catchment occurs in the summer months and mean monthly evaporation exceeds mean monthly rainfall for each month. Annual recharge of alluvial aquifers in semi-arid areas mainly occurs indirectly through river bed infiltration and therefore can be exploited on yearly basis (Owen and Darlin, 2005). Recharge of the Motloutse alluvial aquifer is primarily derived from the ephemeral Motloutse River flow.

Extractable alluvial deposits occur along the sand river course. Owen (1994) has shown that alluvial aquifers have a tendency of occurring at geological contacts. Moreover, rock outcrops can be barriers that divide the sand river into blocks therefore the groundwater quantities are a function of the alluvium and aquifer extent dimensions (Wikner, 1980).

Majority of the communal farmers rely on groundwater and do not know how much groundwater resources are available in river beds and as such, knowledge of the bedrock geology and quantification of groundwater yields are critical which this study seeks to attain.

1.2 STATEMENT OF THE PROBLEM

Communities in the Motloutse River catchment depend on Motloutse River for water to suite their agricultural needs. However, the river is ephemeral resulting in lack of surface water (i.e. dry riverbed) during the six dry months (May-October), (Department of Meteorological services, 1984) for irrigation and watering cattle. Then the obvious option is groundwater resource from the alluvial aquifer in the sand river.

However the hydrogeological characteristics of small alluvial aquifers are not known (Love et al, 2007) and effective water management, water storage planning and management are hampered by very little knowledge of storage capacities (Sawunyama, 2005). This is further aggravated by varying thickness of sand, sand river morphology, increasing demand, therefore groundwater potential of the Motloutse alluvial aquifer had to be studied to support irrigation development and improve the livelihoods of the communal farmers in these areas.

1.3 JUSTIFICATION OF STUDY

The government of Botswana has decided to fully invest on agriculture as one of the recommendations from the national water master plan review of 2006 through NAMPAAD to undertake irrigation along the Motloutse using groundwater resources from the sand river beds and also to incorporate groundwater resources in the NSWC project to augment surface water resources. The MOA also conducted soil mapping and highlighted the area around the Motloutse water course very suitable for arable agriculture (BNWMPR, 2006).

Previous studies done in the Motloutse area by Wikner (1980), Nord (1985) and Department of Lands (1998) were all done before Letsibogo dam was opened in 2000 and since the study

area is downstream of the dam it now relies on flash floods and Letsibogo dam releases. This greatly affects the alluvial aquifers on the river stretches and thereby the groundwater yields established by the studies prior to dam construction. We must also take into consideration that river sedimentation rates have changed, runoff and river flow volumes and increased river sand extraction over the past 2 decades as evidenced by Wagner study commissioned by the DGS in 2003 in the assessment of the Ntshhe, Tati and Sekukwe rivers, which are similar sand rivers as Motloutse. This study thus quantifies groundwater resources at a local scale by characterizing a single alluvial aquifer of Motloutse.

BNWMPR maintains that modelling of rivers studied by Wikner (1980) has to be done in order to ascertain their sustainable yield. In view of the above, this dissertation seeks to study Motloutse water course in order to quantify the subsurface yields of alluvial aquifers and undertake groundwater modelling of the identified resources to optimize its usage and determine exploitable volumes for effective management and utilization of the resource.

1.4 OBJECTIVES OF THE STUDY

Main Objective

- ❖ To evaluate the groundwater potential of Motloutse water course.

Specific Objectives

- To determine depth to bedrock formations and determine aquifer material characteristics.
- To assess the effect of the mine on the groundwater chemistry of the Motloutse alluvial aquifer.
- To determine the suitability of groundwater from Motloutse alluvial aquifer for irrigation
- To determine the groundwater yield of the Motloutse alluvial aquifer.
- To undertake groundwater modelling of the aquifer to optimize its usage and determine exploitable volumes.

1.5 RESEARCH QUESTIONS

- How is the geological nature of the aquifer affecting aquifer material characteristics?
- How is the water quality in the alluvial aquifer for drinking and irrigation purposes?
- To what extent is contamination through existing or other potential land use practices in the study area?
- What are the systems and conceptual model elements affecting groundwater yield in the alluvial aquifer?
- What area of land in the vicinity of the groundwater source can potentially be irrigated and how is the soil suitability of the irrigable areas?
- What is the effect of current/proposed abstraction levels on groundwater levels?

- What is the extent of aquifer boundaries? How long can water be stored in the aquifer and how this storage can be increased?

1.7 SIGNIFICANCE OF STUDY AND ORGANIZATION OF THE THESIS

Results of this study are expected to give an insight into the amount of groundwater resources available for arable farming in the Motloutse area thereby improving livelihoods. This research study proceeds in the rest of the presentation as follows:

Second chapter describes the study area while the literature review for this research focuses on existing or theoretical background of alluvial aquifers incorporating a brief account of the geology of the study area in the third chapter. The fourth chapter expands on how the geophysics, laboratory methods analysis, water quality analysis and groundwater modelling of Motloutse alluvial aquifer were carried out. Chapter five presents the results and discussion. The dissertation ends with chapter six that lays out the conclusion and recommendations.

Chapter 2

2.0 DESCRIPTION OF STUDY AREA

2.1 GEOGRAPHICAL LOCATION AND CATCHMENT DIVISION

Botswana is a semi-arid country, located centrally within southern Africa (Figure 1), with limited surface water resources and hence a significant reliance on groundwater. It shares its borders with Zambia, Zimbabwe, South Africa and Namibia and has a total land area of 582 000 km². The study area lies in eastern Botswana near the Mmadinare, Tobane and Bobonong villages (Figure 1). The study site lies along the Motloutse River, downstream of the Letsibogo dam in the Motloutse catchment, a sub catchment of the Limpopo basin. Four countries in south-eastern Africa share the Limpopo basin: Botswana, Mozambique, South Africa and Zimbabwe. This basin is extremely important to eastern Botswana as a source of surface water.

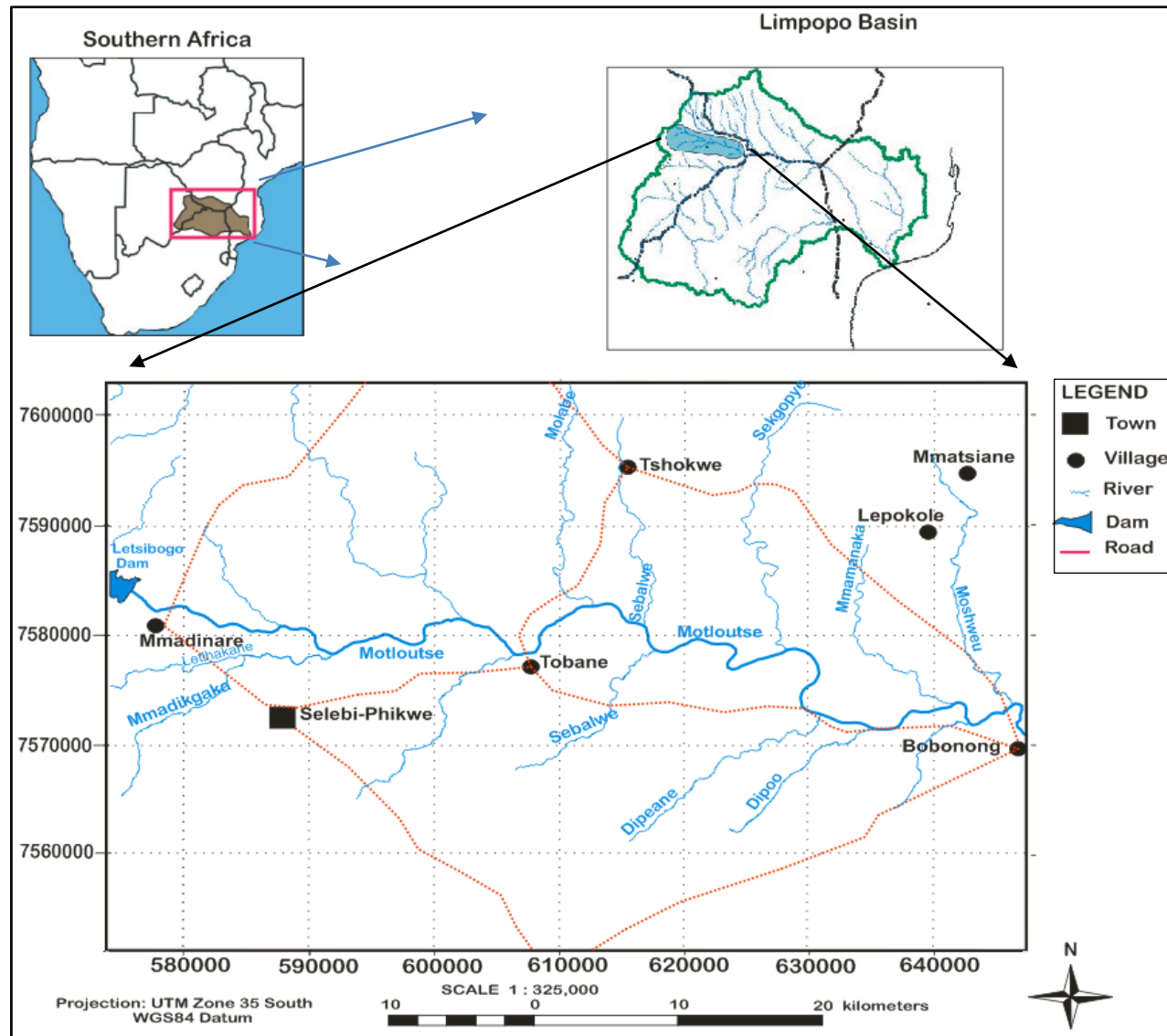


Figure 1: Location map of study area within Southern Africa and Limpopo basin.

2.2 TOPOGRAPHY AND CLIMATE

The majority of the Motloutse catchment as well as the country is characterised by flat savannah and, although devoid of major mountains, few hills are present in the catchment. The Motloutse catchment has topography of approximately 1000 mamsl (Owen, 2012). The Motloutse river basin defines the lowest ridge averaging 770 mamsl.

Botswana lies within the subtropical high pressure zone culminating in calm, established weather and very little rainfall. During summer, low pressure zone develops over the area drawing moist air from Indian and Atlantic oceans. The seasonally occurring rain is due to Inter Tropical Convergence Zone (ITCZ) and tropical cyclones of the south western Indian Ocean. In semi-arid regions such as Botswana these variability in the rainfall is more important than the actual rainfall itself (Pallett, 1997).

The area experiences dry winters and hot summers with an unreliable sparse summer rainfall. Motloutse catchment has a mean annual precipitation of 350mm to 450mm, a mean annual evaporation of 2000 mm with 95% of the highly seasonal rainfall occurring between the months of October and April (Figure 2). The annual number of rain days rarely exceeds 50 and averages 30 rain days per year with only half of these days generating more than 10mm of rainfall (FAO, 2004; MacDonald, 1990). Gibbs (1969) recognised that runoff in the eastern part of the country is exceptionally flashy and is highly probable that the sand rivers can experience years with no flow at all. Monthly PET in the Motloutse typically exceeds monthly precipitation for all the months, resulting in an overall water deficit in the study area as in Figure 2.

During the winter season the disparity between PET and Precipitation is vast and the area experiences severe water shortage during the dry season which is also exacerbated by plants shedding leaves as the season progresses.

Bobonong long-term rainfall dataset representative of the study area is summarized and presented in Figure 3. Bobonong has a MAP of 362mm since 1980. Annual rainfall is mostly below average annual rainfall depicting highly variable annual rainfall intensity with no year-to-year correlation. Figure 4 also displays that year 2000 had high rainfall intensity alongside below average rainfall amounts from 1992 to 2005 save for year 1997. Year 1980, 1992, 1994 and lately year 2004 simulate drought conditions. Figure 4 demonstrates an expected concurrent falling and rising of minimum and maximum temperatures with open water evaporation of the semi-arid study area.

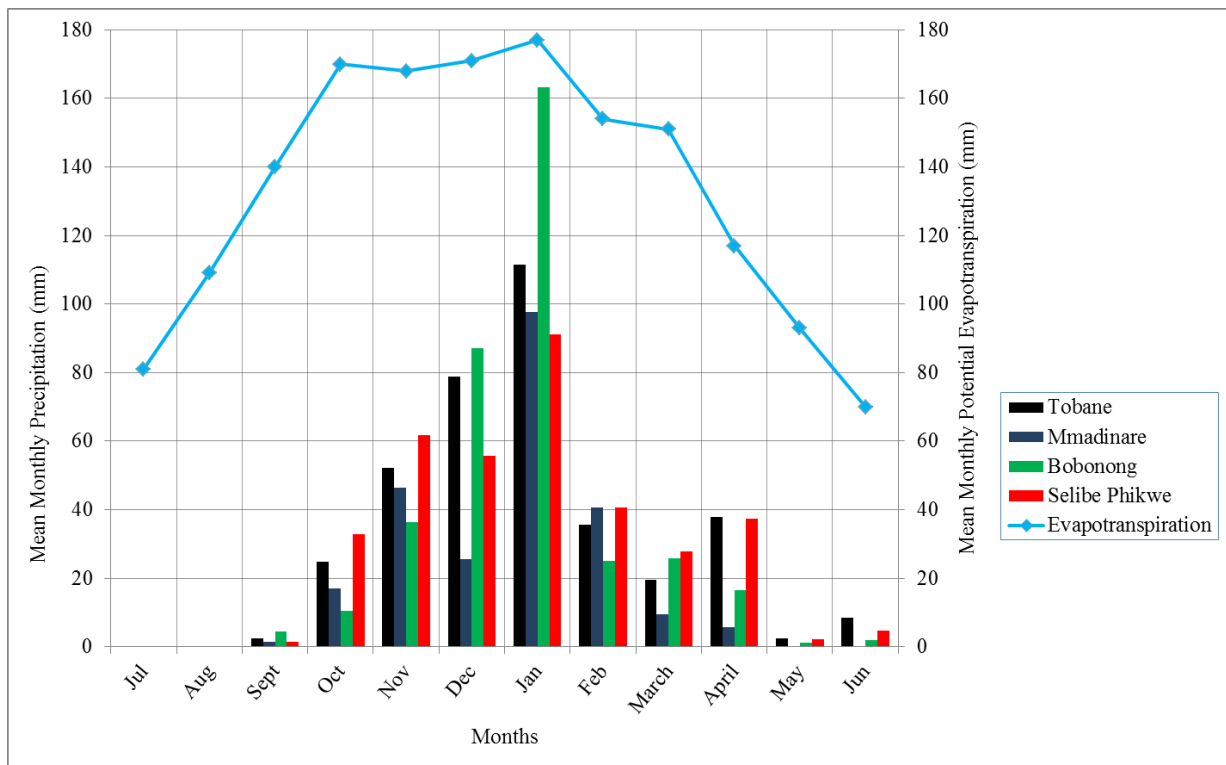


Figure 2: Mean monthly rainfall for Motloutse catchment major town and villages with superimposed plot of Potential evapotranspiration.

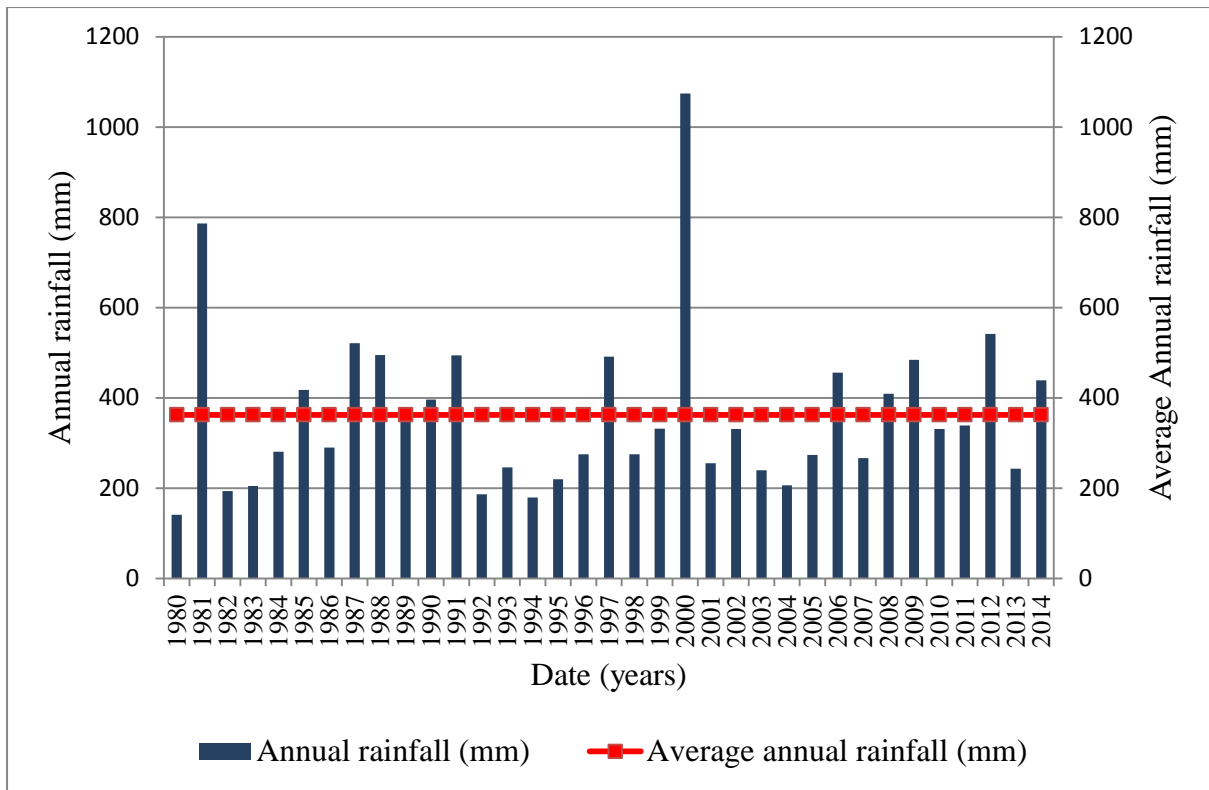


Figure 3: Bobonong Annual rainfall vs Average annual rainfall.

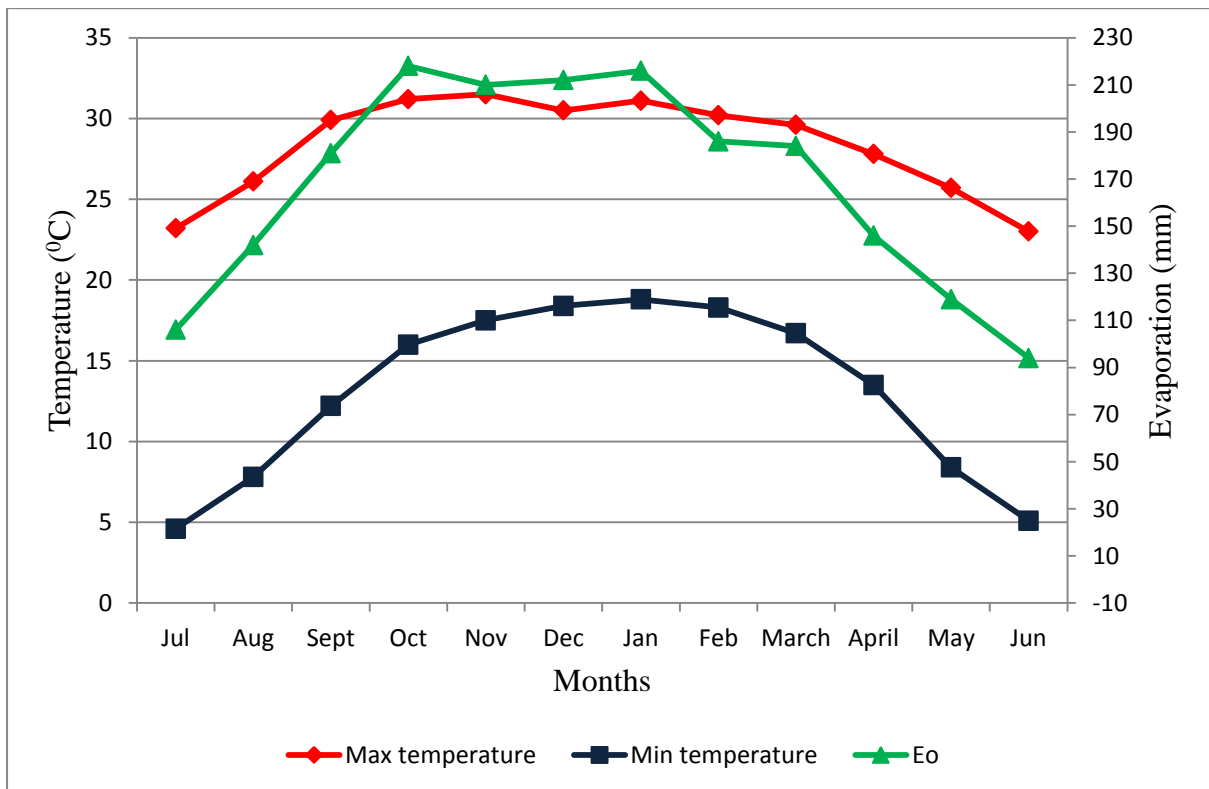


Figure 4: Motloutse catchment temperatures and open water evaporation.

2.3 LANDUSE, VEGETATION AND SOILS

Motloutse catchment area is approximately 20, 000km² and Motloutse river has a length of approximately 250 km and a general east-west trend with its tributaries mainly trending north-south (Figure 1). The main land use is subsistence farming with vast areas of land used as grazing land areas.

Vegetation of the area is mainly mixed mopane woodland, thorny savannah shrubs and occurrence of acacia trees in some places. Sparse vegetation primarily occurs in the area with vast areas cleared for arable agriculture near the villages and rest of the catchment used for cattle rearing. The area is also potent with abundant wildlife and renowned for the African elephant and other mammals.

The catchment area has a lot of freehold land with suitable soil conditions (BNWMPR, 2006). Fourteen blocks of potentially irrigable soils located along the Motloutse river valley between Mmadinare and Bobonong have been identified as in Figure 5 . These areas were assessed and ranked from highly suitable to unsuitable totalling approximately 2000 hectares. The shallow depth to bedrock was singled out as the main limitation of extremely suitable soils in this area and effective land management practises are essential (McDonald, 1990).

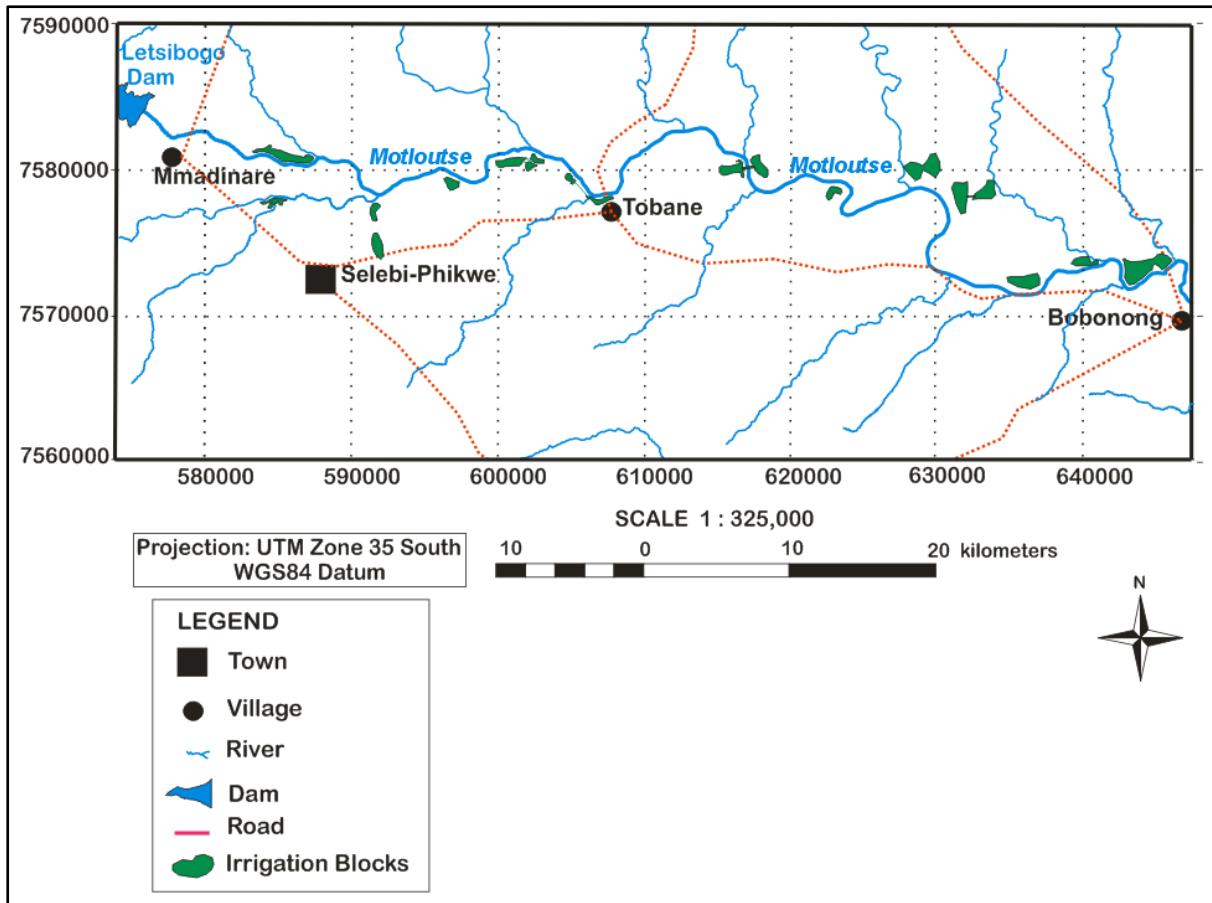


Figure 5: Irrigation blocks recognised by McDonald (1990).

2.4 GEOLOGY OF THE AREA

Area lies on the Limpopo belt between the metamorphosed granite-greenstone-gneiss terranes of Zimbabwe to the north and Kaapvaal cratons to the south. The geology of the area consists essentially of Precambrian basement complex rocks overlain by the bedrock sedimentary and volcanic sequences of the Karoo supergroup. The stratigraphy of the study area is summarized in Table 1.

Table 1: Stratigraphy of the study area

AGE	STRATIGRAPHIC UNIT		
	Supergroup	Group	Formation
Phanerozoic	Karoo	Stormberg Group	Bobonong Lava Formation
		Lebung Group	Tsheung Formation
			Thuni Formation Korebo Formation
Ecca Group	Mofdiahogolo Formation		
Archaean	Limpopo Mobile Belt	Semolale, Phikwe and Mahalapye Complexes	Banded Gneiss and Granitic Gneiss Formations Mahalapye Migmatite

2.4.1 Precambrian Basement Complex

The study area has an Archaean basement of Limpopo mobile belt. Archaean and early Proterozoic crystalline bedrock in the area represents a culmination of rocks produced during the Kaapvaal and Zimbabwe craton collision that form the Limpopo belt. The central zone of the Limpopo belt dominates the area as almost the whole exposure of Limpopo in Botswana is designated to the central zone (Carney et al, 1994). The basement rocks commonly lumped together are granites consisting of; granitoid gneisses, Paragneisses, banded gneisses (Figure 6), anorthositic gneisses, amphibolites and migmatites, all belonging to the Phikwe, Semolale and Mahalapye lithostratigraphic complexes.



Figure 6: Banded Gneiss near Mmadinare

2.4.1.1 Semolale Complex

This complex corresponds to the Northern Marginal Zone of the Limpopo belt and consists of folded greenstone belt fragments and basic intrusions enclosed in granitoid gneisses and megacrystic granites (Carney et al, 1994, Bennett 1971). The granitoid gneisses have multiple zones of mylonitisation and cataclasis (Aldiss 1983b). Fine-grained Archaean amphibolites of different types are most abundant and occur as thin lenses in the study area (Figure 7). Paragneisses in this complex are interlayered with some occurrences of basic to ultrabasic schists (Carney et al, 1994). Granitic gneisses and gneissic granites are also observed in this complex.

2.4.1.2 Phikwe Complex

The Phikwe lithostratigraphic Complex comprises of banded gneisses dominated by supracrustal gneisses situated at the southern part of the study area as in Figure 7. (Key, 1976). Amphibolites form layers within the quartzofeldspathic gneisses and the plagioclase rich gneisses occur known as anorthositic gneiss. Carney et al (1994) describes the granitic gneisses in this complexes ranging from heterogeneous migmatites to augen gneisses and homogeneous granites. Granulites, quartzites, marbles and calc silicate rocks are found in this lithostratigraphic unit occurring on a northeast-southwest trend lumped together as Archaean metaultramafics and metasediment (Figure 7).

2.4.1.3 Mahalapye Complex

An assemblage of migmatites, gneisses and foliated plutonic rocks make up the Mahalapye complex. Carney et al, (1994) divided the complex into Mahalapye migmatite, Mahalapye granite and the Mokgware granite. The Mahalapye complex is included in the Limpopo due to its geographical position and because it typifies intra-cratonic reworking within the Limpopo terrane (Carney et al, 1994). The Mahalapye migmatites which dominates the study area (Figure 7) is a foliated, coarse-grained massive rock of granodioritic composition (Skinner, 1978a). Ermanovics (1980) described the Mokgware granite as a deep seated intrusion with xenoliths of migmatite enclosed by the granite and Mahalapye granite as largely composed of a massive leucocratic quartz monzonite and porphyroblastic dioritic facies.

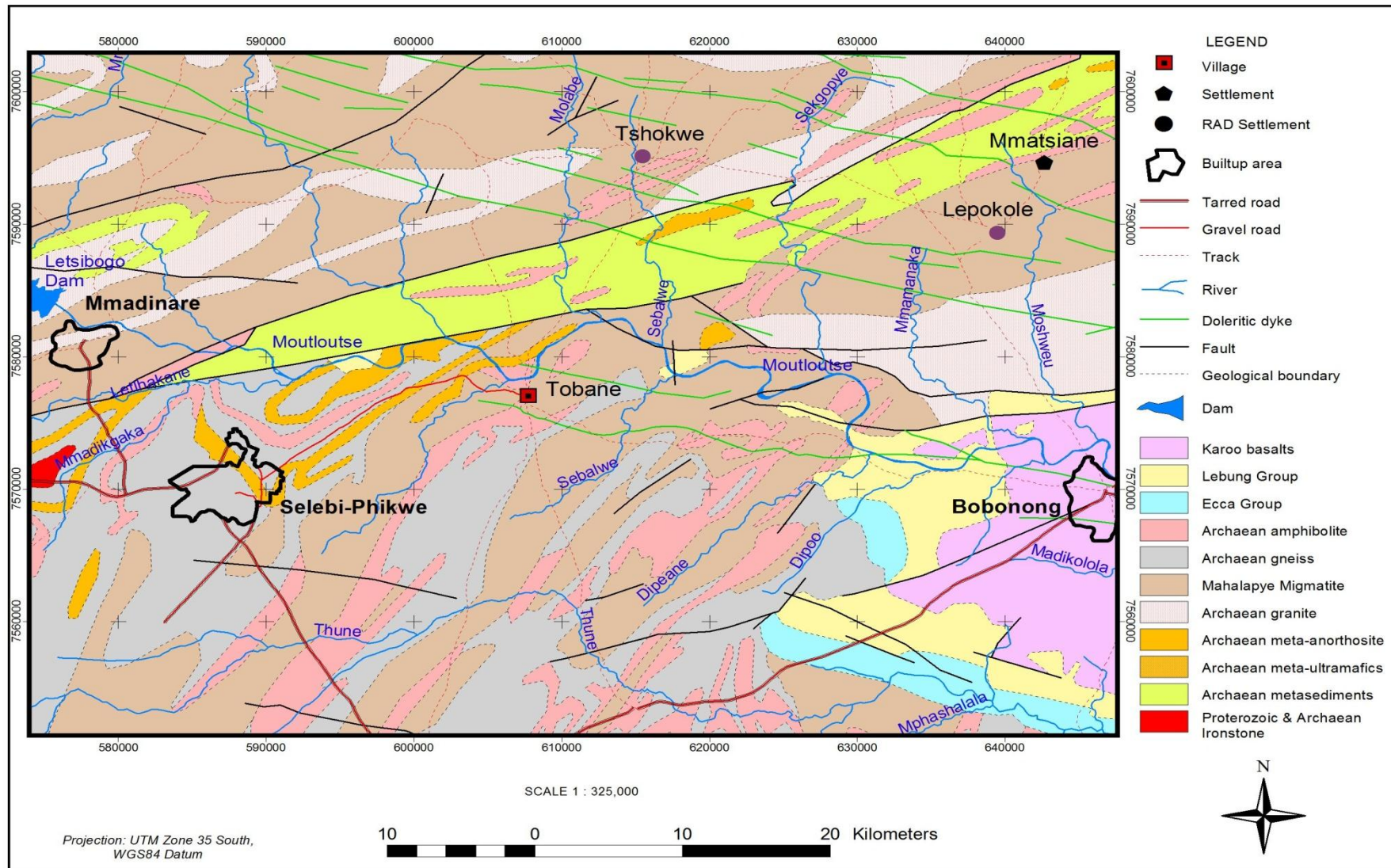


Figure 7: Geological Map of study area (Modified from WSB, 2007).

2.4.2 Karoo Supergroup

The Karoo supergroup rocks cover most parts of Botswana, South Africa and Lesotho and very minute in other southern Africa countries. This assemblage of sedimentary and volcanic rocks is poorly exposed since it is in turn overlain by the Kalahari beds in Botswana. The Karoo succession is made up of a series of mudstones, siltstones, sandstones and grits underlying the aeolian sandstone of Lebung Group, which is overlain by basaltic flood lavas (WSB, 2007).

2.4.2.1 Ecca Group

This Formation represents fluvial and deltaic depositional environments which lie unconformably over basement rocks. It largely consists of coarse to conglomeratic sandstones and is prominent only in the south western part of Bobonong (Paya 1996).

2.4.2.2 Lebung Group

A succession of uniform, red clastic sediments is classified as the Korebo, Thuni and Tsheung Formations. These are equivalent to the Mosolotsane and Ntane sandstone formations of the Lebung Group.

2.4.2.3 Stormberg Lava Group

Lava extension followed the sedimentation forming Bobonong Lava Formation which flowed over the Aeolian sand of Lebung Group. Basaltic lava is well exposed over the Bobonong area as in Figure 7 belonging to the Stormberg Group consisting of dark grey tholeiitic basalt lavas and associated minor intrusions (Paya, 1996).

2.4.3 Structural Geology

The study area has a complex structural geology typical of deformed and metamorphosed Archaean terranes. Cox et al, (1965) divided the Limpopo belt into central zone, Northern and Southern Marginal zones based on structural trends. The study area has a ductile shear zone about 10 km in width which formed during later stages of deformation in the Limpopo known as Magothate Shear Zone (MSZ) (Wakefield, 1977). This shear zone has various zones of mylonite which deform the granitoid gneisses and cuts across the Limpopo in a north-north east-south-south west trend occurring north of Tobane. The MSZ terminates in the north east close to the international boundary, also acts as the northern limit of Semolale complex and Paya, (1996) considered the shear zone to demarcate the boundary between Zimbabwe craton and Limpopo belt.

The Gonbojango Fault zone truncates the Semolale complex against the Karoo supergroup in the Tuli basin (Aldiss, 1983a). Various interbanded, mylonitic gneisses informally known as Maibele supracrustal belt are recognized in the MSZ (Paya, 1996). Coward et al (1976) summarized the 4 deformational episodes of Limpopo belt as being intracratonic as small blocks of crust moved relative to each other resulting in local shear zones. Northeast-southwest trending dolerite dykes cut across the Karoo and Archaean rocks in the northern part of the study area (Figure 7) which are part of the regional Kalahari dyke swarm of northern Botswana (Reeves, 1978).

2.4.4 Hydrogeology

Motloutse Sand River consists mainly of sand and gravel at variable depth, with coarse sand along the middle of the river and silt and clay banks occurring adjacent to river banks. Sedimentology studies show that the sediments on the few uppermost metres of sand rivers have

been deposited on the last 100 years (Herbert et al, 1997). BNWMPR (1991) classifies Motloutse River as a major sand river and this sand bed is recharged from runoff that comes from upstream.

Fetter (1994) defines transmissivity as a flow rate through a unit width under a hydraulic gradient of one by the saturated thickness of the aquifer, and thick alluvium deposits (>3m) make highly transmissive aquifers. Transmissivity values ranging from 400-3000 m²/day have been recorded in sand rivers of Botswana (BNWMPR, 2006). Table 2 shows storage values and transmissivities from pumping tests done on sand river aquifers found in major and intermediate rivers of the Limpopo basin drainage system. Average width of river is about 80m, however from reconnaissance; the channel in some areas can reach up to 140m.

Table 2: Hydrodynamic properties of aquifers of Botswana major and intermediate rivers. (Modified from BWNMPR, 2006)

River Location	Reference	Transmissivity (m³/day)	Storage (%)
Motloutse Phikwe	Gibb 1969	1470	17
Motloutse Mmadinare	Wikner 1980	310-345	15-20
Motloutse Mmadinare	Nord 1985	1300	7-40
Motloutse Tobane	Wikner 1980	1730	15-20
Shashe Sebina	Wikner 1980	600	15-20

2.4.4.1 Study area Water level hydrographs

Figure 8 and Figure 9 shows hydrographs of water level data collected on the riverbed near Tobane. The data set has two records from two periods ranging from year 1979 to 1982 and 1990

to 1995 for the second data set. In Figure 8 it can be observed for the most part of the record that the water levels mimic the sand levels and generally steady with minor deviations and an average of 738.6 mamsl. During May 1981 the water levels dropped to their lowest readings.

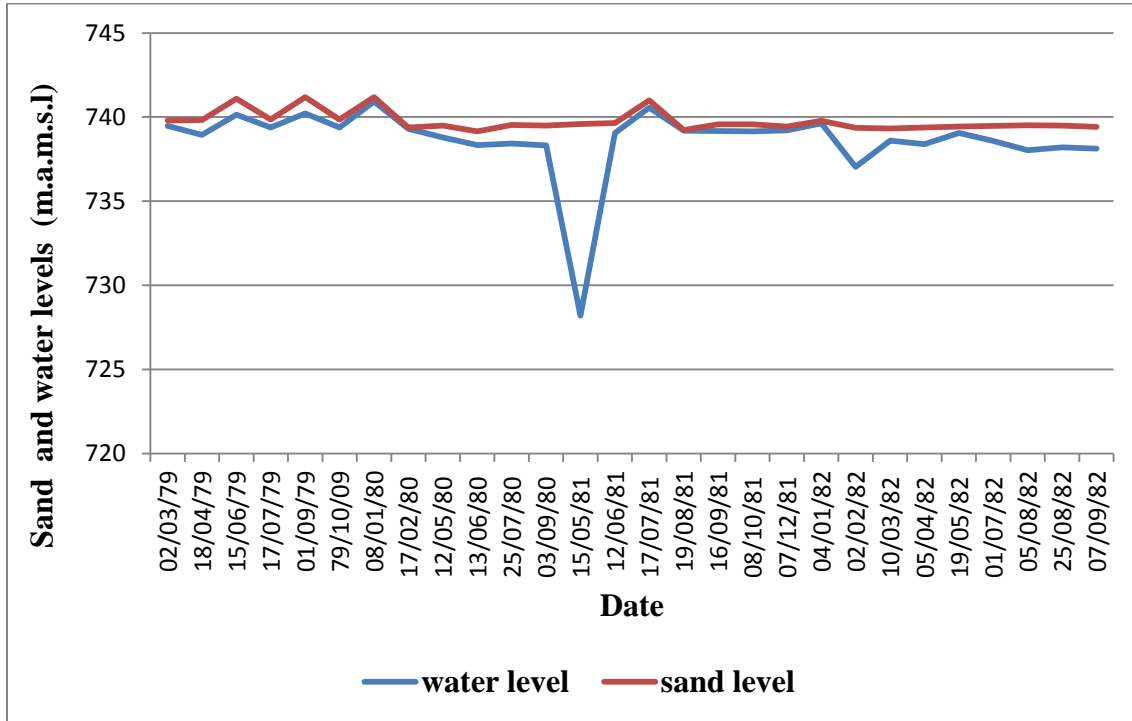


Figure 8: Hydrograph showing water and sand levels for 1979-1982 period (BNWMP, 1991).

Figure 9 shows the long-term hydrograph for the second data set and here water levels do not mimic the sand level demonstrating the seasonal recharge of the riverbed. The maximum water levels occur in December 1994 to February 1995, which is consistent with the wet season rainfall amounts.

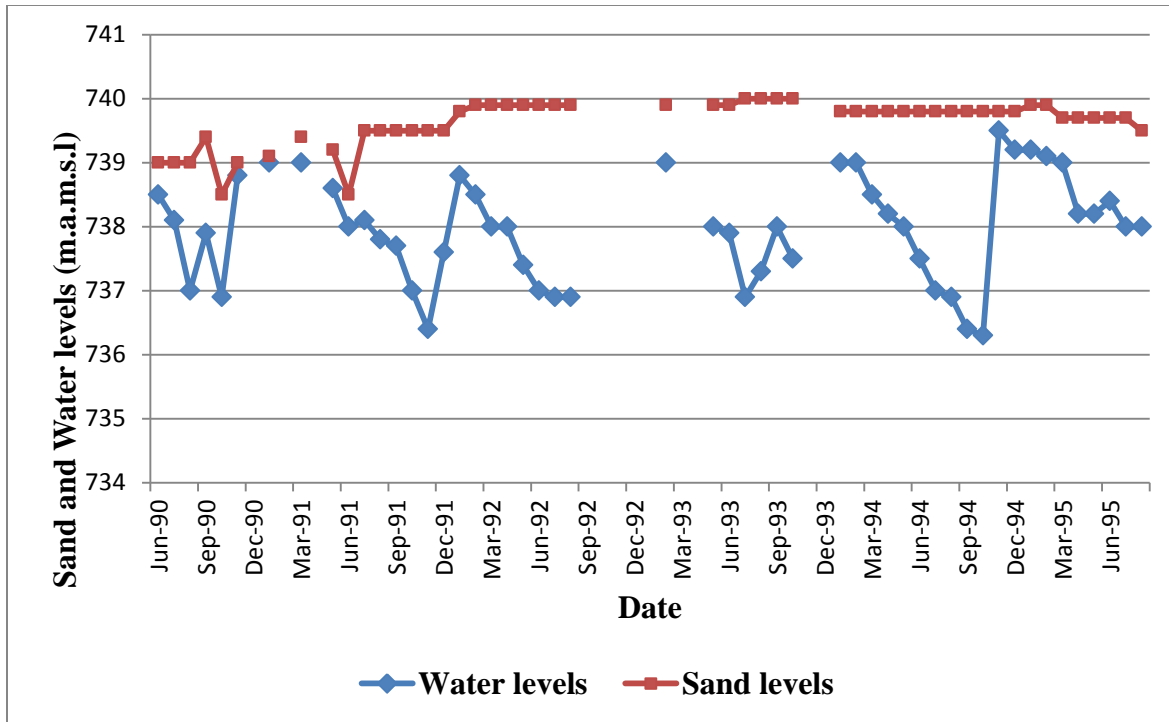


Figure 9: Hydrograph showing sand and water levels for June 1990 to June 1995 period (Anderson,1997).

2.5 SOCIO-ECONOMIC CONDITIONS

The Limpopo River basin is home to around 14 million people in the four riparian states of Botswana, South Africa, Zimbabwe and Mozambique (Owen, 2012). Botswana has the highest percentage of the population living in the Limpopo basin as in Table 3. Many people in the rural areas rely on the Motloutse catchment as a secure water supply for subsistence agriculture therefore water allocation between upstream and downstream areas and between urban and rural users is therefore a serious test for water management.

Selibe Phikwe is the only town in the catchment with principal villages being Mmadinare, Bobonong and Tobane and urban supply to Selibe Phikwe town is the major user. The Limpopo River basin is located in an arid to semi-arid area where water is of critical need and very vital to

all development in the region. The majority of rural population in the Motloutse catchment mostly subsistence farmers rely on irrigation which in turn relies on stored water on the sand riverbeds.

Table 3: Percentages of Population in Limpopo by country (Owen, 2012).

Country	Estimated Total Population by Country in 2007 (million)	Estimated Population Living in Limpopo Basin in 2007 (million)	% in Limpopo River basin
Botswana	1, 756,651	1, 205,580	69
South Africa	47, 900,000	10, 720,838	22
Zimbabwe	11, 392,629	1, 140,833	10
Mozambique	20, 366,795	1, 389,703	7
Total	81, 416,075	14,456,954	18

2.6 WATER USES AND DEMAND

Urban or industrial water supply is the largest and fastest growing water use sector in Limpopo river basin at 60Mm³ per annum (Environmentek, 2003). The Motloutse catchment is categorised as a water stressed region of the Limpopo River basin (Owen, 2012). Smallholder farmers have limited access to irrigation water in semi-arid areas such as Limpopo basin (Love et al, 2006) and with a widespread unanimity that small scale water supply technologies are financially sound and or affordable (Lasage et al., 2007; Van der Zaag and Gupta, 2008). Currently different methods are used to extract water from sand rivers such as hand-dug shallow pits for cattle watering purposes and collector wells, a technique developed by the British Geological Survey (Herbert et al, 1997). These low cost abstraction systems are suitable due to the small head difference between the alluvial bed and the fields (Mansell and Hussey, 2005).

Rainwater harvesting has been used for many years in higher rainfall areas but it is less practical in low rainfall areas with flat topography such as the Motloutse catchment (Love and Walsh, 2009).

Primary use of groundwater is in irrigation for example in the Talana Farms area downstream of Bobonong village. The catchment as in Figure 1 has a 100 MCM capacity dam (Letsibogo) near Mmadinare village, opened in year 2000 principally to supply the industrial town of Selibe Phikwe and surrounding areas. However, the dam now supplies Gaborone and major villages along the pipeline route through the NSWC project. Water demand for the Selibe Phikwe mining town in 2004 was at 97l/c/d and averagely 65l/c/d for the villages which is well taken care of by the dam . Through the NSWC project this will lead to increased or over abstraction on the reservoir resulting in poor environmental releases as already noted by the BNWMPR, (2006) which can harm the ecology downstream of dam. Water demand is based on availability, source and price of water, of course the sources are present but the availability is hampered by the NSWC project affecting price thereby increasing demand. This further leads to irrigation water needs relying solely on groundwater.

3.0 LITERATURE REVIEW

3.1 PREVIOUS WORK

Previous investigations on the Motloutse water course have been done as follows; the Bamangwato Concessions Ltd and Gibbs and Partners (1969, 1970, and 1971) carried out a temporary water supply investigations on a 29km section of the Motloutse River between Mmadinare and Tobane. They focused on the Letlhakane fault underlying the Letlhakane River and part of Motloutse. The United Nations Development Programme (UNDP) mapped and established a groundwater level profile from Mmadinare to the confluence of Limpopo in 1972.

Wikner (1980) and Nord (1985) investigated the major sand rivers in eastern Botswana. The riverbed was probed by Wikner (1980) and Nord (1985) and their work produced vertical cross sections through the sand aquifer along the Motloutse. Wikner provided an approximation of expected average yields per km of major sand rivers based on total storage data on alluvium depth based on a large number of cross sections. He used test pumping obtained at different locations along riverbed to estimate aquifer properties.

Nord (1985) reviewed different methods for sand river abstraction and he categorized the sand rivers according to average yield per km resulting into major, intermediate and smaller sand river classification as in Table 4.

Table 4: Sand river classification of Botswana Rivers after Nord (1985)

Rivers	Classification	Yield (m³/d x km)
Lower Shashe, Mahalapye, Motloutse	Major sand rivers	100-133
Upper Shashe, Tati, Ntshhe	Intermediate sand rivers	30-45
Upper Sebina, Metsimotlhabe	Smaller sand rivers	0-20

The smaller sand rivers were considered not suitable for exploitation. He also investigated the effect of artificial barriers such as cut-off dams and sand storage dams. He found out that artificial barriers founded on subsurface rock barriers or thresholds to minimize seepage losses leading to efficient abstraction schemes as they do lower evaporation losses and increase yield to some extent. However, he concluded that success of artificial barriers in Botswana is hampered by lower velocities of sand rivers and no reliable sediment load investigations in Botswana.

Water Resource Potential

Gibbs (1970) used a model where the water resource was classified into “short term”, “midterm” and “long term” resources. A short-term resource referred to the dewatered volume calculated through monitoring the gradual decline of the water table by keeping the hydraulic gradient constant until the saturation level intersected one of the barriers occurring across the riverbed. Midterm resource was estimated to be the amount of water held in storage by the sand aquifer between the water table height when the barrier (dyke or fault) is first intersected and that water table level when all the drainage over the barrier has ceased. He lastly defined “long term” resource as that quantity of water remaining trapped below the lowest drainage outlet from a basin between the water table and bed bottom.

Gibbs found out that in the 22km reach of Motloutse; 72.5%, 16.6% and 10.9% was held in short, midterm and long term storage respectively. However, Nord (1985) realized that the so-called “barriers” have been found out not to react as barriers and Gibbs model implied that when short term resources are lost there is no groundwater flow at all. A fact that Nord disputes as he proved that there is still groundwater flow in the larger sand rivers of Botswana at the end of the dry season and therefore he considered Gibbs model irrelevant for major sand rivers. He further disapproves the notion of underground barriers as they do not seem to play that important role for the hydraulic conditions in sand rivers as described by previous reports.

Thomas and Hyde (1972) used another model based on the lowest found water table at the end of the dry season. He took year 1971 as a case study and categorized sand river storage into “shallow” depth storage, mid-term and deep storage. The shallow depth storage was assumed to be water volume lost over the dry season, and the storage below the water level at the end of 1971 dry season down to 3.5m depth was described as midterm-storage. Aquifer below the midterm-storage was defined as “deep-storage”. This were all under the assumption based on an extremely dry season of 1967/68 and also assuming a dry period of 30 months. However, Nord (1985) in his report revised the model and divided the aquifer into 2 zones, namely the upper zone” defined as natural losses and lower zone” referring to water in storage”. He found out that 33% of the water was held in shallow storage while 48% and 19% was held in mid and deep storage respectively.

Field Methods

2 methods have been employed in previous investigations being Auger drill probing and resistivity. Probing using an auger drill is the old and common method in Botswana utilized by

DWA in which continuous sampling of bed material can be done and information gathered. However, the method is labor and time consuming as many holes have to be drilled in a river section.

Thomas and Hyde (1972) used resistivity in conjunction with probing but there was a poor correlation between the methods due to distortion by clays in the sandriver aquifer. Buckley (1982) also used resistivity at the North-east district rivers and found interpretation of resistivity data difficult. His result shown that the riverbed were underlain by a thick bedrock. DWA in 1981 at Mmadinare used a similar method when drilling production holes, they found solid bedrock below the sand beds at all drilling sites and no weathered bedrock was found.

Environmental Impacts of Dam

Sir MacDonald and partners (1989) when carrying out Letsibogo dam feasibility study observed no significant upstream impact of the dam, however he envisaged little erosion risk associated with increased cattle density due to decreased grazing land. To date, no subsequent upstream impact of dam is significant, save for small, rare flooding associated with dam.

Concerning environmental downstream impacts, MacDonald also noted insufficient compensatory flows that cause riverine vegetation not to regenerate leading to increased erosion and reduced grazing pastures. Illegal sand mining could adversely affect the sand river aquifers yield by reducing the depth of alluvium of which the water is held in storage.

BNWMPR (2006) states that subsequently to Nord's study there have been no comprehensive re-evaluation of sand river resources the only work being MacDonald (1990) and Department of Lands (1998) on the Motloutse. MacDonald identified potential dam sites and suitable lands for irrigation and assessed the economic and technical feasibility of the proposed dam. Department

of Lands (1998) quantified the water resources of Motloutse only in areas where soil is suitable for agriculture.

3.2 DESCRIPTION OF ALLUVIAL AQUIFERS

Barker and Molle (2004) defines an alluvial aquifer as a groundwater system, generally unconfined, that is hosted in laterally discontinuous layers of gravel and sand, deposited by a river in a river channel, banks or flood plain.

Water retention on an alluvial aquifer is more efficient than in a surface dam due to lower evaporation losses (Love et al, 2010). Surface dam operations can also have unwanted effects on alluvial aquifers such as channel incision due to changed flow regime connected with the dam (Allan and Castillo, 2007) that drain aquifers downstream of dam (Bornette and Heiler,1994). Deposition of sediment downstream of dam may be reduced which by default form the alluvial aquifer (Kondolf and Wanson, 1993; Shield et al, 2000) because of descending channel migration (Ward and Stanford, 1995). Alluvial aquifers also avoid environmental effect related to surface dam such as inundation and flow regime changes (King et al, 2003).

It has been shown that groundwater losses by transpiration are minimal while evaporation losses diminish to zero when water levels fall one metre below surface, termed “extinction depth” (Wikner, 1980; Nord,1985; Wipplinger,1958.; Aerts et al., 2007).

Love et al, (2007) noted that alluvial aquifers are related to stream flow due to their shallow depth and vicinity to streambed and Mansell and Hussey, (2005) further argues that groundwater flow in alluvial aquifers is an extension of surface flow. Townley (1998) and Owen (1991) proposed that in semi-arid areas surface water bodies can be categorized as discharge water bodies when they receive base flow in the dry season and as recharge bodies when they replenish

an alluvial aquifer during the rainy season or under a managed dam release. Alluvial aquifer recharge occurs through direct rainfall on the sand bed surface and mainly through surface runoff into the channel (Wikner 1980).

River flow only occurs after full saturation of the aquifer channel sands and depletion of the groundwater resource begins once river flow ceases, such full recharge in semi-arid places normally occurs early in the rainy season (Owen and Dahlin, 2005; Nord, 1985; Halcrow, 1982). Alluvial aquifers in the eastern side of Botswana are usually hosted in the ephemeral sand rivers and these sand rivers have well-defined, steep-sided channels, with flat floors, in filled with thick alluvial sands. The alluvial aquifers are replenished perpetually on perennial rivers and usually, annually on ephemeral rivers through flushing out by flood waters and dam releases (Barker and Molle, 2004; Owen, 1994; Owen, (2000) and salinity intrusions from older lithologies can occur if there is over abstraction from the aquifers –or during drought years.

Construction of sand dams or gabions-weirs increase the depth of the aquifer when constructed above surface (Aerts et al., 2007) and reduce downstream groundwater flow when constructed below the surface. Managed releases from an upstream dam replenish the aquifers thereby ensuring also a year-round availability of alluvial groundwater (Moyce et al., 2006).

3.3 GEOMETRY AND PHYSICAL PROPERTIES OF ALLUVIAL AQUIFERS

Groundwater resources often occur in isolated basins/compartments along the river course which are controlled by buried rock thresholds (Wikner, 1980). Love et al, (2007) in studying sand rivers noted that alluvial deposits occur in large rivers and minor tributaries as narrow bands less than 1km in width on large rivers to a few metres on small rivers. Owen (1991) further suggests that distribution of alluvial aquifers depends on river gradient, channel geometry, sudden change

of stream power as a function of decreasing discharge downstream caused by evaporation and infiltration losses, and sedimentation rates due to erosion. However Love et al, (2007) points out that due to the physical homogeneity of alluvium the infiltration rates are fairly uniform spatially.

The extent and thickness of the alluvial fill in the river channel and under the lateral alluvial plains determines the aquifer dimensions or is the main limiting factor, and areas where the alluvium is naturally augmented render potential sites for groundwater development (Owen and Darlin, 2005). Depth of alluvium is also enhanced at the confluence of larger tributaries and the main river channel (Wikner, 1980). Owen and Darlin (1994) shows why and how alluvial aquifers are located at geological boundaries through a conceptual model (Figure 10).

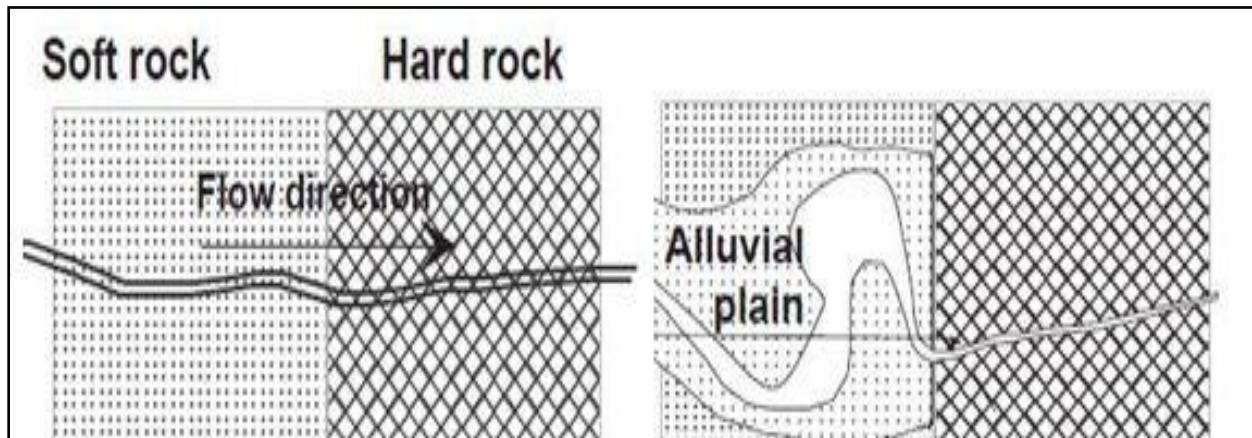


Figure 10: River channel cuts through a hard rock downstream of geological boundary and due to the resistant lithology downstream coupled with the soft rock erodibility, meanders form upstream of contact.

Changes or an increase in sediment supply to the stream result in deposition of alluvial sediment (Richards 1982). Geometry and position of alluvial fill depends on whether the resistant lithology

occurs upstream or downstream (Owen and Darlin, 2005; Cobbing et al., 2008). A detailed understanding of the bedrock geology and alluvial deposition process are vital for identifying localities with potentially enhanced alluvial aquifer dimensions.

3.4 HYDRAULIC CONDUCTIVITY

Hydraulic conductivity is the rate at which a unit cube of geologic material will transmit water under a hydraulic gradient (Kasenov 2002). Darcy in 1856 studied the movement of water through a porous medium to empirically define a relationship between flow rate (Q) and hydraulic conductivity (K), Cross sectional area (A), length of soil column (L) and difference in water level (h_1-h_2) given as

$$Q = KA \frac{(h_1-h_2)}{L} \quad (11) \text{ from which K is expressed as}$$

$$K = \frac{Q}{Ai} \quad (12)$$

Where K=Hydraulic conductivity (m/day)

Q = Discharge/flow rate (m^3/day)

i = hydraulic gradient dh/dl

Fetter (2001) noted that K depends on porosity, particle size, distribution, arrangement and shape of particles. Determination of K in hydrogeology is critical for groundwater modelling and pollutant transportation in the saturated and unsaturated zones between stream and its sediments.

There are many ways of determining hydraulic conductivity that can be grouped into different classes such as empirical, experimental and correlation methods among others (Oosterbaan and Nijland, 1994). For simplicity these methods can be categorized into 2 main approaches namely; in situ field methods and laboratory methods. In this dissertation, both approaches have been utilized in establishing hydraulic conductivity of the Motloutse alluvial aquifer.

Both approaches are based on Darcy’s law and can either be field measurements (in situ) or laboratory methods with the former consisting of augering and borehole pumping tests among others while the latter is composed of constant and falling head permeability tests and correlation methods (Todd and Mays 2005;Oosterbaan and Nijland,1994) as in Figure 11.

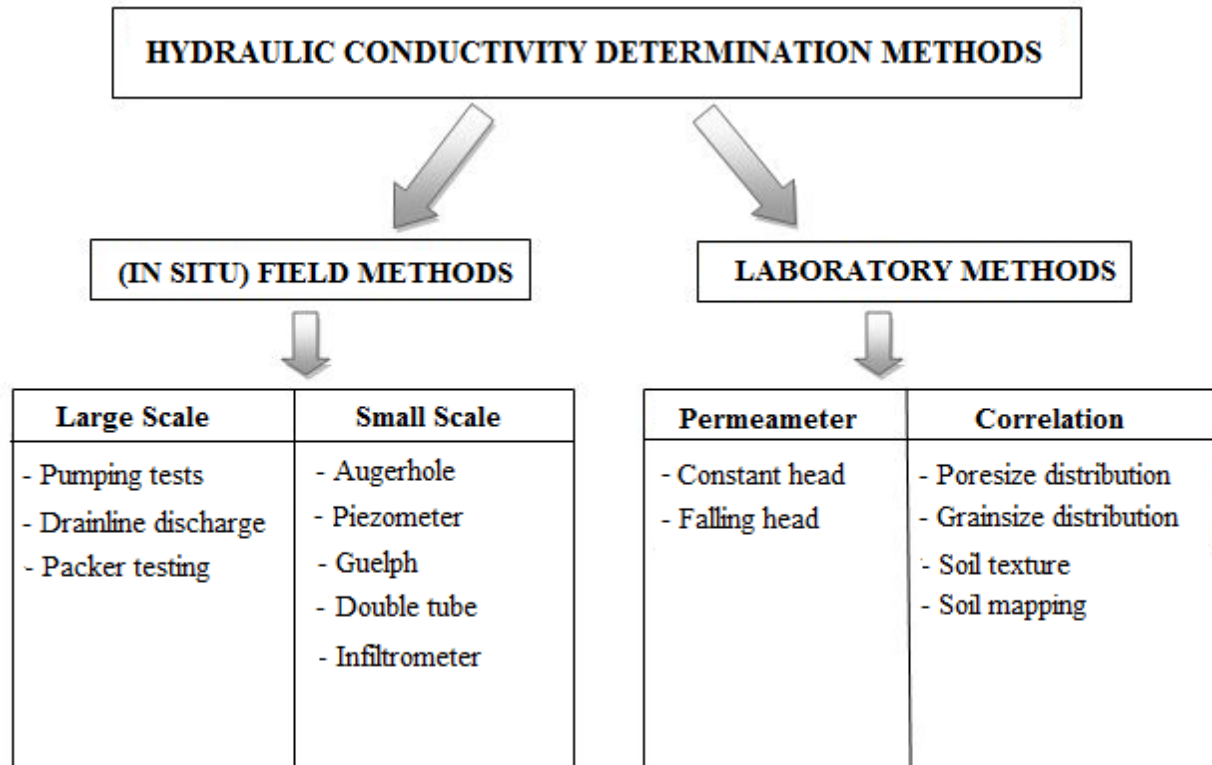


Figure 11: Methods for determining hydraulic conductivity (Modified from Oosterbaan and Nijland, 1994)

Pumping tests are a large scale and conventional method of assessing aquifer properties as it measures the actual field values while other methods only measure samples, which are unlikely to reflect the full heterogeneity of the alluvium. However its field operations are expensive due to the specialized drilling equipment used, diesel consumed and not forgetting that water has to be pumped from the aquifer in such a way that the water does not return to the aquifer and this requires more energy requirements to power the pumping process (Karanth, 1987). The accuracy

of field methods is also hindered by insufficient knowledge in determining aquifer geometry and hydraulic boundaries (Uma et al, 1989).

In view of the above deficiencies associated with field measurements, empirical methods have been developed correlating hydraulic conductivity to properties of the medium namely grain size, porosity and to some extent soil texture.

3.5 COMPARISON OF DEPTH ESTIMATION METHODS

Murray (1996) when assessing methods for estimating groundwater resource highlighted that often the main difficulty is quantifying area, thickness and storativity. However, in this study these concerns are mitigated by a high-resolution geophysics technique for thickness and area.

Ground Penetrating Radar is a rapid and cost effective means alongside other reasons of obtaining information on the thickness and lithology of river alluvium as shown in Table 5 hence was chosen for this study.

Table 5: Comparison of Geophysical methods in sand river study.

METHOD	ADVANTAGES	DISADVANTAGES
EM	<p>Since it is based on induction, it does not require electrodes in ground.</p> <p>Can be carried out under most geological conditions including those of high surface resistivity such as sand and gravel. (Kearey and Brooks, 1991).</p> <p>Faster surveys over larger areas.</p>	<p>EM anomalies can result from sources such as graphite, water filled shear zone, bodies of water and man-made features.</p> <p>Wet clays and graphite bearing rocks may limit depth of penetration.</p> <p>Penetration is not very deep – limited to frequencies that are generated and detected (Tx-Rx separation).</p> <p>Depth information only obtained by calibration against probing.</p>
VES	<p>Suitable for the subsurface investigation of geologic environments consisting of horizontal stratigraphy such as in unconsolidated sedimentary sequences (Kearey and Brooks, 1991)</p> <p>Method readily identifies the depth to the crystalline bedrock – sand alluvium interface and responds well to water content.</p>	<p>Poor resolution in the areas underlain by Karoo Super group sediments due to abrupt lateral changes in lithology.</p> <p>Interpretation very ambiguous and depth of penetration limited by electrical power that can be introduced into the ground.</p>
GPR	<p>Provides the broadest range of geological feature detection; including sediment thickness, bedrock, fractures, faults, groundwater, voids and sinkholes.</p> <p>Offers the highest resolution of the subsurface.</p> <p>Can map both depth to bedrock and the water table with outmost accuracy.(Smith et al, 1992).</p> <p>Simple instrumentation setup and portability</p> <p>Deeper penetration (10-30m) can also be achieved with high accuracy.</p> <p>Particularly effective in coarse, electrically resistive sedimentary aquifers such as alluvial sands and gravels (Beres et al., 1999)</p>	<p>Principal limitation of the method is the electrical conductivity of the ground effected by conductive clays (Bristow and Jol, 2003).</p> <p>Depth range also limited by the transmitted centre frequency and the radiated power.</p>

3.5.1 Overview of Ground Penetrating Radar

GPR is a high-resolution geophysical technique made to penetrate the ground using electromagnetic energy to image the subsurface. The electromagnetic pulses permeate from a transmitting antenna into the subsurface until they encounter a layer with contrasting dielectric properties (Annan, 2009). Contrasting dielectric properties cause some of the electromagnetic energy to be scattered back to a receiving antenna ferried along above the ground.

A GPR system measures the time taken by the electromagnetic energy to travel from an antenna to an interface (such as the water table, soil horizon, stratigraphic layer, buried objects etc) and back. A time-distance record of the subsurface is produced and displayed immediately on a screen, (Figure 12) with the abscissa being a distance scale based on the speed of the antenna across the ground surface. The vertical scale represents the two-way travel time of the radar pulse through the subsurface as shown in Figure 12.

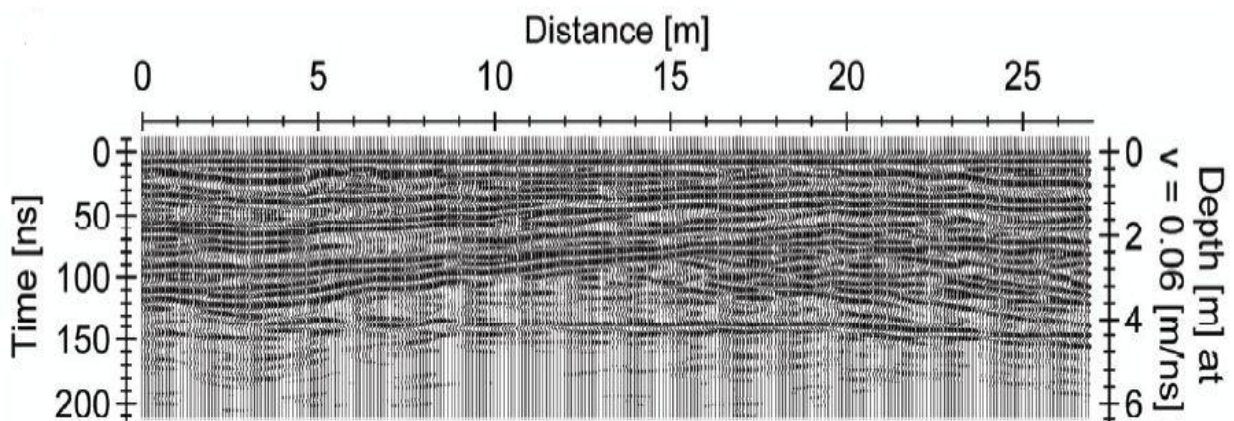


Figure 12: Raw radargram showing time in nanoseconds, depth in metres on vertical scales and distance in metres on horizontal scale after Burval working Group,(2006) .

If the travel path length of the radar wavefront is known, the electromagnetic wave velocity can be estimated from the two-way travel time of the reflected wave. The propagation velocity can then be used to convert the time scale into a depth scale (Doolittle et al, 2006).

In soils with low conductivity and energy dissipation, propagation velocity can be approximated using equation 2 (Daniels, 2004).

$$V=2D/T.....(2)$$

Where V is the propagation velocity, D is depth and T represents the two way pulse travel time. Time converted depth scales have been proven to be reasonably accurate, and most modern GPR software packages contain them by default (Smith et al, 1992). Bentley and Trenholm (2002) under favorable conditions used GPR to estimate depths to shallow water tables to an accuracy of about 20cm.

The penetration depth is controlled by the GPR center frequency, electrical conductivity and attenuation of the subsurface media. Dry clean sands, gravel and sandstone provide the maximum penetration depths (Jol and Bristow, 2003). Conductive materials such as clay, saline pore water attenuate the signal faster thereby decreasing penetration significantly. Vertical resolution depends primarily on wavelength of the electromagnetic wave, which is determined by the GPR frequency, f, and velocity, v, of the concerned material.

3.6 WATER BALANCE OF AN ALLUVIAL AQUIFER SYSTEM

Hydrological processes affecting the flow of water in an alluvial aquifer are critical in increasing an understanding of sustainable water resources management. Balance between inflows into the aquifer and outflows from the aquifer are fundamental and represented by equation 1 (Schicht & Walton, 1961). A positive value implies that inflows are greater than outflows and vice versa for a negative value, therefore net groundwater flows refer to changes in storage in the alluvial aquifer.

Seepage losses often times can be difficult to quantify but they are controlled by bedrock geology (Dehamer, 2008). Love et al (2007) monitored drying periods after a dam overflow event minus evapotranspiration losses at different sections of the river, one underlain by granite and the other by heavily weathered granite, he realised that seepage values (rate in mm/day) can be derived by comparing drying curves of the two sections. Masvopo et al (2008) also observed water level fluctuations after a dam release on Malala alluvial aquifer bounded by dam and dolerite dyke and calculated seepage values of 3.7 percent from a total volume of a fully saturated alluvial aquifer. Seepage can be a considerable flux; however, Nord (1985) in studying the Motloutse alluvial channel has noted seepage losses to be insignificant as water will have moved 1.5 km downstream over a 300-day dry season.

$$\Delta S_G = P + Q_{IN} - Q_{OUT} + Q_L - Q_S \pm Q_P - E \quad (1)$$

Where

ΔS_G = Change in groundwater storage

P = Precipitation which percolates through the unsaturated zone

Q_{IN} = Flow from upstream of the aquifer through the sand formation

Q_{OUT} = Flow in the downstream direction through the sand formation

Q_L = Leakage or recharge from the river bed to the aquifer

Q_S = Seepage from the alluvial aquifer to the underlying geological formation

Q_P = The amount of pumping out of the aquifer.

E = Evapotranspiration from the unsaturated zone.

Nord (1985), noted lateral inflow from the Mahalapye river banks. This theory has been supported by Viak, 1973 who recorded saline groundwater conditions in a limited area of the Mahalapye River. This water gave chloride content of 2500mg/l after water quality monitoring increasing in the dry season and decreasing in the wet season but this observation is not repeated upstream/downstream of river indicating inflow from riverbank at that point in Mahalapye River.

3.7 GROUNDWATER RESOURCE EVALUATION

In order to establish the sustainable exploitation potential of a groundwater resource its essential to assess how much water is held in storage and what amount can be removed for the resource to last through years of less than average rainfall. Owen and Darlin (2005) highlighted that the three dimensional extent of alluvial aquifers confines the groundwater resource and this resources in an alluvial aquifer can be estimated by multiplying the aquifer volume by a specific yield value of the aquifer material. In addition it is of great importance to determine the mean thickness of the aquifer and its area as part of the hydrogeological study of the area.

Nord (1985) identified natural losses and measured the water level depletions for Botswana sand rivers and these losses have to be considered and these include through flow, evaporation and seepage. Nord (1985) in studying alluvial channels in considered the top

90cm to be an evaporation zone and that evaporation losses may account for 25 % of the available water in the aquifer once annual recharge has ceased. In order to adequately quantify groundwater resources from alluvial aquifers it is important to identify the bedrock geology and to also have an understanding of the processes of alluvial aquifer dimensions.

4.0 METHODOLOGY

4.1 GEOPHYSICS INVESTIGATION

4.1.1 Site Selection

An analysis of the available data, maps and aerial photographs was done. Bulletin no. 40, quarter degree sheet 2128C which offers an explanation of the geological map of the country around Bobonong area and other geological literature was consulted to give a background on the existing geological formations in the study area. Google Earth™ was also considered in choosing the sites to be considered for Ground Penetrating Radar Survey. The choice of location where GPR profiles were taken was based on river width, accessibility, settlement radius, riverbed slope, rock outcrops and lithology. The wider reach of the river to maximise the resource potential, an easily accessible section and close vicinity to settlements being the desired options. In addition, gentle slope of the riverbed as it results in low sediment velocity, no or little outcrops, resistant lithology upstream as explained in chapter 3, Figure 10 all these being the criteria for location choice.

4.1.4 GPR Method Fieldwork

A GPR Survey was carried out in Tobane on the 15th of June 2014, the timing concurrent with the dry season thus avoiding rainy season which usually disturbs smooth running of GPR fieldwork. Five radar traverse lines across the Motloutse river width near Tobane village were established. These profiles were trending north-south and their length determined by the river width ranging from about 100-135m. These profiles had an interspacing of 250m as illustrated in a plan view of the radar grid setup shown in Figure 12. Along each of these profiles, elevations and coordinates were captured with Trimble Differential Global Positioning System (DGPS) from the two (2) banks and along the middle section of the river

for topographic corrections. The radar grid was confined to the channel width and not extended to the alluvial plains due to riverine vegetation that impedes access. In addition, there was concern of severe attenuation of radar signals in silts and clays of the alluvial plains.

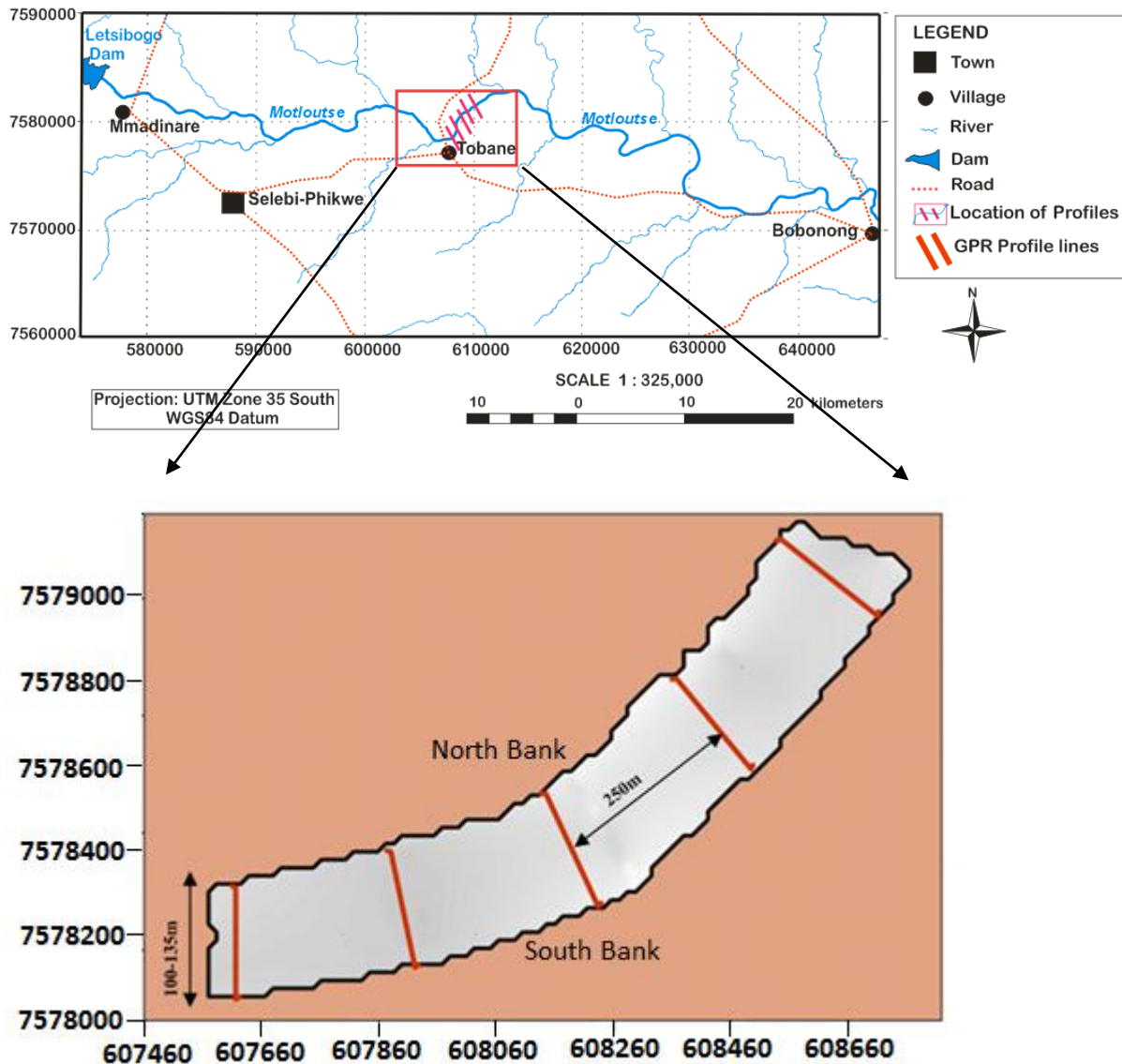


Figure 13: Location of GPR profiles and simplified Plan view of the GPR Survey

Optimum offset GPR reflection profiles were recorded along the profile lines using a Ramac™ GPR system from Mala Geoscience. The unshielded antennae were kept at a constant separation of 2 m with a center frequency of 50 megahertz because lower

frequencies result in greater penetration depths (Conyers, 2004; Leckebusch, 2003; Daniels, 2004; Reynolds, 1997). The antennas were orientated parallel to each other and perpendicular to the profile (Figure 13). To improve the signal to noise ratio every trace was vertically stacked sixteen (16) times. A “hip chain” which is simply a cotton thread that unwinds as the operator walks along the profile and is calibrated to actual length was used to measure the distance between each trace measured (Turesson, 2006). Due to its ease of use and portability an individual carried both the storage unit, control unit, display device on a backpack and the antennas alongside him as in Figure 13. The velocity of the profiles was also recorded directly from the display device at $59\text{m}/\mu\text{s}$. This value was be used to calibrate the processing software packages so that correct depths are determined.



Figure 14: Display monitor, storage and control units and the antennae used for the survey

4.1.5 Data Processing

GPR data processing is essential before the data can be interpreted because it leads to signal enhancement thereby improving target recognition and easing interpretations. In GPR data

processing, amplitude reflections recorded with travel times are digitized into individual traces which represent a series of waves collected and imaged in different ways such as wiggles-form, slices, grayscale or colour (Conyers, 2004).

The data processing of GPR is analogous to seismic data processing therefore a few seismic basic processing steps were applied (Fisher et al, 1992). The first step was simple data editing to correct mistakes in the field such as merging files, reversing profile directions and low-cut filtering (dewow), which removes low-frequency induction effects on the radar equipment (Jol and Bristow, 2003, Turesson, 2006). The raw data had the following reflection data collection parameters (Table 5).

Table 6: GPR Reflection data collection parameters.

Reflection Data parameter	Parameter measurement and units
Antenna Separation	2 m
Sampling Frequency	2148 MHz
Trace spacing/Interval	0.3 m
Number of Stacks	16

Raw data of all the profiles before processing is shown in appendix A1 using a free *GPRSoft Viewer* viewing software, that is, a software without processing capabilities but can only display the files usually for academic purposes. Second step was to adjust time zero in order to achieve correct two-way travel times and depths (Sensors and software, 2003). Next step is application of gains; due to attenuation and wave spreading of the signal, gains boost signal strength by enhancing low amplitude reflections (Dojack, 2012).

4.1.6 Interpretation

Interpretation of GPR data is primarily limited by two factors namely; methodological limitations affecting the quality of the signal and quality of the comparative data by which the signal is deduced (Dojack, 2012). Furthermore, radarfacies analyses and radar stratigraphic analyses are commonly used techniques in which interpretation is derived, this techniques focus on or takes into account radar sequence boundaries (Van Overmeeren 1998; Neal, 2004).

Various authors have demonstrated that for aiding in interpreting subsurface strata a ground-truth control is required such as trenching, coring and cut face experiments (Taylor and Macklin 1997; Bridge et al 1998; Liner and Liner 1995). On the 13th and 14th of November as a ground truthing method post the ground penetrating radar survey, the Motloutse River was augered at the sites where GPR data was collected.

Interpretation of the radar records is based on reflection amplitude changes. Amplitude changes are due to contrasting subsurface material properties and high amplitude reflections are expected between layers of highly varying physical and chemical properties. However low amplitude values are of almost similar properties or uniform matrixes of materials (Conyers, 2004; Neubauer et al., 2002). This is why interpretation of radargrams was based on free *Visual Seismic Unix (SUNT)* for windows program due to its capability to show traces in wiggle form which displays reflection amplitudes (appendix A2). GP Workbench and *Reflex 2D* were used in conjunction with (*SUNT*) for interpretation.

4.1.7 Ground truthing excursion

At Tobane village the riverbed was augered to a depth of 3.5m and the water was strucked at a depth of 0.6m. Augering to a further depth was not possible because the auger tool itself nearly got damaged, any further twist it would have broken. It was initially dug to a depth of

about 2m (Figure 19) using shovels and from there the auger was installed but the water that collected was too much and hindered the augering process.

It must be noted that the riverbed in some areas had deeper sand thicknesses from observation that were avoided so the augering was done in areas where the sand was thinner. Water levels were recorded from hand dug wells for November, December and January months on a weekly basis.



Figure 15: Measuring depth to water level



Figure 16: A 1m hole dug in the riverbed before auger installation

4.2 AQUIFER MATERIAL PROPERTIES ANALYSIS

4.2.1 General

Sand samples were collected from the alluvial aquifer for further laboratory analysis of aquifer medium characteristics;

- Porosity test
- Specific yield test
- Hydraulic conductivity
- Permeability test
- Grain size distribution and soil classification

4.2.2 Sample Collection

Nine sand samples representative of the aquifer material were collected as well with coordinates at different places along the corresponding GPR profile lines and at the riverbanks for further analysis of hydraulic conductivity (m/day), porosity (%) and specific yield (Figure 17). Samples were obtained from a depth of 2 and 3m on the aquifer to avoid surface sampling ,this is due to some physical and biological processes such as surface shrinkage, silty layers or lenses referred to as “planosols” that result in varying aquifer properties (Oosterbaan and Nijland,1994).

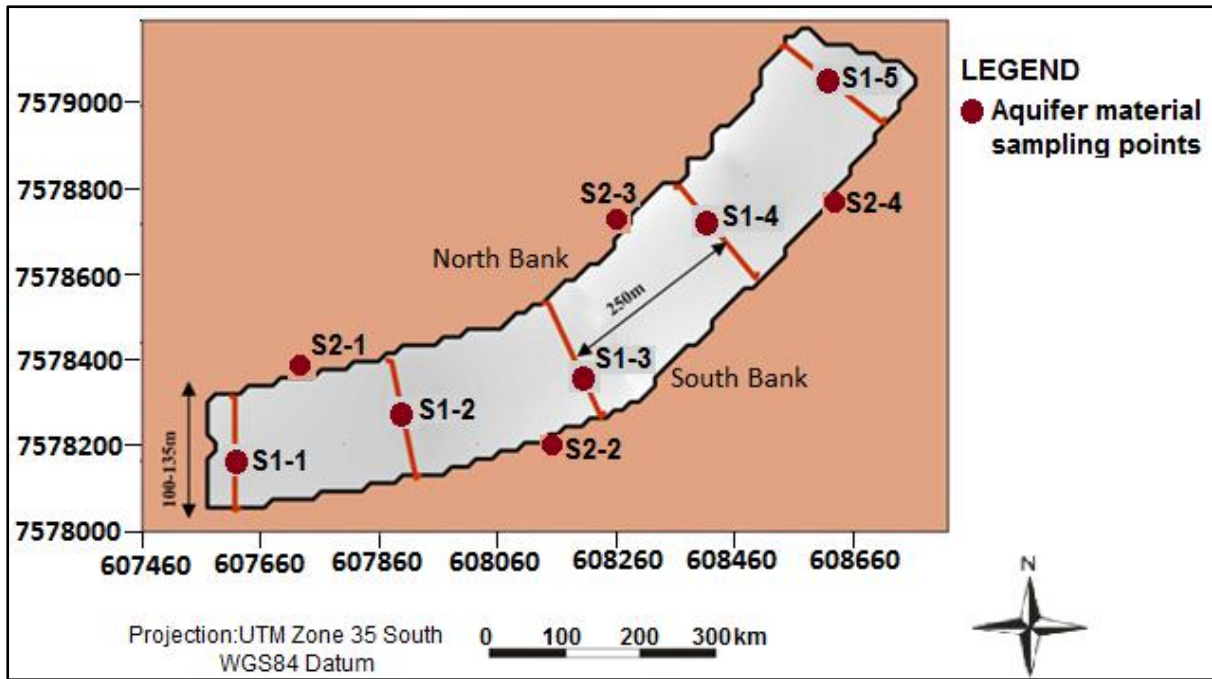


Figure 17: Location of aquifer material sampling site in relation to GPR profiles

4.2.3 Porosity

Porosity is one of the basic aquifer properties that define a porous medium and its ability to facilitate groundwater flow. The Motloutse alluvial aquifer is made up of a porous material so its porosity is of paramount importance as it is in this pore spaces that groundwater occurs. Fetter (2001) defined porosity as the percentage of voids in a medium given by equation 2.

$$n = \frac{100V_v}{V} \quad (2)$$

Where n=Porosity expressed in percentage

V_v =Volume of voids in a unit volume of earth material

V =Unit volume of rock inclusive of both voids and solids

Two common methods were employed in determining porosity described below.

Method 1

A graduated measuring cylinder was filled with water.

A 200ml beaker was filled with the sample.

Water from the measuring cylinder was then poured into beaker with sand sample.

Volume remaining in measuring cylinder recorded and used to calculate porosity.

Method 2

Samples were oven dried in order to expel moisture that is clinging to grain surfaces of the sample.

The dry sample was then put in a beaker and its weight measured and recorded.

The dry sample was then saturated with water and also its weight noted down.

The volume of voids and beaker were recorded and used to calculate porosity.

According to Vukovic and Soro (1992) and Kasenow (2002), porosity (n) can be sourced from grain size analysis through the empirical relationship with the coefficient of grain uniformity (U) given by;

$$n = 0.255 (1+0.83^{Cu}) \quad (3)$$

Where Cu is the coefficient of grain uniformity and represented by $Cu = \left[\frac{d_{60}}{d_{10}} \right]$ (4)

Here, d_{60} and d_{10} are the particle diameters derived from cumulative distribution curves and represent size fractions at which 60% and 10%, respectively, of the sample by weight is composed of grains of a smaller size.

Method 3- Determining Porosity from GPR

It must be noted that in method 3 unlike the previous methods where porosity was determined from samples, porosity was this time determined directly from the study area using GPR.

Water content and porosity are critical in hydrogeological investigations and various authors have demonstrated that GPR can be used for estimating water content in soils (Huisman et al, 2001; Turesson et al, 2006; Doolittle et al, 2006; Topp et al, 1980; Lunt et al, 2005; Schmalz et al., 2002). This is because related parameters such as dielectric constant and radar wave velocity are highly dependent on moisture content. In low loss medium (that is, soils with low salinity and clay content) which is expected of river sand, the velocity (V) of the soil can be related to the dielectric constant by equation 5 (Davis and Annan, 1989).;

$$V \approx \frac{c}{\sqrt{K'}} \quad (5)$$

Where c is the electromagnetic wave velocity in free space and K' is the real part of the dielectric constant

Velocity of 0.06m/ns that was read from the Ramac Mala Geoscience display device which is also in conjunction with velocity for unsaturated sands was used and dielectric constants read from tables of dielectric constants for different materials (after Davis and Annan, 1989; Daniels , 1996). Topp et al, (1980) when using various soil samples found out that the real part of the dielectric constant was increasingly sensitive to volumetric water content, while also weakly sensitive to soil type and density and derived an empirical relationship (equation 6) between apparent dielectric constant and volumetric water content:

$$\theta_v = -5.3 \times 10^{-2} + 2.92 \times 10^{-2} K_a - 5.5 \times 10^{-4} K_a^2 + 4.3 \times 10^{-6} K_a^3 \quad (6)$$

Where Θ_v is the volumetric water content (the ratio of water volume to total sample volume). For low-loss materials $K_a \approx K'$ where K_a is the apparent dielectric constant.

The water content (Θ) equals the product of porosity (\emptyset) and water saturation (S_w) as in equation 7 (Turresson, 2006).

$$\theta = \phi \cdot S_w \quad (7)$$

However in water saturated soils the water content (Θ) is a measure of porosity (\emptyset), that is, $\Theta_v \approx \emptyset$.

4.2.4 Specific Yield

Specific yield is the ratio of water that can be drained by gravity from a saturated sample to the total volume of sediment in laboratory terms. Freeze and Cherry (1979) defined it as the amount of water released from storage of an unconfined aquifer per unit surface area of the aquifer per unit decline of the water table. Specific yield is given by equation 8 after Meinzer, (1923).

$$S_y = \frac{V_d}{V_t} \quad (8)$$

Where;

V_d = Volume drained from aquifer by gravity

V_t = Total volume

Storage in an unconfined aquifer comes from the changes in saturation of individual pore spaces within the medium because water molecules inevitably cling to particle surfaces therefore not contributing to the overall drainage of the sample (Fetter, 2001).

Only pores which are interconnected are available for fluid flow will yield groundwater therefore the specific yield reflects the effective porosity (Todd and Mays, 2005). A test to determine specific yield was executed as follows;

A dry sample was put in a beaker and saturated with water with both the beaker and saturated sand weights recorded.

The sample was then put in a sieve and covered to reduce evaporation

Water was then allowed to drain under gravity

The weight of drained sample was recorded and Specific yield calculated using the following equation

$$\begin{aligned} Sy &= \frac{\text{Volume of water drained}}{\text{Total material volume}} & (9) \\ &= \frac{\text{Mass of water}}{\text{Mass of sand} / (\text{specific gravity of sand})} \end{aligned}$$

4.2.5 Hydraulic Conductivity

4.2.5.1 Hydraulic Conductivity determined from Grain Size Analysis

These empirical formulas are part of the laboratory methods that utilize grain size distribution of granular material as shown by Freeze and Cherry (1979).

The empirical approach is based on representative samples and are simpler, cheaper and do not rely on geometry and hydraulic boundaries of the aquifer as highlighted by Alyamani and Sen (1993); Odong (2007), but reflect the transmitting characteristics of the media. Many authors have proposed multiple relations between K and grain size. Vukovic and Soro (1992) summarized multiple empirical methods from various studies and came up with a general formula as follows;

$$K = \frac{g}{\nu} \cdot C \cdot f(n) \cdot d_e^2 \quad (10)$$

Where K=Hydraulic conductivity

g = acceleration due to gravity

ν = kinematic viscosity for a given temperature

C = sorting coefficient

f (n) = porosity function

d_e = effective grain diameter

The kinematic viscosity (ν) is related to dynamic viscosity (μ) and the fluid (water) density (ρ) by the following expression;

$$\nu = \frac{\mu}{\rho} \quad (11)$$

The sorting coefficient(C), porosity function f (n) and effective diameter (de) values depend on the different methods used in grain-size analysis. Porosity here has been calculated as in equation 3 by Kasenow (2002), mentioned earlier. According to Vukovic and Soro (1992) and Kasenow (2002), porosity (n) may be sourced from the empirical relationship with the coefficient of grain uniformity (U) given by equation 4.

On this dissertation, 4 methods have been used based on their suitability summarized by Vukovic and Soro (1992) that take the general form of equation were selected as follows;

$$\text{Hazen (1892): } K = \frac{g}{v} \times 6 \times 10^{-4} ([1 + 10(n - 0.26)]d_{10}^2) \quad (12)$$

This equation is known as new Hazen formula which takes into consideration porosity and fluid viscosity unlike the general and older one given as;

$$K=C(d_{10})^2 \quad (13)$$

after Fetter (1994). Hazen coefficients ranged from 1-1000 resulting in a large uncertainty of K values (Carrier 2003).

The Hazen formula is useful for fine sand to gravel range, provided the sediment has a uniformity coefficient less than 5 and effective grain size between 0.1 and 3mm.

$$\text{Kozeny-Carman (Kozeny, 1927 and Carman, 1956): } K = \frac{g}{v} \times 8.3 \times 10^{-3} \left[\frac{n^3}{(1-n)^2} \right] \quad (14)$$

This equation was originally proposed by Kozeny (1927) and was then modified by Carman (1956) to yield the Kozeny-Carman equation. It is not suitable for material with effective size above 3mm or for clayey soils as noted by Carrier (2003).

$$\text{Beyer (1964): } K = \frac{g}{v} \times 6 \times 10^{-4} \log \frac{500}{Cu} d_{10}^2 \quad (15)$$

Breyer method does not take porosity into account thus porosity function takes on a value of 1. This formula is usually useful for materials with heterogeneous distributions and poorly sorted grains with uniformity coefficient between 1 and 20, and effective grain size between 0.06mm and 0.6mm.

$$\text{Alyamani \& Sen (1993): } K = 1300 [I_0 + 0.025(d_{50} - d_{10})]^2 \quad (16)$$

Where K = hydraulic conductivity (m/day)

I_0 = intercept (in mm) of the line formed by d_{50} and d_{10} with the grain-size axis, or simply the x-axis.

d_{50} = median grain diameter (mm)

d_{10} = effective grain diameter (mm)

The Alyamani-Sen formula is also one of well-known equations that considers both sediment grain sizes d_{10} and d_{50} as well as the sorting characteristics. It must be noted that the terms in the Alyamani formula above bear the stated units for consistency and this formula is different from the afore mentioned formulas that take the general form of equation (10) above.

As seen above the suitability or applicability of these formulas rely on the type of soil for which K is to be estimated. Vukovic and Soro (1992) however highlighted that the use of empirical formulas can produce K values that differ by a factor of 10 or even 20.

Odong (2007) concluded that the Kozeny-Carman formula followed by Hazen and Beyer respectively, give the best overall estimation of K when he applied seven empirical methods on four different sand samples hence their usage in this study.

Chen (2000) reported that values of streambed K determined from grain size show disparities to those determined by other methods such as permeameter tests. In addition, Landon et al

(2001) also suggested that K determined from empirical methods is statistically greater in deeper sediments than K determined from other methods in unison with Chen's findings. Furthermore Song (2009) when evaluating the feasibility of grain size analysis methods in accurately estimating K of streambeds from 52 samples in seven sites noted that values of K determined from grain sizes are consistently higher than K determined from in situ permeameter tests at corresponding test locations

Song then concluded that smaller values of coefficient C must be used when deriving K from grain size data by downscaling the C values in the original grain size formulas. In this study the original C values have been scaled down and new values of C inevitably proposed by Song have been applied in determining K from grain size data. The new C values are as follows; 1.3×10^{-4} , 1.4×10^{-3} , 1.5×10^{-4} and $\log 500/C_u$ for Hazen, Kozeny-Carman and Beyer respectively. It must be noted that Song (2009) did not use the Alyamani method but on this study, the original value by Vukovic and Soro has been applied.

4.2.5.2 Grain size analysis

Grain size analysis was carried out only on samples collected on the riverbed since the riverbank samples were not granular, they had a lot of silt and clay. Grain size analysis was carried out using the following equipment shown in Figure 18 ; Balance, set of sieves and pan, cleaning brush and sieve shaker. Grain size analysis of soil was done in accordance to the **ASTM D-422 or D2487** standard (American Society for Testing and Materials) and Unified Soil Classification System (USCS) as both are the most widely used technical standards.



Figure 18: Equipment used for gradation

Uniformity coefficient (C_u) which is a rough measurement of the shape of gradation curve and Coefficient of curvature (C_c or C_g) were also calculated and it must be noted that;

- The smaller the value of C_u the more uniform the gradation (or the steeper the curve)
- $C_u = 1$, is the minimum possible value that indicates a material of only one size.
- A well graded soil will have C_u that is bigger than or equals to 6.
- A soil with a C_c between 1 and 3 is thought to be well graded as long as C_u is also greater than 4 for gravels and for sands.

A plot of grain size vs. percent finer was made from grain size analysis results as shown in Figure 32.

4.2.5.3 Hydraulic Conductivity determined from Permeability tests

The Permeability method was applied to core samples of the aquifer material. Even though these methods are labour consuming than the correlation methods, the uncertainties associated with estimating K from empirical formulas are avoided (Oosterbaan and Nijland, 1994). The constant head permeameter test was applied because it is used for permeable soils while the falling head is mainly used for less permeable soils ($k < 10^{-4}$ cm/s). A beaker, stopwatch, vernier calipers, 2 porous stones, Permeameter, filter papers, funnel, tamping device, steel ruler, flexible water tubes, graduated measuring cylinder, inflow reservoir and thermometer were the equipment used for carrying out the Permeameter test as per the ASTM D 2434 – Standard, Figure 19.



Figure 19: Constant head parameter test equipment

Hydraulic conductivity was calculated using the following modified Darcy equation:

$$K = \frac{QL}{Ath} \quad (17)$$

Where K= Hydraulic conductivity (m/day)

Q = volume of discharge (m³/s)

L = length of specimen (m)

A = cross-sectional area of permeameter (m²)

t = time for discharge in seconds

h = hydraulic head difference across length L , in m of water; or it is equal to the vertical distance between the constant funnel head level and the chamber overflow level.

In appendix D, the data for calculating K from permeameter test has been appended.

4.2.5.4 Hydraulic Conductivity determined from Slug test

This method is a small scale insitu field method carried out on the Motloutse riverbed. Song (2009) highlighted the limitation of laboratory methods being that the original sediment structure of samples is disturbed during sampling and therefore they do not represent the actual K and directional K so an insitu method was carried out.

The slug test method entails observing the rate of drawdown of the raised head after the application of water has been stopped. The method is of course based on Darcy's law and is referred as 'unsteady state permeameter method or modified inverted auger hole method (Bouwer and Jackson, 1974). In general, the results of small-scale methods are more valuable in shallow aquifers such as the Motloutse than in deep aquifers (Oosterbaan and Nijland, 1994) and were carried out as follows.

- A one metre PVC tube was pressed vertically into the aquifer until the slots in the tube were submerged under the water level
- The tube was submerged up to 24cm under the water level with 76cm remaining over the water table.
- Sufficient water was then poured into the tube until it reached top of the tube and this is to ensure the saturation of a large area of the aquifer around and below place of measurement.
- Time taken for the head to fall or attain initial water level was recorded.

K from Slug test was estimated using equation 18 after Masvopo et al (2008) as follows;

$$K = \frac{Q}{Ai} = \frac{[\pi R^2 h]}{T[2\pi RH + \pi R^2]} \quad (18)$$

Where K= Hydraulic conductivity (m/day)

Q= Discharge (m³/day)

A= Cross sectional area of soil sample (m²)

i= hydraulic gradient (which equals 1 as Kz; i=1)

R=radius of tube (m)

T= Time taken for water column to attain initial water level (day)

H= Length of PVC tube under the water level (m)

Note that since the tube had perforations in its lower section infiltration occurs both through the bottom and the sidewalls of the tube. Hence we have $A = \pi r^2 + 2\pi rh$.

In all cases above, K was calculated as geomean to keep the average from being affected by erroneous extreme values.

4.3 HYDROCHEMISTRY

4.3.1 General

Groundwater quality evaluation is fundamental in groundwater potential assessment as the suitability of groundwater for domestic, irrigation and industry use is based on its chemical and physical aspects. Analysis of hydrochemical parameters in groundwater aids in the apprehension of hydrogeological conditions such as the chemical and biochemical interaction between groundwater and the geological materials through which groundwater flows (Freeze and Cherry, 1979).

In order to understand the groundwater quality of the Motloutse alluvial aquifer, representative water samples were collected from different locations of the study area from both the surface water and groundwater. During sampling some physical and chemical water quality parameters such as temperature, electrical conductivity (EC), Total Dissolved Solids (TDS) and pH were measured in situ.

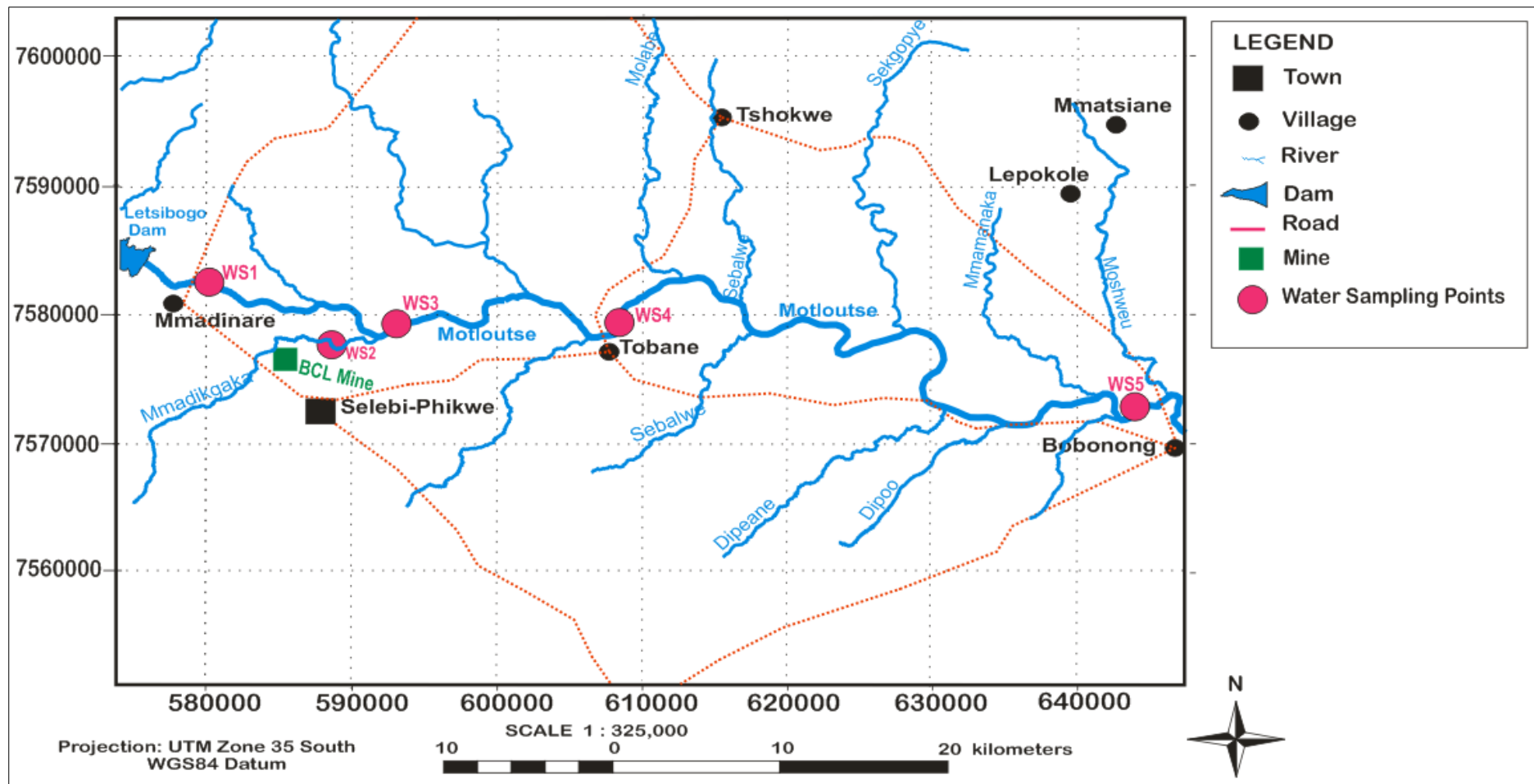


Figure 20: Locations of water sampling points.

4.3.2 Water Sampling and Analysis

Water samples were collected at different points along the Motloutse River upstream and downstream of the BCL mine tailings dump. This was done in order to assess the effect of the mine on the water chemistry of the alluvial aquifer. Based on this configuration, five water samples were collected along the Motloutse river in Mmadinare, Tobane, Bobonong, Letlhakane-Motloutse river confluence near Selibe Phikwe and lastly near the BCL tailings dam. The water sampling points were designated as follows:

- ❖ Sample WS1 was collected in Mmadinare from a hand dug well. This water sampling point is located about 15 kilometers westwards before the BCL mine as shown in Figure 20 .
- ❖ WS2 was sampled near the BCL mine tailings dam from the Motloutse River. The water sampling point is located after the BCL mine.
- ❖ Sample WS3 was collected in the Letlhakane-Motloutse rivers confluence from the river after the BCL mine.
- ❖ In Tobane sample WS4 was amassed from a hand dug well. As shown in the figure 1the sampling point is approximately 20 kilometers after the BCL mine.
- ❖ Water sample 5, (WS5) was collected in Bobonong from a hand dug well. The water sampling point is the farthest away after the BCL mine; it is located almost 60 kilometers east of the mine.

Two of the five samples collected were surface water from the BCL mine tailings dam and the rest of the samples were from hand dug wells. WS1 is sampled before the mine and the rest of the samples after the BCL mine to evaluate the impact of the mine releases on the Motloutse alluvial aquifer. The water samples were collected into new screw-cap, high density polyethylene

bottles and sent to the DGS laboratory for chemical analysis. The samples were analyzed for major cations, anions and also for some trace elements and the result is given in appendix C.

Physical parameters as above were collected onsite using a portable, calibrated TDS meter.

The accuracy of water analysis data is estimated using balance error given by the following equation (Domenico and Schwartz, 1998) and the balance error is expressed in percentage.

$$\text{Where, E.N (\%)} = \left[\frac{(\text{sum cations}, (\frac{\text{meq}}{\text{L}})) - \text{sum anions}, (\text{meq/L})}{(\text{sum cations}, (\frac{\text{meq}}{\text{L}})) + \text{sum anions}, (\text{meq/L})} \right] * 100 \quad (19)$$

As a general rule, the charge balance error should be within 5% of zero using equation 19, although in most cases the error will be less than 1 or 2% if good field and lab procedures are followed. If the charge balance is outside 5%, it could mean one of several things: (1) problems with field measurements (e.g., alkalinity), (2) problems with the lab analysis (e.g., poor standardization or failure to correct the results for laboratory dilutions), (3) incorrect assignment of the charge for one or more of the major solutes or, (4) the list of compounds that were analyzed was incomplete.

All the water samples analyzed in the study area are within the limit of acceptable error (< 5%) and used for the purpose of data processing and interpretation.

4.3.3 Unstable Chemical and Physical Parameters

Properties of groundwater evaluated in a physical analysis include temperature, color, odor, and taste. Temperature (T°), Electrical Conductivity (EC), Total Dissolves Solids (TDS) and pH were measured in situ during the field investigation period.

4.3.3.1 Temperature

Water temperature is considerably important in water quality as it alters dissolved oxygen values, which refers to the weight or volume of oxygen dissolved in water. The solubility of a gas in water decreases as the water temperature increases, so warmer water simply holds less oxygen. Temperature also plays a significant role in affecting the various physical and chemical parameters such as alkalinity, salinity, electrical conductivity, pH and even its taste.

4.3.3.2 Color, Taste and Odor

Color in groundwater may be due to mineral or organic matter in solution and is reported in mg/l by comparison with standard solutions. Taste and odor can originate from natural inorganic and organic chemical contaminants and biological sources or processes. Water was smelt in the field immediately after sampling and tasted in the lab after determining its portability explained in the coming sections. These characteristics are subjective sensations that can be defined only in terms of the experience of a human being.

4.3.3.3 pH

The pH of natural water is a useful index of the status of equilibrium reactions in which the water partakes (Hem, 1985). The balance of positive hydrogen ions (H^+) and negative hydroxide ions (OH^-) in the water determines how acidic or basic the water is. Drinking water with a pH value of between 6.5 and 9.5 is generally considered as acceptable (BOBS, 2009).

4.3.3.4 Total Dissolved Solids (TDS) and Electrical Conductivity (EC)

One basic measure of water quality is the Total Dissolved Solids (TDS), which refers to any minerals, salts, metals, anions or cations dissolved in water. This includes anything present in

water other than the pure water molecule and suspended solids expressed in milligrams per liter (mg/l).

Several processes such as groundwater percolation through rocks, waste disposal concentration or concentration by evaporation may cause an increase in TDS content when the rocks contain soluble mineral matter (Karanth, 1987). Fetter (2001) summarized that more than 90% of the total dissolved solids in groundwater can be attributed to eight ions, Na^+ , K^+ , Ca^{2+} , Mg^{2+} , Cl^- , CO_3^{2-} , HCO_3^- , and SO_4^{2-} and are usually present at concentrations greater than 1 mg/l.

Electrical conductivity (EC) of water is a measure of the ability of water to conduct electricity. This depends on its dissolved constituents and in practice EC is often expressed in terms of milli Siemens per centimeter (mS/cm) and micro Siemens per centimeter ($\mu\text{S/cm}$). The TDS and the EC are in a close connection that the more salts are dissolved in the water, the higher the electric conductivity. Table 7 shows a classification of water based on TDS content.

Table 7: Classification of water based on TDS (Freeze and Cherry, 1979)

Class	TDS(mg/l
Fresh water	0-1,000
Brackish Water	1,000-10,000
Saline Water	10,000-100,000
Brine Water	More than 100,000

4.3.4 Water type Classification

Determining water type based on various physical and chemical parameters is crucial to evaluate its suitability for domestic, irrigation and industry uses. The water type in the study area classified based on the following chemical parameters, which were determined at the field and in the laboratory.

- Hardness

- Total Dissolved solids(TDS) and Electrical conductivity (EC)
- Major cations and anions

4.3.4.1 Hardness

Hardness of water is defined as its content of metallic ions which reacts with sodium soaps to produce solid soaps or scummy residue and which react with negative ions forming solid boiler scale (Camp, 1963). It is predominantly caused by divalent cations such as calcium, magnesium, alkaline earth metal such as iron, manganese, strontium, etc. It is a water quality indication of the concentration of alkaline salts in water, mainly calcium and magnesium. Hardness is normally expressed as the total concentration of Ca^{2+} and Mg^{2+} as milligrams per liter equivalent CaCO_3 . The total hardness is defined as the sum of calcium and magnesium concentrations, both expressed as CaCO_3 in mg/l (Hiscock, 2005). It can be determined by substituting the concentration of Ca^{2+} and Mg^{2+} , expressed in milligrams per liter, in the expression

$$\text{Total Hardness} = 2.5 (\text{Ca}^{2+}) + 4.1 (\text{Mg}^{2+}) \quad (20)$$

Each concentration is multiplied by the ratio of the formula weight of CaCO_3 to the atomic weight of the ion; hence the factors 2.5 and 4.1 are included in the hardness relation. Sawyer and McCarty (1967) derived a hardness classification system as in Table 7 which depends on the concentration of calcium carbonate.

Table 8: Hardness classification of water (after Sawyer and McCarty, 1967)

Hardness rating	Concentration of Calcium Carbonate (mg/l)
Soft	0 -75
Moderately hard	75 - 150
Hard	150- 300
Very hard	300 and greater

4.3.4.2 TDS and EC

Categorizing and classifying water based on percentage composition of major cations and anions is paramount. To classify and categorize water on the basis of these criteria, a systematic graphic presentation is essential such as Durov plots. The major cations and anions species in most natural waters and are plotted on this diagram are Na^+ , K^+ , Ca^{2+} , Mg^{2+} , Cl^- , CO_3^{2-} , HCO_3^- , and SO_4^{2-} (Figure 35 and Figure 37).

4.3.5 Metal Concentrations

Due to the presence of copper-nickel mine in the study area, analysis of metal concentrations is therefore of great importance. Eleven metal elements were tested in the water samples namely: Aluminum, Barium, Chromium, Copper, Iron, Manganese, Nickel, Lead, Strontium, Vanadium and Zinc. Out of these eleven metals three were not detected in all water samples and those detected are displayed in Figure 37.

4.3.6 Water Quality

In specifying the quality characteristics of water, chemical, physical and biological analyses are normally required (Todd, 1980). Therefore to decide a certain water to be fit for a certain purpose, its physical, chemical and biological qualities has to be determined and compared with different water quality standards of the country though the standards range vary from place to place and from country to country. In this research, the water qualities of Motloutse alluvial aquifer are compared with water quality standards of World Health Organization (WHO, 1993) and Botswana Bureau of Standards (BOBS 32:2009).

4.3.6.1 Water Quality for Irrigation Purpose

Water quality for agricultural purposes is determined on the basis of the effects of the water on the quality and yield of the crops, as well as the effects on drainage efficiency and characteristic changes in the soil (Richards, 1954; Wilcox, 1955).

The quality standards for irrigation water are based on:

1. Total dissolved solids which may affect the intake of water and other nutrients by plants through osmosis;
2. the relative concentration of alkalis and alkaline earths which affect the soil texture due to cation exchange, and thereby its permeability and drainage characteristics; and
3. The concentration of specific ions, viz. boron, selenium, cadmium etc., which are toxic to the growth of plants beyond certain levels.

4.3.6.2 Salinity

A salinity problem exists if salt accumulates in the crop root zone to a concentration that causes a loss in yield. Yield reductions occur when the salts accumulate in the root zone to such an extent that the crop is no longer able to extract sufficient water from the salty soil solution, resulting in a water stress for a significant period of time. The critical salt concentration in the irrigation water depends upon many factors. However, amounts in excess of 700 ppm are harmful to some plants, and more than 2000 ppm is injurious to all crops (Garg, 1987).

The salt concentration is generally measured by determining the electrical conductivity of water. The primary effect of high EC water on crop productivity is the inability of the plant to compete

with ions in the soil solution for water. The higher the EC, the less water is available to plants, even though the soil may appear wet.

4.3.6.3 Infiltration problems

An infiltration problem related to water quality occurs when the normal infiltration rate for the applied water or rainfall is appreciably reduced and water remains on the soil surface too long or infiltrates too slowly to supply the crop with sufficient water to maintain acceptable yields. Although the infiltration rate of water into soil varies widely and can be greatly influenced by the quality of the irrigation water, soil factors such as structure, degree of compaction, organic matter content and chemical make-up can also greatly influence the intake rate.

The two most common water quality factors which influence the normal infiltration rate are the salinity of the water and its sodium content relative to the calcium and magnesium content. High salinity water will increase infiltration. Water with high sodium to calcium and magnesium ratio will decrease infiltration, because sodium reacts with soil to reduce its permeability. When sodium-rich water is applied to soil, some of the sodium is taken up by clay; the clay gives up calcium and magnesium in exchange which can alter the physical characteristics of soil.

Therefore before applying certain water for irrigation purpose, knowing its sodium concentration is paramount.

The sodium content can be expressed in terms of percent sodium (sodium percentage) defined by

$$\%Na = \frac{(Na+K)}{(Ca+mg+Na+K)} * 100 \quad (21)$$

Where all the concentrations are expressed in milli equivalent per liter.

The sodium hazard in irrigation water can also be expressed by determining the Sodium Adsorption Ratio (SAR) by the relation;

$$SAR = \frac{Na^+}{\sqrt{\frac{Ca^{2+} + Mg^{2+}}{2}}} \quad (22)$$

Where all the concentration are expressed in milli equivalent per liter after Richards, 1954.

Accordingly to evaluate the suitability of water of Motloutse alluvial aquifer for irrigation purpose; EC and Sodium content in terms of percentage and SAR value have to be determined. Based on these criteria, the suitability of water for irrigation purpose of Motloutse alluvial aquifer will be determined and compared with the standard values in Table 9 (Todd, 1980).

Table 9: Water quality classification for irrigation.

Water class	%Na	SAR	EC(mS/cm)
Excellent	<20	<10	<250
Good	20-40	10-18	250-750
Permissible	40-60	18-26	750-2000
Doubtful	60-80	>26	2000-3000
Unsuitable	>80		>3000

(Source: After Todd, 1980).

4.4 GROUNDWATER MODELLING

4.4.1 General

Groundwater models represent hypothetical flow situations providing generic understanding of the flow system behaviour (Anderson and Woessner, 1992).

Groundwater modelling was undertaken using a three dimensional groundwater flow code, MODFLOW (McDonald and Harbaugh, 1988). Visual MODFLOW, a proprietary product of Waterloo Hydrogeologic Inc. (2005), was employed as it is a groundwater flow modelling standard used by government agencies and consulting firms as it is effective, ideal for small-scale modelling of sites and due to its dynamic usage (Fetter 1994; Fetter 2001; Hughes et al., 2010). This modelling code solves the general governing equation which is partial difference equation describing the three-dimensional movement of groundwater in unconfined aquifers. (Anderson & Woessner, 1992);

$$\frac{\partial}{\partial x} \left(K_x \frac{\partial h}{\partial x} \right) + \frac{\partial}{\partial y} \left(K_y \frac{\partial h}{\partial y} \right) + \frac{\partial}{\partial z} \left(K_z \frac{\partial h}{\partial z} \right) = S_s \frac{\partial h}{\partial t} \quad (23)$$

Where

K_x, K_y, K_z -are directional components of hydraulic conductivity assumed to be parallel to the major axis of hydraulic conductivity

S_s -Specific storage of porous material

h –is the potentiometric head

t –time

4.4.2 Previous Modelling

Mott McDonald (1990) in his study of Motloutse Dam feasibility modelled the Motloutse for the purpose of assessing the downstream impacts of upcoming Letsibogo dam construction on the sand river resource. He constructed two steady state groundwater models covering a 58 km reach from the dam site to around 20km downstream of Tobane. BCL mine flows near the Letlhakane confluence measured in the order of 10 000 m³/day. At this point the sand river aquifer is fully recharged with minute surface flow for some distance. A separate steady state evaporation modelling exercise using full cross sections by Wikner (1980) were used to assess evaporation losses. A back water energy balance method was employed to estimate surface water flow and Darcy's law to calculate groundwater flow across successive cross-sections.

An evaporation loss of 6l/s/km was found and by comparison with results from an investigation of combined losses due to evaporation and seepage along 17km downstream of Selibe Phikwe it was concluded that subsurface evaporation was dominant over surface evaporation and ET and accounting for all significant losses along the reach. A daily water balance model was developed for the entire reach. The model consisted of 70 cells and since in some areas they were no cross-sections, a general cross-section was developed and applied throughout the river reach covered by the model. Run off from each sub-catchment was estimated and local population abstractions for village supply and irrigation applied. Model Calibration was done using 81/82 measured groundwater levels which was the driest year on record.

The simulated groundwater levels were within 0.3 & 0.8 of observed water levels for wet & dry seasons, respectively. An explanation for this residual was that the observed water levels were not referenced to the lowest point of the riverbed. The main gradient of water decline was well depicted suggesting no significant quantities of water are lost to riverine vegetation. The Dam

effect was simulated by running the model without Letsibogo catchment, that is the catchment area upstream of dam and comparing this to the previous run. Major variations in groundwater levels were observed immediately downstream and gradually reducing and terminated at Letlhakane confluence. This demonstrated that drawdown effect becomes negligible after a few kilometres. A 3 year drought was simulated resulting in a maximum water decline of 0.15m in groundwater levels and supported by local population that groundwater was still available in the sand river following a recent drought tapped through shallow wells. It was also shown that direct rainfall was the main recharge regime and aquifer is fully recharged at the end of wet season.

Department of Lands (1998) modelled five target areas to evaluate the effect of proposed abstraction schemes on the groundwater resource. Time-variant inflows & outflows were used in determining the availability of groundwater during a day season only therefore rainfall & runoff were omitted from the model. Majority of input data was acquired from previous reports. Due to river floods preventing construction of long-term monitoring structures in the sand aquifer the model was not calibrated. However the modelling was still considered to be feasible and an 8 month period transient model was developed broken into monthly stress period.

A processing Modflow (PMWIN) was employed using a single layer model. Target areas ranging from 2-6 km were modelled. Injection and drains were used to simulate upstream inflow and downstream outflow, respectively. Abstractions were simulated using well package in PMWIN for irrigation based on highest consuming crop pattern. The model was initially run without abstractions to verify the reasonability of the simulation; once a reasonable model was achieved the groundwater abstractions were then introduced into the model. Maximum sustainable rates were determined per target area for monthly periods.

5.0 RESULTS AND DISCUSSION

5.1 GEOPHYSICS RESULTS

5.1.1 Interpretation

Processed radargrams of all profiles are shown in the following figures (Figure 21 -25) through *Reflex 2D* which is a software package with processing capabilities.

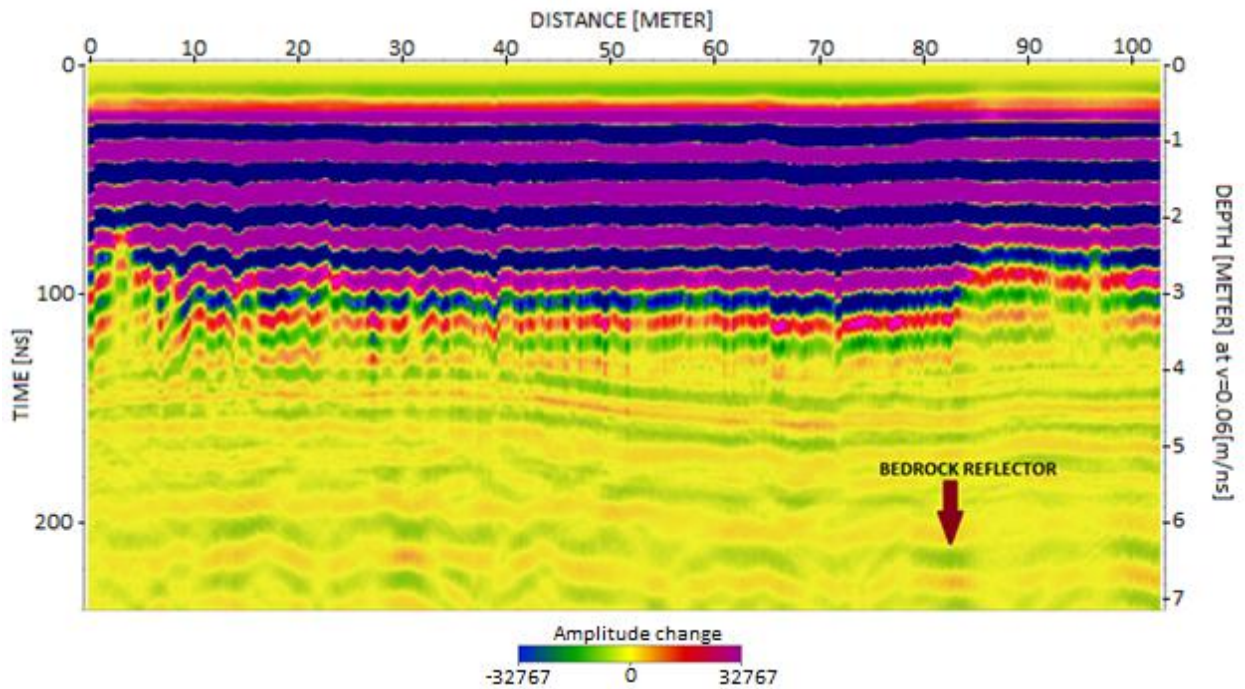


Figure 21: Reflex 2D software Processed radargram for first profile.

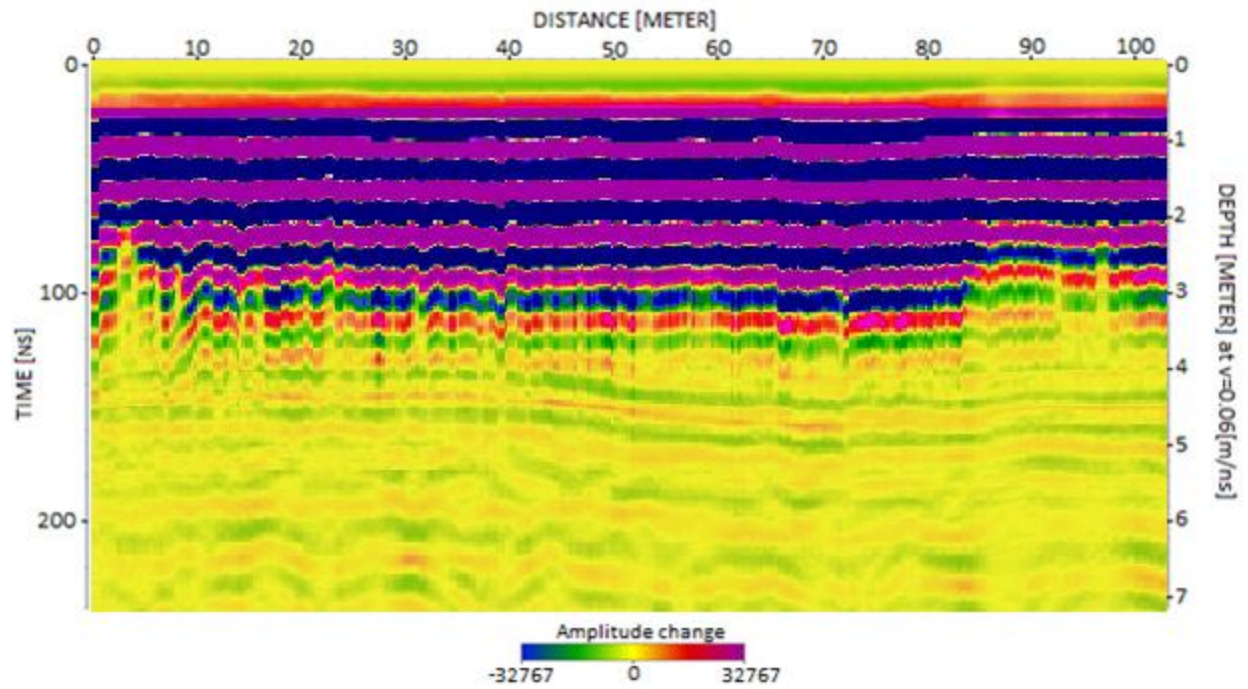


Figure 22: Reflex 2D software Processed radargram for second profile.

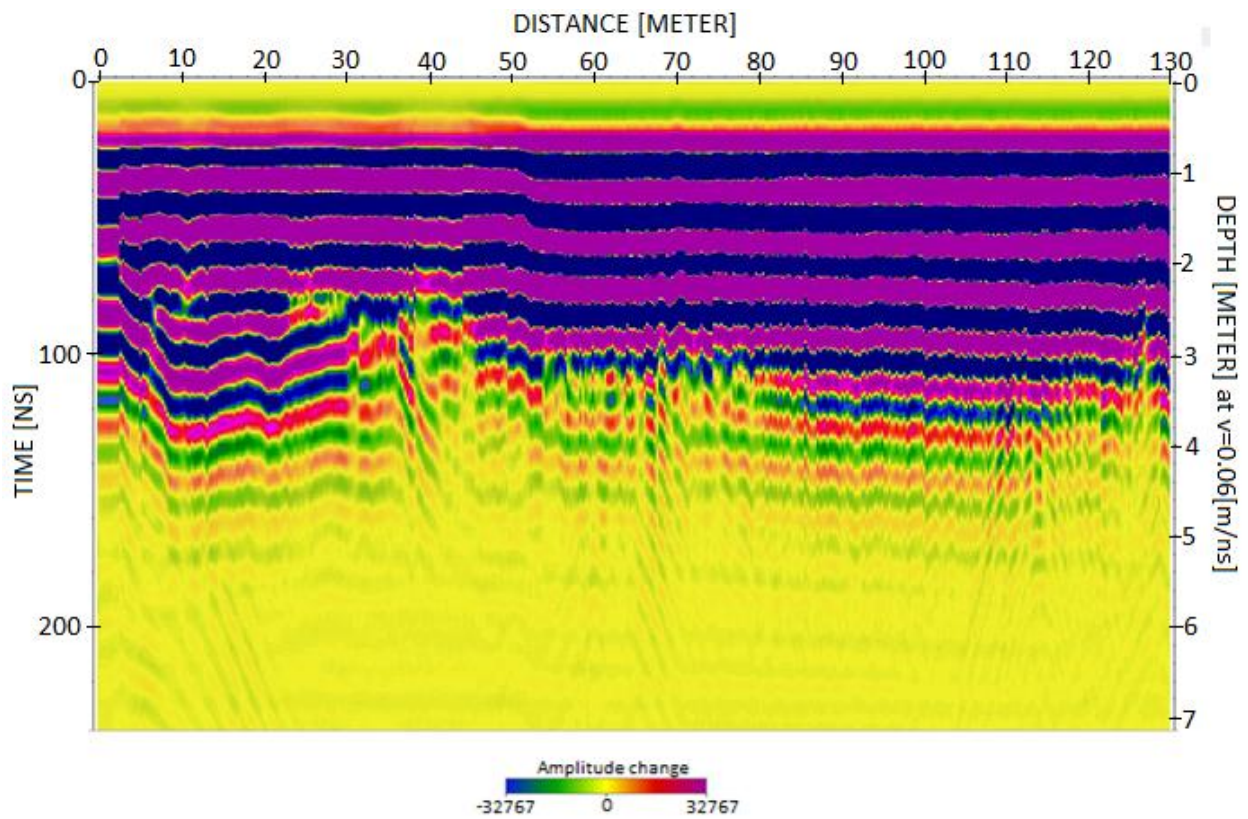


Figure 23: Reflex 2D Processed radargram for third profile.

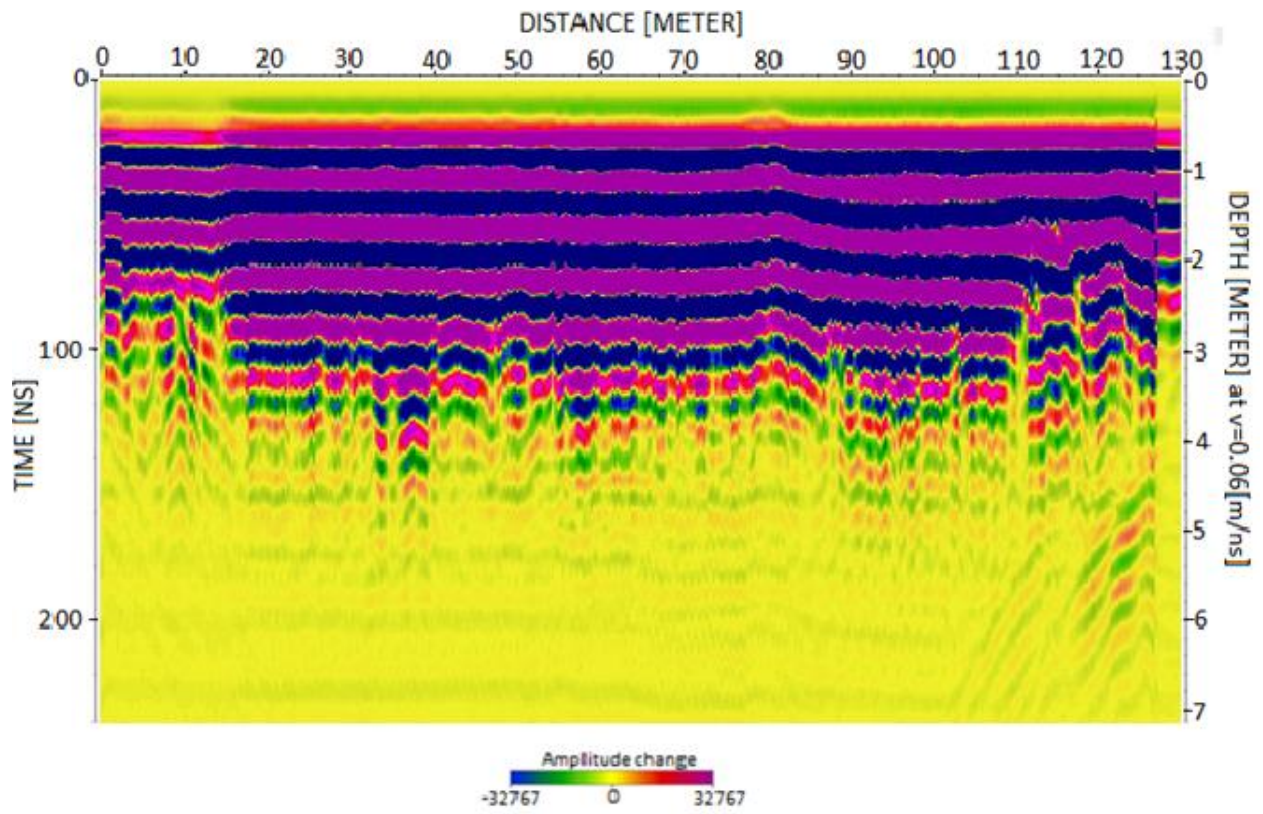


Figure 24: Reflex 2D Processed radargram for fourth profile.

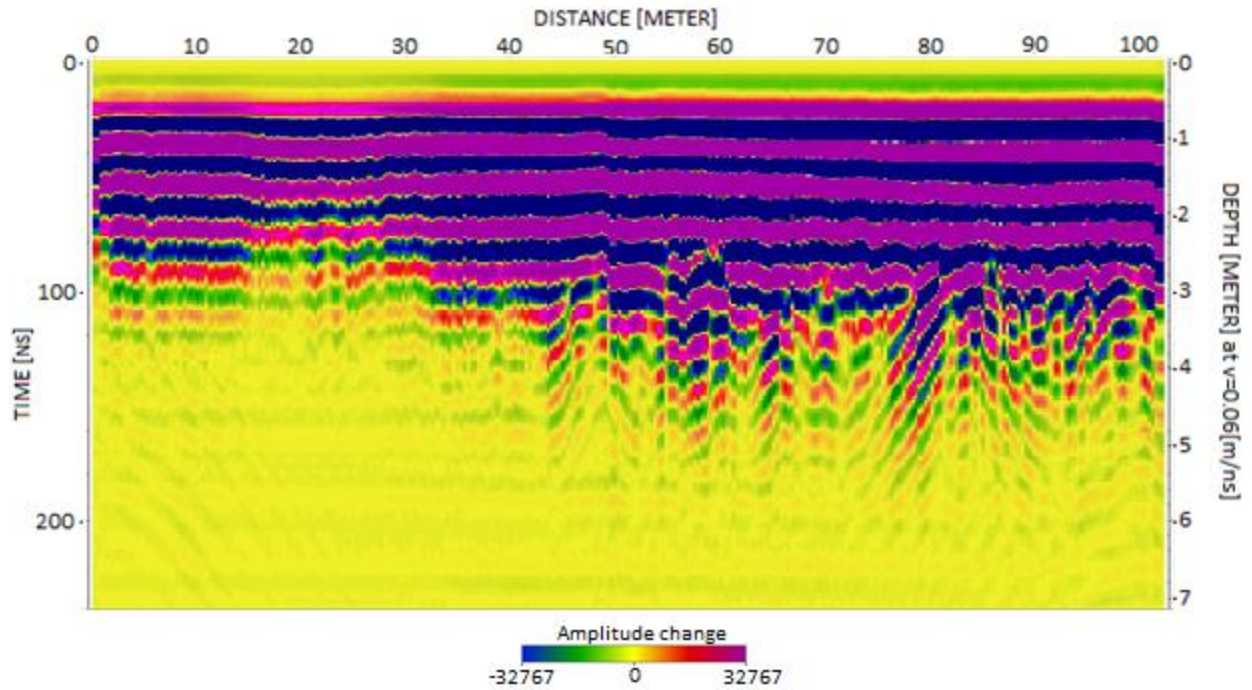


Figure 25: Reflex 2D processed radargram for the fifth profile

The radargrams are generally the same and have been interpreted as follows;

The first reflections are a characteristic airwave and groundwave, respectively. The very first reflection that is to the left on all the radargrams is caused by the direct electromagnetic wave interaction with air as can be seen in Figure 26 and Figure 27 .

The groundwave is represented by black, continuous reflection amplitudes that form a very straight, horizontal solid bar as on Figure 26 and the first reflection to the right in Figure 27. Below the groundwave reflection is the unsaturated zone of the sediment, interpreted as the unsaturated sand.

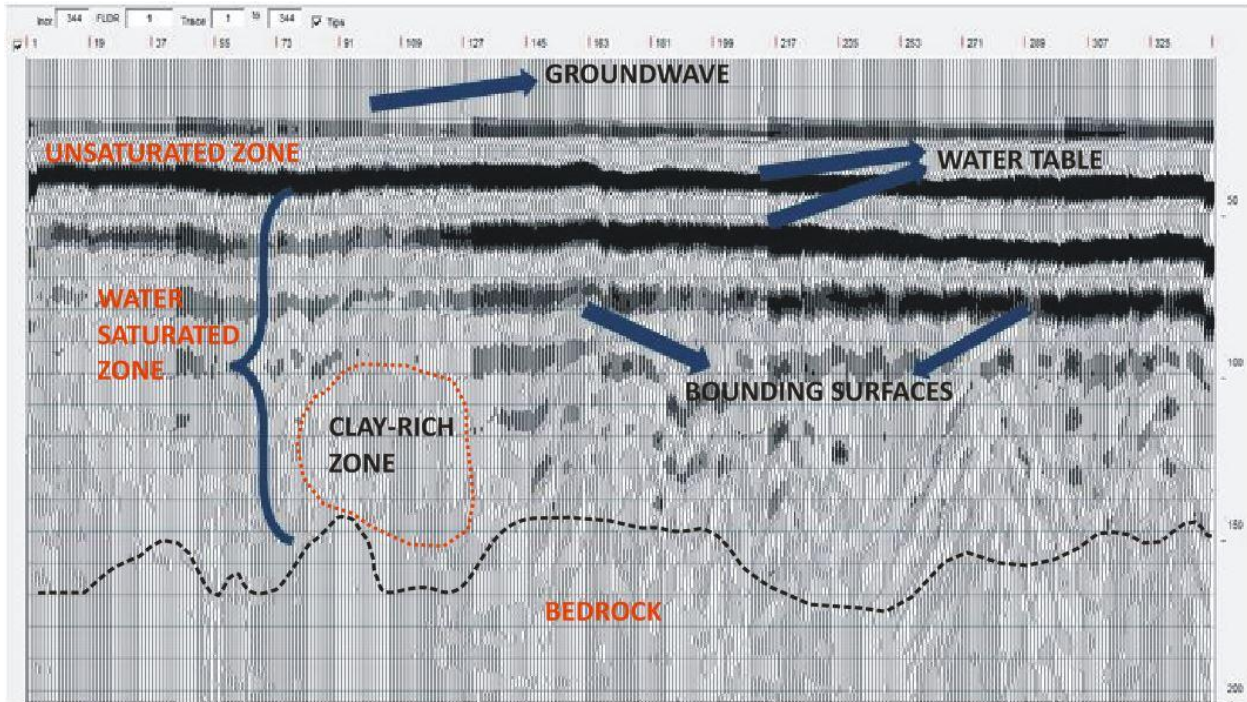


Figure 26: SUNT processed and interpreted radargram in wiggle form showing the aquifer stratigraphy.

The next two or three prominent, high amplitude reflections that are easily identified and traced across all the radar records are interpreted as the water table (Figure 26). This is because in sediments, the water content primarily causes the changes in dielectric properties (Annan et al, 1999). A change from dry to wet sand results in a change from a three- phase system (air, water and sediment) to a two- phase system (water and sediment) in which other factors apart from porosity control the dielectric properties (Van Dam et al, 2000). In addition, this transition usually changes the amplitude and polarity of the signals in Figure 27 where the water table gives the largest amplitude to the right (Woodward et al, 2003).

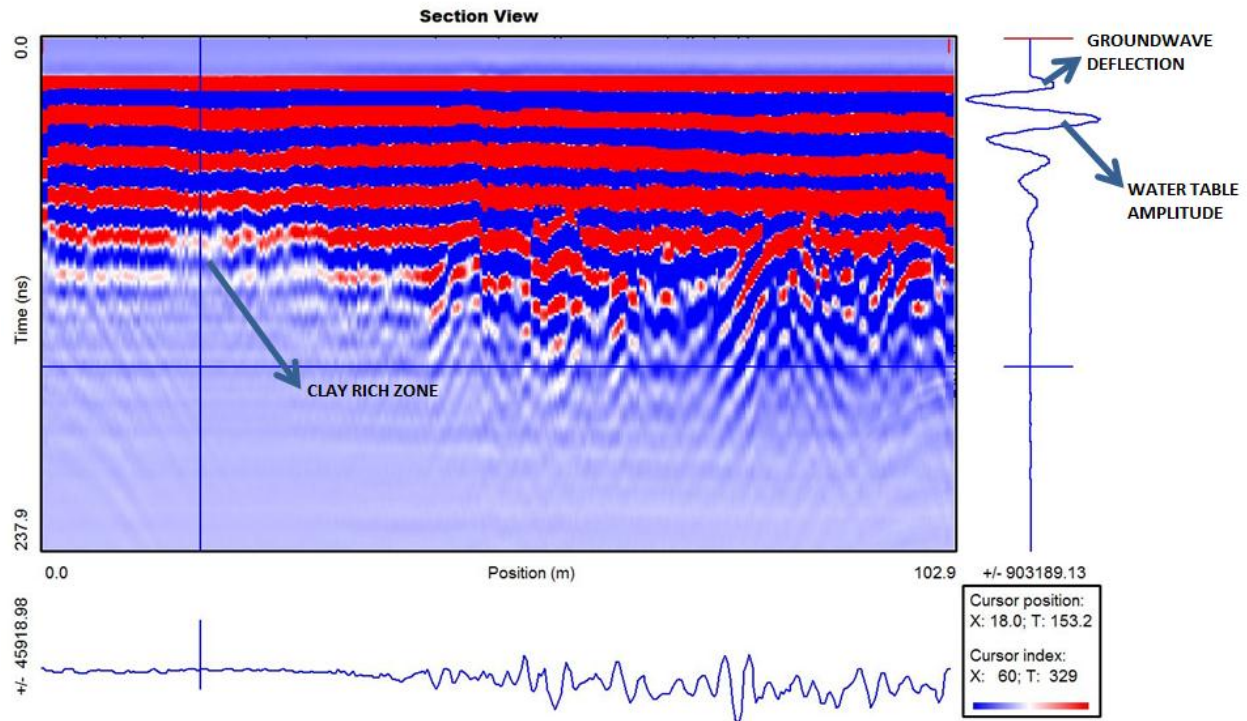


Figure 27: A single trace wavelet alongside a radargram showing the amplitude of the wavelet in response to the heterogeneity of the aquifer.

A transitional zone that is partially saturated to saturated with water known as the capillary fringe occurs above the water table. In coarse textured soils the capillary fringe is narrow and dielectric properties between the unsaturated and saturated zones is abrupt and contrasting leading to a distinguishable reflection of the water table in radargrams which normally appears as a series of 2-3 bands due to oscillations in the reflected radar pulses (Doolittle et al, 2006).

The next reflections after the water table are generally weak in all the radargrams (Figure 26 and Figure 27) and this can be due to many factors. Conyers (2004) affirms that the water content often increases with depth resulting in attenuation of radar waves with increasing depth. These reflections are thus suggested to be bounding surfaces between two sand layers of different periods of deposition.

A portion of almost no reflections can be observed in radargrams from at trace 91-127 at depth of 100ms (Figure 26) is interpreted as a clay rich zone because clays are highly conductive and this conductivity is increased when they are wet resulting in almost complete attenuation of the wave.

In most radargrams; low, right and oftentimes left dipping reflections are observed at the beginning and ending of the radargrams, or simply at the river banks as deduced from the horizontal distance scale (Figure 29). This are interpreted as bounding surfaces between differing lithologies of sand, silt and clays that expected at the banks due to differences in density and grain size (Shenk et al 1993; Harari, 1996).

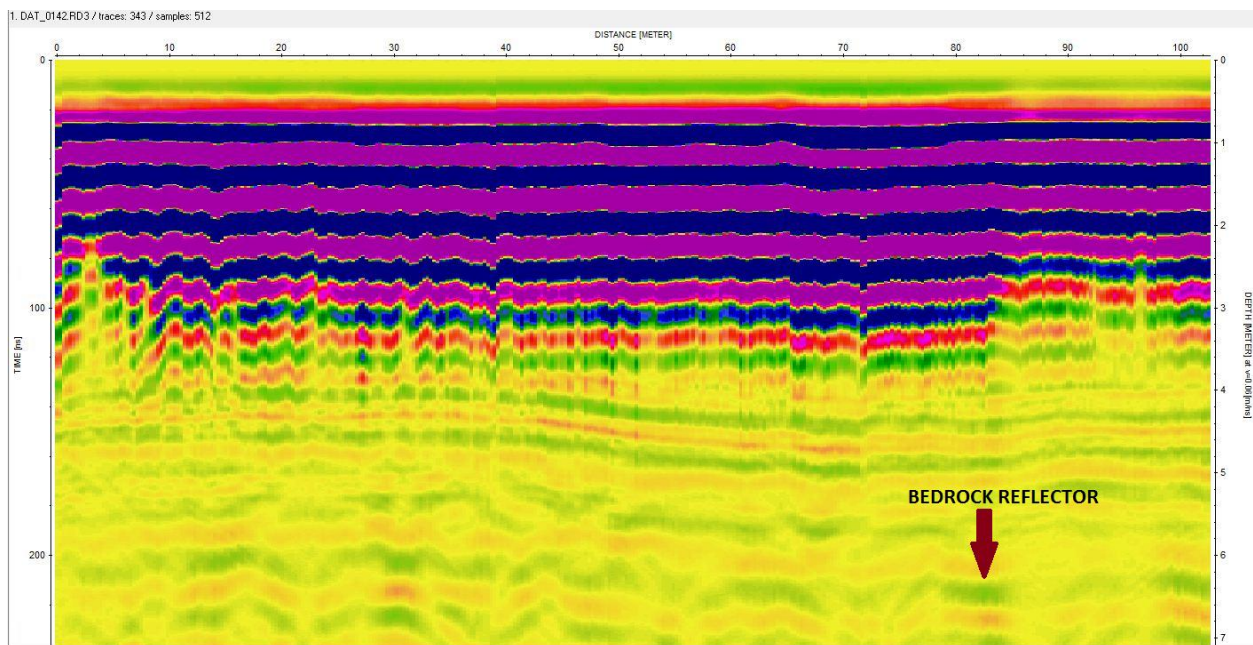


Figure 28: Bedrock reflector in the first profile line.

Below these reflections, no further reflections are observed in wiggle form in most radargrams as in Figure 26 suggesting a marked change in reflective characteristics. This is interpreted as an interface between the channel fill and the bedrock because at the resolution used, radar signals

will not be able to penetrate the granite bedrock; the dotted line represents the outline of the inferred bedrock. However, in some radargrams as in Figure 28 the bedrock reflector can be seen.

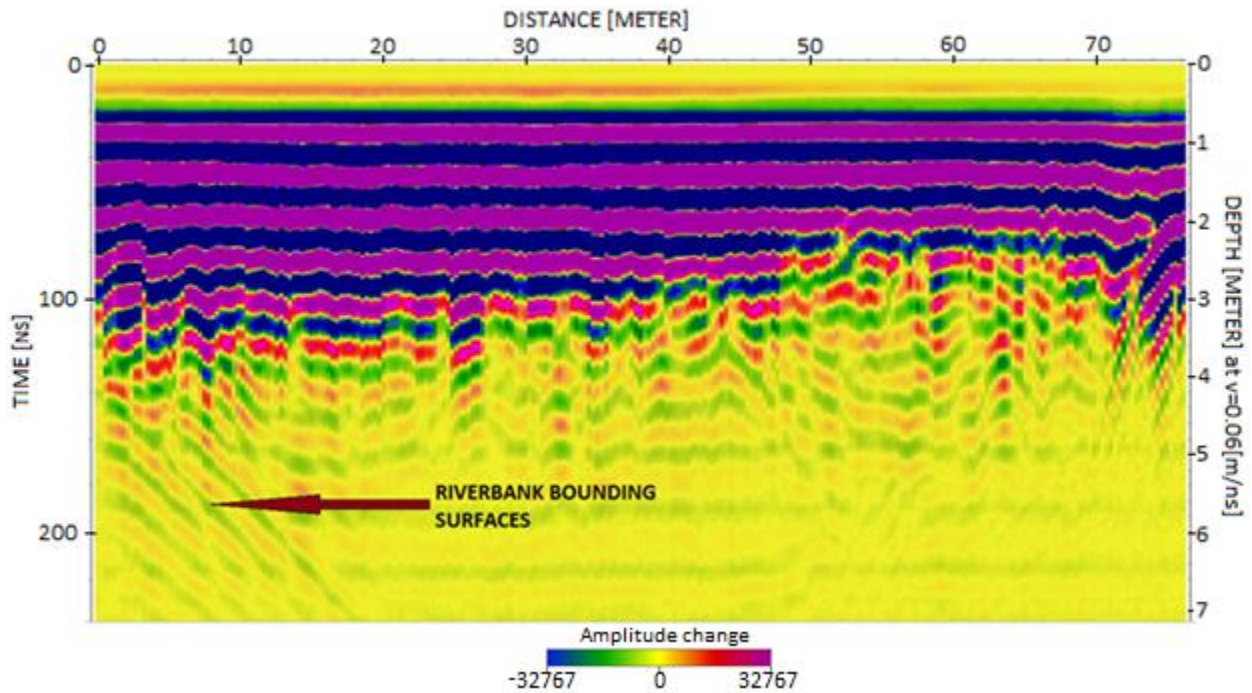


Figure 29: Radargram depicting riverbank bounding surfaces common in most radar records.

The average depth of the water table from the sand surface deduced from *Reflex 2D* software with velocity set at 0.06m/ns for saturated sands after (Daniels ,2004) is 0.8m at Tobane sites with an error of 0.2m (Bentley and Trenholm 2002).

Average depth to the bedrock deduced from radargrams is 6.0m with an error of 0.5m due to uneven bedrock and sand surfaces. The acquired depths from the GPR profiles have been contoured (Figure 30) and areas of deeper alluvium have been deduced from GPR. The sand

river formations and depth to bedrock have been resolved successfully as depicted in a schematic cross section (Figure 31).

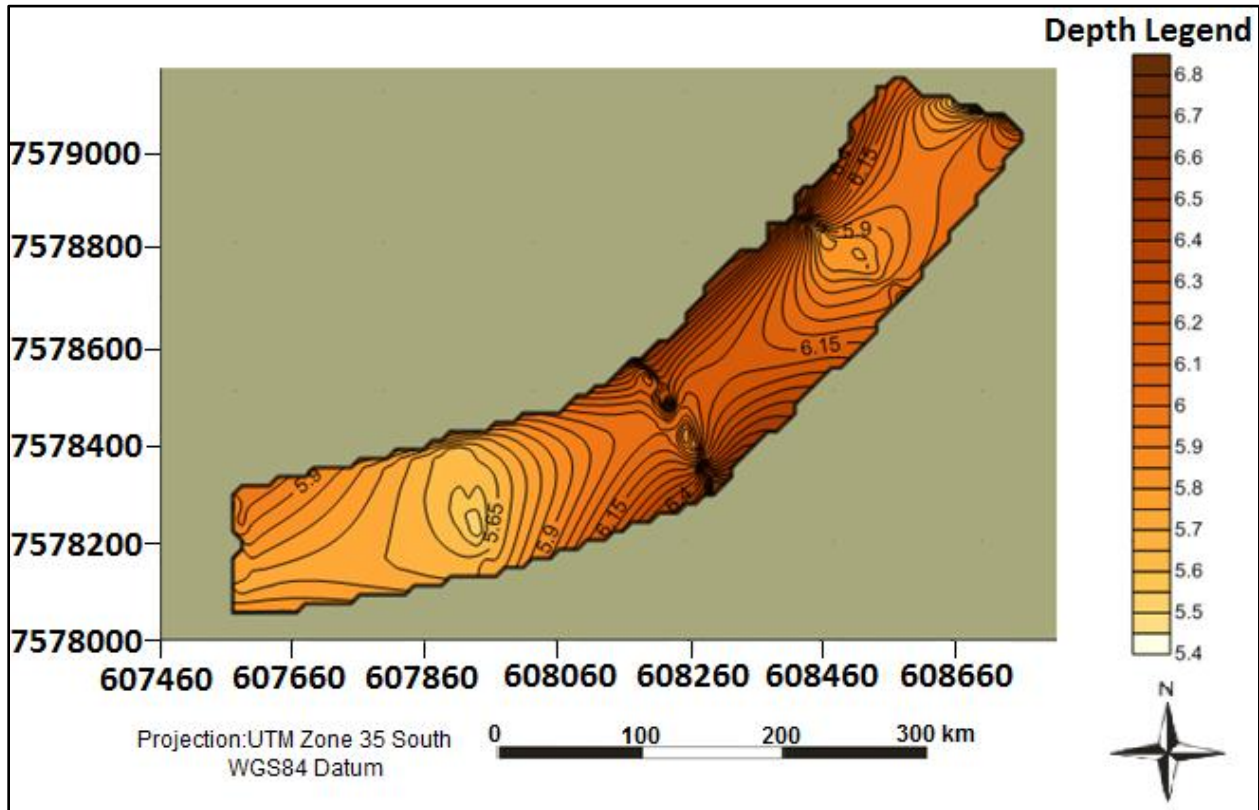


Figure 30: Motloutse sand depth to bedrock contour map.

The GPR results obtained match or corroborate with the augering findings. As earlier noted from augering observation the sand was much thicker than 3.5m for sure and about 6-7m in thickness. Based on water strikes the water levels seem to be a bit shallower from those in GPR interpretations because at the time of augering it was already rainy season and as a matter of fact it had rained on the previous day leading to the field excursion resulting in the aquifer being replenished.

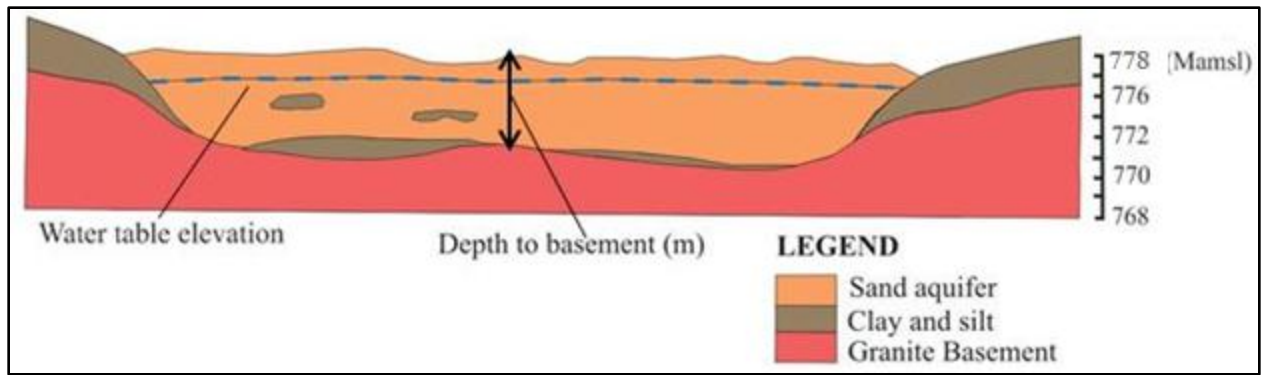


Figure 31: Schematic cross section of Motloutse alluvial aquifer.

5.2 AQUIFER MATERIAL PROPERTIES ANALYSIS

5.2.1 Porosity

Porosity was one of the aquifer media characteristics studied for the Motloutse Alluvial Aquifer.

Measured porosity values for samples taken in the river reach of the alluvial aquifer are summarized in Table 10 and Table 11 for Method 1 and Method 2 respectively.

Table 10: Method 1 of determining Porosity

Sample ID	Volume in measuring cylinder (ml)	Volume remaining in cylinder (ml)	Volume of voids (ml)	Volume of Beaker (ml)	Porosity
S1-1	100	28	72	200	36
S1-2	100	34	66	200	33
S1-3	100	32	68	200	34
S1-4	100	28.5	71.5	200	35.75
S1-5	100	29	71	200	35.5
S2-1	100	26	74	200	37
S2-2	100	23	77	200	38.5
S2-3	100	22	78	200	39
S2-4	100	18	82	200	41

Table 11: Method 2 of determining Porosity

Sample ID	Weight of dried sample +Beaker (g)	Weight of saturated sample + Beaker (g)	Volume of voids	Volume of Beaker	Porosity
S1-1	431.83	512.44	80.61	250	32.24
S1-2	436.16	519.04	82.88	250	33.15
S1-3	432.14	516.77	84.63	250	33.85
S1-4	420.65	507.64	86.99	250	34.80
S1-5	433.36	517.23	83.87	250	33.55
S2-1	451.60	536.44	89.84	250	35.94
S2-2	459.17	541.65	87.48	250	34.99
S2-3	435.13	523.55	88.42	250	35.37
S2-4	426.96	514.19	87.23	250	34.89

Porosity determined from GPR

The porosity determined from the Ground Penetrating Radar is 0.4 with K' calculated to be 25 after using equation 3 where $c=3 \times 10^8 \text{m/s}$ and $V=6 \times 10^{-2} \text{m/ns}$. This porosity is within range of 0.25-0.5 of sand material (Freeze and Cherry, 1979).

The values from the methods used in estimating porosity are high. This high porosity values are expected for river sands and for clays, silts from riverbank samples. Nord (1985) obtained a porosity of 35% for Motloutse River sand so most the porosity values compare well with results from other studies.

5.2.2 Specific Yield

Table 12: Calculation of Specific Yield.

Sample ID	Mass of beaker + saturated sand (g)	Mass of empty beaker (g)	Mass of saturated sand (g)	Mass of beaker +drained sand (g)	Mass of drained sand (g)	Mass of water (g)	Specific Yield
S1-1	476.40	33.80	442.6	464.24	430.44	12.16	7.49
S1-2	521.07	32.65	488.42	486.65	454.00	34.42	20.09
S1-3	494.06	32.65	461.41	460.78	428.13	33.28	20.60
S1-4	452.32	33.80	418.52	434.04	400.24	18.28	12.10
S1-5	480.35	33.80	446.55	467.05	433.25	13.3	8.14
S2-1	527.38	32.65	494.73	501.62	468.97	25.76	14.56
S2-2	476.96	33.80	443.16	464.35	430.55	12.61	7.76
S2-3	501.43	33.80	467.63	476.25	442.45	25.18	5.69
S2-4	485.96	32.65	453.31	455.01	422.36	30.95	7.33

Specific gravity of sand was taken as 2.65 because river sand has the main component as quartz and this value is applicable to sands that are not packed. Table 12 shows an average specific yield of 13.68% for samples collected only on the riverbed which is low for this river section as

compared to that derived by Nord (1985) of 20% and very low for a typical sand formation which has a range of 21 to 27 (Moyce et al, 2006). This value will result in a higher groundwater estimates while the value acquired in this dissertation is low so will give a conservative estimate of the groundwater resource.

5.2.3 Hydraulic Conductivity

Particle size distribution of samples only collected on the riverbed ranges from 0.008mm to 10 mm in diameter as can be seen in Figure 32 which is a very wide range attesting to the poorly graded sand and the heterogeneous nature of the aquifer. The median (d_{50}) and effective grain diameter (d_{10}) are 1.6 and 0.4 respectively.

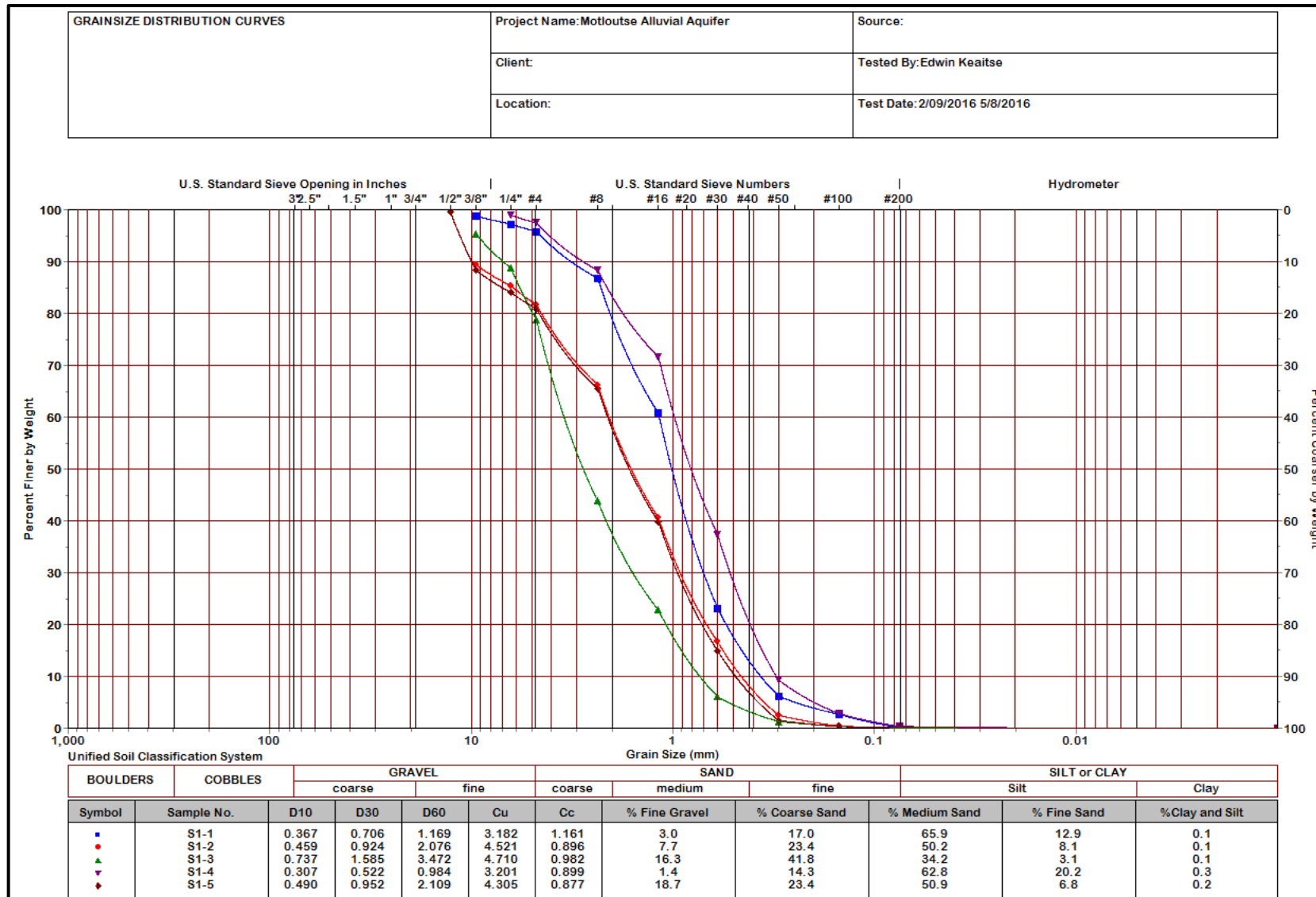


Figure 32: Grain size Distribution curve of the Motloutse

Analysis of grain size data given in appendix B according to the Unified Soil Classification System (Holtz and Kavacs, 1981) the Motloutse alluvial aquifer material is poorly graded sand with gravel as depicted in Table 13 below:

Table 13: USCS classification of aquifer material samples.

Sample ID	S1-1	S1-2	S1-3	S1-4	S1-5
Percent fines	0.14	0.1	0.1	0.3	0.2
Percent sand	95.8	81.8	79.1	97.3	81.1
Percent gravel	3	7.7	16.3	1.4	18.7
Cc	1.16	0.89	0.98	0.89	0.88
Cu	3.2	4.5	4.7	3.2	4.3
USCS classification	SP	SP	SP	SP	SP

Table 14: Hydraulic conductivity determined by different empirical formulae.

Sample ID	d ₁₀	d ₃₀	d ₆₀	Cu	Cc	n	Io	Hazen	KC	Breyer	Alyamani
S1-1	0.3	0.7	1.1	3.2	1.1	0.4	0.3	191.0	190.6	177.7	113.9
S1-2	0.4	0.9	2.1	4.5	0.9	0.4	0.3	259.5	211.2	258.6	144.8
S1-3	0.7	1.6	3.4	4.7	0.9	0.4	0.5	656.1	520.2	661.2	443.1
S1-4	0.3	0.5	0.9	3.2	0.8	0.4	0.3	133.1	131.9	124.2	89.6
S1-5	0.4	0.9	2.1	4.3	0.8	0.4	0.3	301.54	251.8	297.9	161.9
K geomean								264.9	233.6	257.1	160.4

A value of 9.80065 m/s^2 for acceleration due to gravity and kinematic viscosity value of $8.46 \times 10^{-7} \text{ m}^2/\text{s}$ derived for a water temperature of $27.4 \text{ }^\circ\text{C}$, this temperature was measured in the field and so this values were used in this study. Hazen method gave the highest hydraulic conductivity value of 264m/day. The calculated K proves that the aquifer can be fully recharged by water flowing through the sand from upstream. On the other hand this means the aquifer is vulnerable to pollution events as the point source pollutants will move rather relatively quickly through the aquifer. A higher value of K found by Nord (1985) could be expected depending on the method used and the nature of K having an error of magnitude of

orders, demonstrating the heterogeneity of the river sand typified by few isolated clay and silt lenses.

Table 15: Hydraulic conductivity from constant head Permeability test.

Sample ID	K
S1-1	106.61
S1-2	108.13
S1-3	115.50
S1-4	105.17
S1-5	114.59
S2-1	96.24
S2-2	83.57
S2-3	69.23
S2-4	61.24
K geomean	93.52

The constant head permeability test yielded an average value of 93.52m/day that is lower than that determined from empirical formulae. A temperature correction factor of 0.8696 for a water temperature of 26⁰c as measured in the lab was used to correct the hydraulic conductivity since viscosity changes with temperature (California department of transportation, 1998). A radius of 7.9cm, length of 23.6cm and head difference of 58cm were used in estimating hydraulic conductivity from constant head permeability tests.

Table 16: Hydraulic conductivity from slug test.

Sample ID	Radius(m)	h(m)	T(s)	H(m) ²	K(m/s)	K(m/d)
S1-1	0.01	0.76	21	0.24	0.000738581	63.81341108
S1-2	0.01	0.76	23	0.24	0.000674357	58.26441881
S1-3	0.01	0.76	19	0.24	0.000816327	70.53061224
S1-4	0.01	0.76	25	0.24	0.000620408	53.60326531
S1-5	0.01	0.76	22	0.24	0.000705009	60.91280148
S2-1	0.01	0.76	29	0.24	0.000166776	14.40947992
S2-2	0.01	0.76	2000	0.24	0.000378298	32.68491787
S2-3	0.01	0.76	3500	0.24	0.000534835	46.20971147
S2-4	0.01	0.76	6000	0.24	0.000143613	12.40816327
K geomean						39.44

Slug test produced a mean value of 39.4m/day, which is the lowest of all six methods used to estimate K. It can also be noted that riverbank samples have very low K's which is expected since they contain a lot of silt and clay.

5.3 HYDROCHEMISTRY RESULTS

5.3.1 Unstable Chemical and Physical Parameters

In the study area the temperature of groundwater ranges from 25.7-29.2°C and an average of 26.7 for surface water. The water is colorless, tasteless and odorless.

In the study area, all the samples have a field pH value ranging from 7.80 to 8.24 as shown in the Table 17 below, which presents a slight trend of alkaline chemical reaction within the groundwater system.

Table 17: pH values of the Motloutse water samples.

Sample code	Name of water source	pH value	Remark
WS1	Motloutse-Mmadinare	7.96	acceptable
WS2	Motloutse-Near BCL tailings dam	8.24	acceptable
WS3	Motloutse-Letlhakane river confluence	8.0	acceptable
WS4	Motloutse-Tobane	7.8	acceptable
WS5	Motloutse-Bobonong	7.90	acceptable

5.3.2 Water type Classification

The water quality indicators have been analysed to characterize the physical and biological water quality indicators. Table 18 illustrates the variation of TDS and EC values of Motloutse water samples and their classification.

Table 18: TDS and EC values of Motloutse water samples and Classification.

Sample code	Name of water source	TDS	E C ($\mu\text{S}/\text{cm}$)	Class
WS1	Motloutse-Mmadinare	529	800	Fresh water
WS2	Motloutse-Near BCL tailings dam	3725	5050	Brackish water
WS3	Motloutse-Letlhakane river confluence	2434	3460	Brackish water
WS4	Motloutse-Tobane	982	1510	Fresh water
WS5	Motloutse-Bobonong	681	530	Fresh water

Table 18 shows the TDS and EC measured values for the water samples of Motloutse categorized according to TDS using scheme by Freeze and Cherry (1979) and plotted on Figure 33.

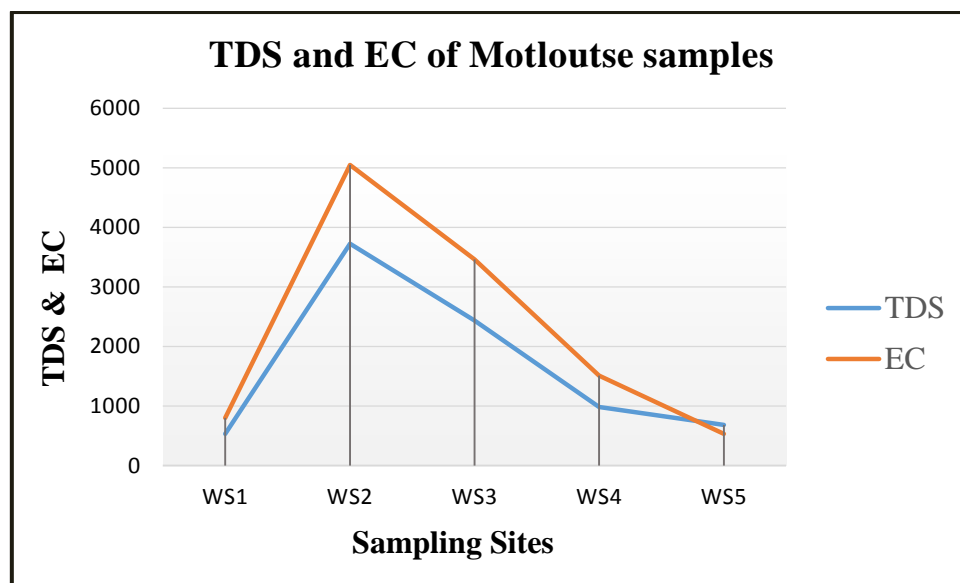


Figure 33: TDS and EC of Motloutse samples.

Sample WS1 has low TDS and EC levels as compared to the other samples thereby outlining the effect of the mine on the water quality. Sample WS2 depicts very high levels of TDS and EC values and this is due to the fact that the water sampling point is immediately after the tailings dam so more salts are dissolved in the water at that stage. It can be seen from Figure 33 that TDS and EC levels of the rest of the samples decreases with the increase in distance from the source (BCL mine) as would be expected of the alluvial aquifer due to the lithological nature of the strata. Dilution by water from the downstream tributaries will also decrease these levels as the river progresses.

Table 19: Water type classifications of Motloutse based on hardness.

Sample code	Name of water source	Hardness value (mg/l)	Group
WS1	Motloutse-Mmadinare	224.3	Hard
WS2	Motloutse-Near BCL tailings dam	2294.5	Very hard
WS3	Motloutse-Letlhakane river confluence	1370.7	Very hard
WS4	Motloutse-Tobane	536.2	Very hard
WS5	Motloutse-Bobonong	417.06	Very hard

Four out of the five samples are very hard while the Mmadinare one is hard as observed in Table 19, which could be attributed to weathering products of basic and intermediate igneous rocks in the area. All the samples after the BCL mine contain high concentrations of calcium and magnesium than those upstream and this again could be due to the BCL mine effluent input. Figure 34 exhibits the same trend observed in TDS and EC levels (Figure 33), that is of hardness decreasing with the increase in distance from the source of the water sampling points located after the mine. It must also be noted that these observation coincides with the groundwater flow direction.

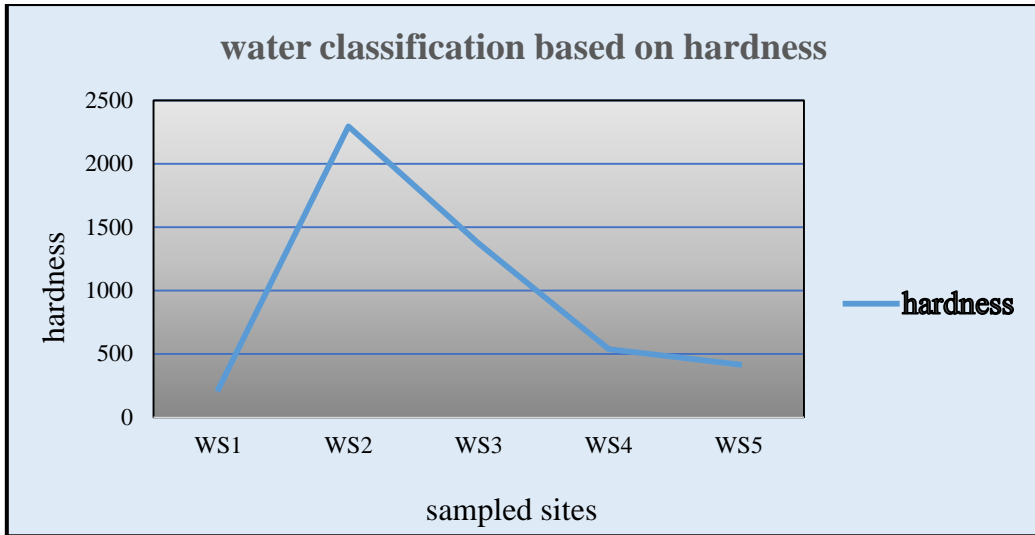


Figure 34: Hardness values of Motloutse water samples.

The chemical analysis results of the major cations and anions of the water samples from the study area are plotted on this diagram using Aqua-chem computer Software program (Figure 35).

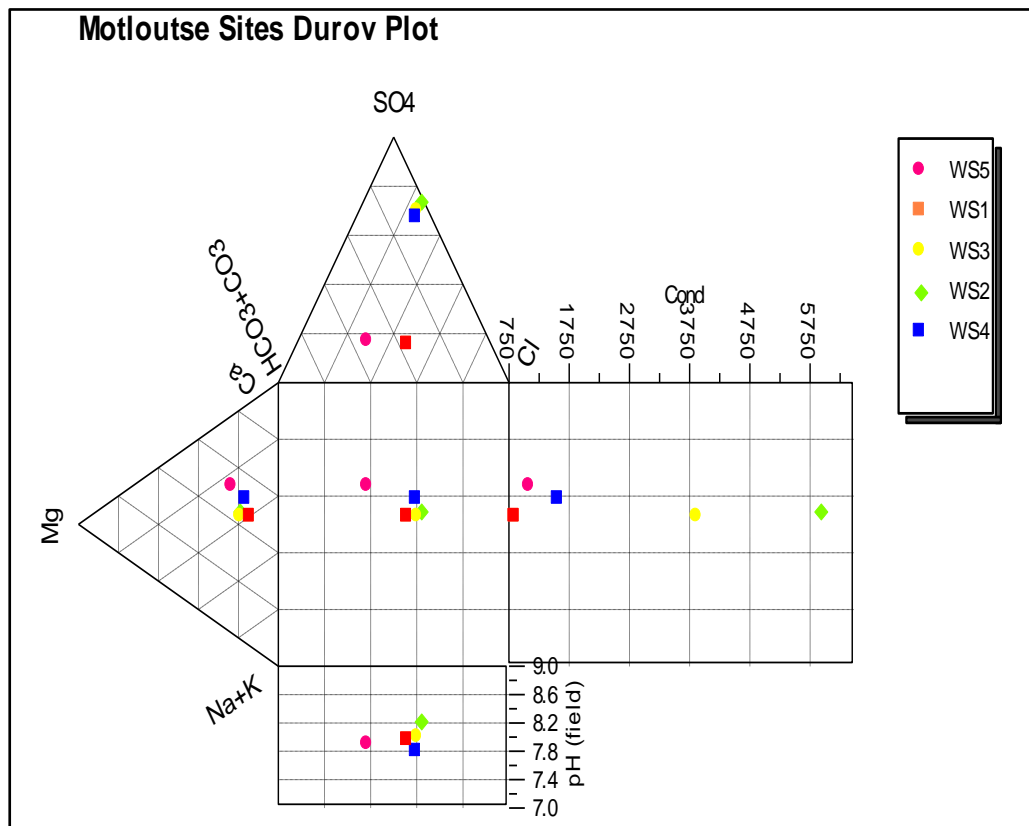


Figure 35: Durov plot of Motloutse water samples.

The water samples of Motloutse sites are classified according to water type derived from the above Durov plot. Three sites (WS2, WS3 and WS4) have identical water type of Ca-Na-SO₄-Cl and WS1 has Ca-Na-Cl-HCO₃ while WS5 has Ca-Mg-Na-HCO₃-Cl water type (Table 20).

Table 20: Water type of Motloutse samples.

Sampling Sites	Water Type
WS1	Ca-Na-Cl-HCO ₃
WS2	Ca-Na-SO ₄ -Cl
WS3	Ca-Na-SO ₄ -Cl
WS4	Ca-Na-SO ₄ -Cl
WS5	Ca-Mg-Na-HCO ₃ -Cl

The dominance of Calcium and Sodium probably suggests their origin by dissolution of basic and acidic silicate minerals from rocks forming the geology of the area and/or caused by cation exchange on riverbank clays.

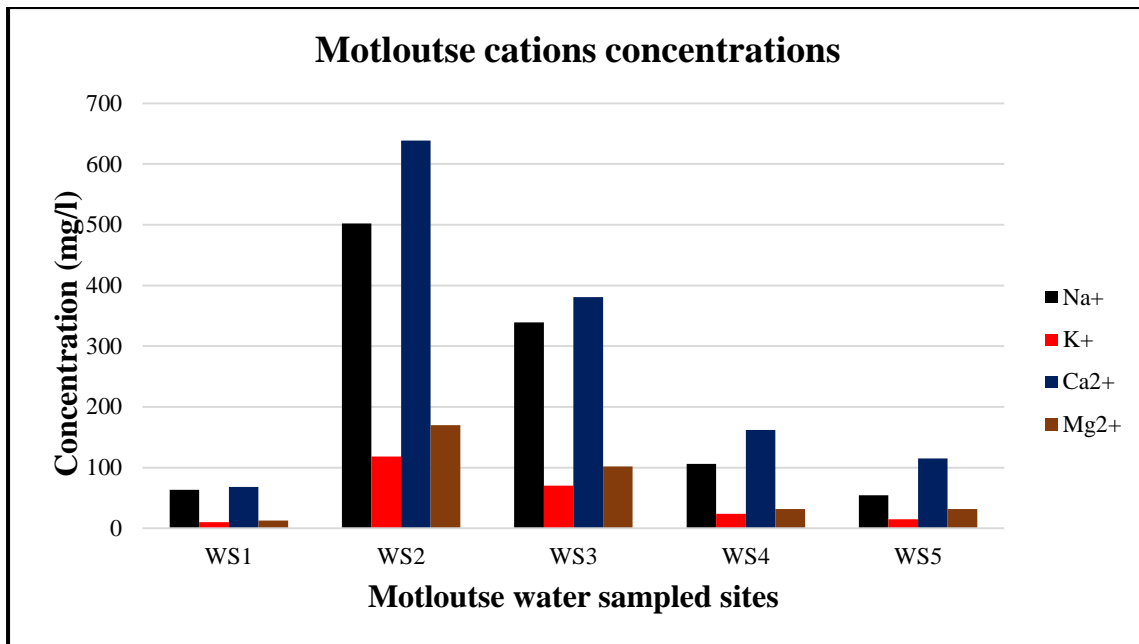


Figure 36: Concentrations of cations in the water samples.

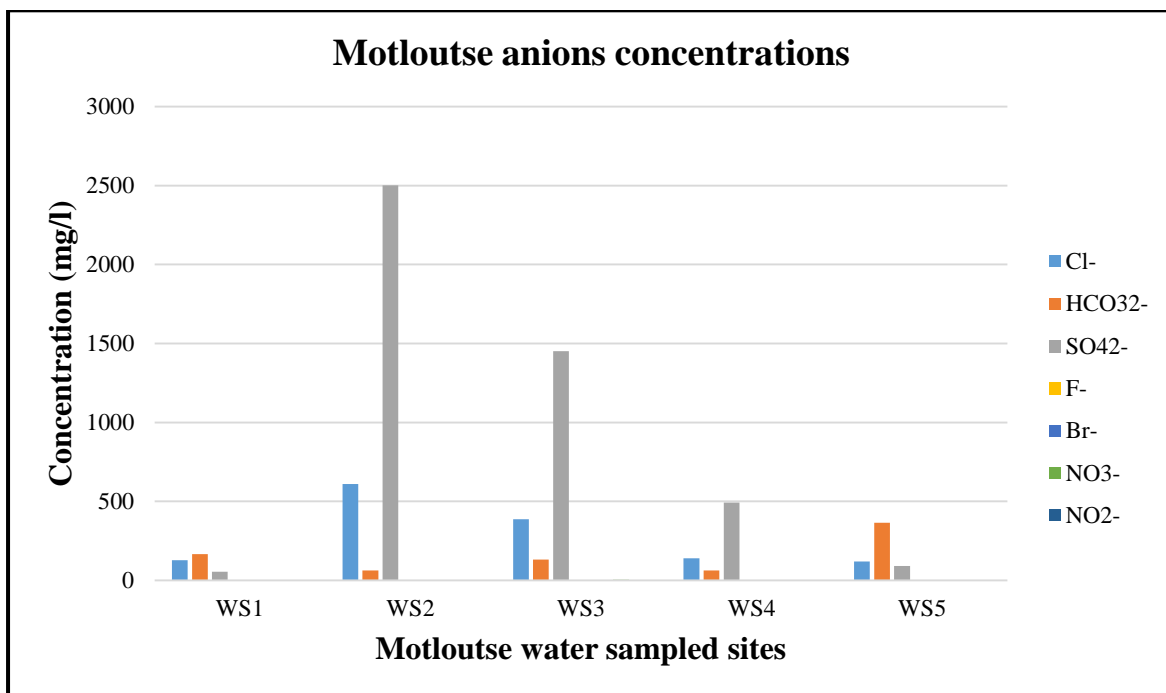


Figure 37: Concentrations of anions of water samples.

From Figure 36 and Figure 37 it can also be observed that the concentrations of both cations and anions are elevated in water sampling WS2 and decrease steadily to WS5.

5.3.3 Metal Concentrations

The distribution of metals concentrations in the samples considered is shown in Figure 38 . Strontium amounts in all water samples are high and this is probably due to localized geologic conditions that supply considerable amounts of strontium to ground and surface waters of the area. Nickel is detected in sample WS2 and WS3 as expected from the copper nickel mine tailings and fades out in WS4. Barium is significantly present in all samples and up to 265 ppb in WS5 and high levels of barium are usually associated with elevated level of strontium. Other metals are existent in less significant amounts but the presence of iron in Bobonong is noted.

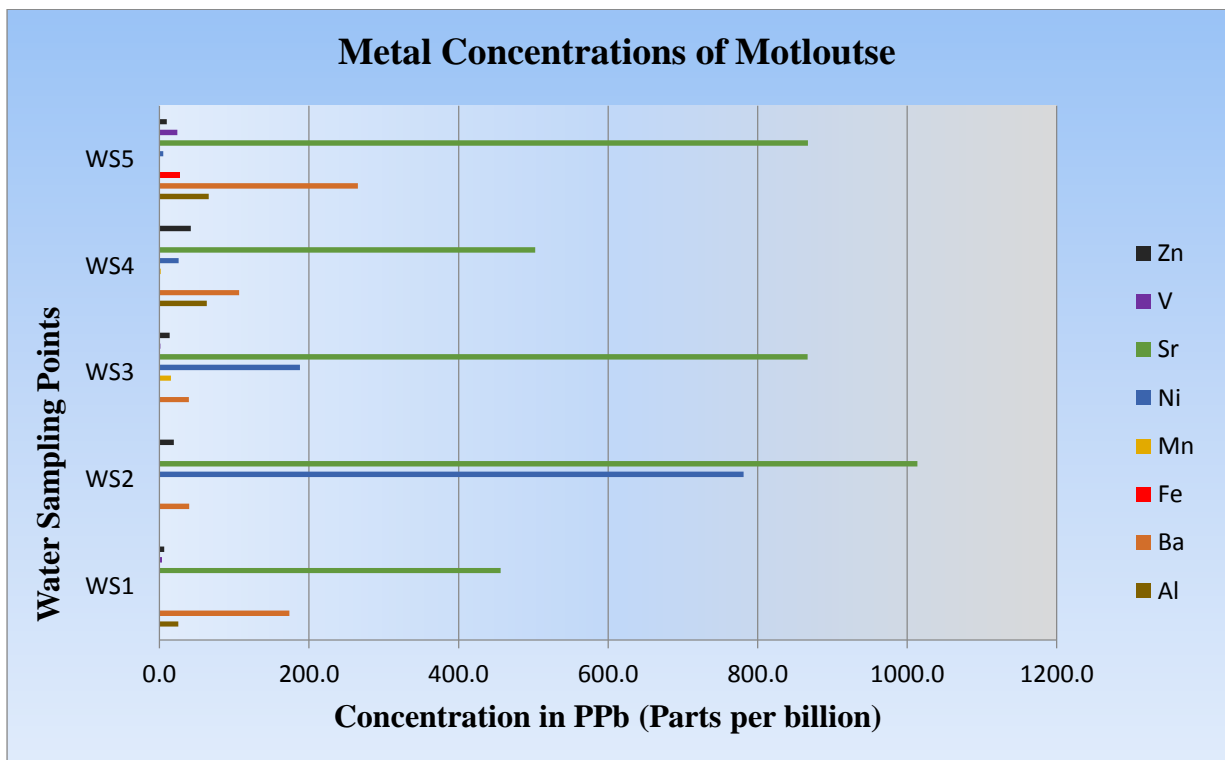


Figure 38: Comparison of metal concentrations of Motloutse sampling points.

5.3.4 Water Quality

Water quality of Motloutse aquifer in relation to various water quality standards in use is presented in Table 21 . From it can be noted that WS1 sample is within all the requirements

of BOBS standards and all except TDS for WHO water quality standard therefore it is fit for drinking purpose. WS2 and WS3 do not meet most of the requisites of both standards therefore not fit for drinking; another clear indication of high chemical concentrations introduced into the alluvial aquifer by the BCL mine. WS4 attains most of the demands of the standards except for its very high sulphate and calcium concentrations but safe for human consumption. WS5 fulfils most of the stipulations of the water standards but its nitrite content must be noted and the water can conclusively be passed for drinking purposes. Overall 3 out of 5 samples in the study area are fit for human consumption.

Table 21: Water quality of Motloutse aquifer compared to different water quality standards

Water quality Parameter	WHO	BOBS class II	Water Sampling Points (mg/l)				
	Guideline (mg/l)	Maximum Allowable	WS1	WS2	WS3	WS4	WS5
pH	6-9	5-10	7.96	8.24	8	7.8	7.9
Conductivity	2500	3100	800	5050	3460	1510	530
TDS	500	2000	529	3725	2434	982	681
Hardness	20-200		224.3	2294.5	1370.7	536.2	417
Sulphate SO ₄	250	400	55.7	2501	1451	492	91.7
Calcium Ca	75	200	68.4	639	381	162	115
Nitrite NO ₂	3	3	1.96	2.46	3.27	2.18	3.26
Sodium Na	200	400	63.2	502	339	106	54.5
Magnesium Mg	100	100	13	170	102	32	31.6
Nitrate NO ₃	45	50	2.15	0.47	5	0.22	0.91

(Source: WHO (1993) and BOBS 32 (2009) water quality standards).

Table 22: Motloutse alluvial water quality suitability for Irrigation.

Parameter	Sampled site				
	SW1	SW2	SW3	SW4	SW5
SAR	9.9	24.9	21.8	10.7	6.4
Water class	Excellent	Permissible	Permissible	Good	Excellent
%Na	47.4	43.4	45.9	40.1	32.1
Water class	Permissible	Permissible	Permissible	Permissible	Good
EC	800	5050	3460	1510	530
Water class	Permissible	Unsuitable	Doubtful	Permissible	Good

As can be seen from Table 22 , all the SAR values of all the water samples of the study are within the permissible limit therefore the groundwater of the basin can be classified as no sodium hazard but with different levels or classes of SAR. Based on the classification scheme made using percent sodium, the water sample of the study area exhibits different classes. As far as EC is concerned, SW2 and SW3 EC values can be regarded as unsuitable for irrigation.

Generally based on the analysis made above and comparison of the water quality results of the study area and the listed standard value (Table 21), Motloutse alluvial aquifer has 3 out 5 samples having appropriate water quality for irrigation hence fit for agricultural use.

The groundwater quality of majority of samples is suitable for drinking and irrigation, it can be utilized by the Motloutse communities with caution and continued water quality monitoring must be practiced due to detected contamination. For all major ions examined, concentrations are very high in the vicinity of mine and decrease with increasing distance downstream of mine. This positive correlation suggests the impact of mining activities on groundwater chemistry through seepage from tailings dam and mine effluent of readily soluble salts and metals into the sand river aquifer. The impacts of the mine on the groundwater chemistry are of small significance on the irrigation and human consumption requirements since the water is portable due to dilution by frequent wet season river flows. However, the impacts are after all noteworthy because during the dry season there are no

flows and Department of Lands (1998) have noted and observed seasonal variations in water quality which could easily outgrow the allowable standards limits.

5.4 GROUNDWATER MODELLING RESULTS

5.4.1 Model Development

The purpose of modelling effort is to produce a basic groundwater flow modelling in order to quantify, assess the resource potential and optimize its sustainable usage on a one kilometre river stretch scale. To achieve the above, a simple steady state, finite difference groundwater model was implemented to simulate and plot groundwater flow to improve the fundamental understanding of groundwater flow in the Motloutse sand river aquifer. The steady state simulation is based on the assumption of predevelopment conditions (those prior to pumping) in the study area.

5.4.1.1 Conceptual Model

A conceptual model is a representation of a natural system designed in order to understand its operations. Development of a conceptual model results in the construction of a numerical model with equal details but simplified conditions of reality to reproduce observed conditions in attaining the set goals of the model. The criteria used in developing the conceptual model consisted of striking a balance between simplicity in that the basin definition had to be general enough to be representative of a typical sand river basin, and detailed to provide boundary conditions and interpretation of cause and effect relations from model results.

Geological logs, water level records and results of geophysics have been examined to produce a conceptual hydrogeological model. The modelled area is located downstream of the contact between Banded Gneiss Formation to the north and Granitic Gneiss Formation to the south according to the local geological map (Magogaphate, 2128C). The contact should intersect the river upstream of the modelled area. The Position of the resistant lithology upstream as already explained by Owen and Darlin (1994) in chapter 2 results in an increased deposition of alluvial sediment of alluvial aquifers located around geological boundaries

hence the choice of the modelled area shown in Figure 39 below. This model area is 1000m in length by 135m defined by average river width at that river section.

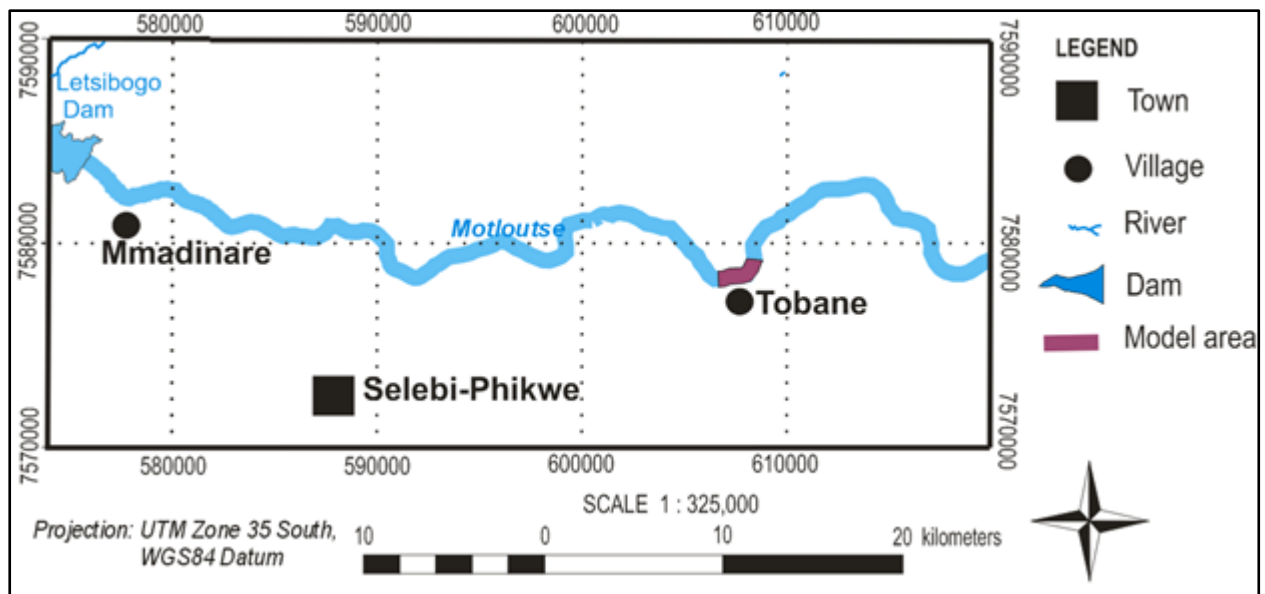


Figure 39: Model area for Motloutse

The vital processes taking place in the study area include areal recharge from precipitation, stream inflow and discharge as river outflow, evaporation and evapotranspiration (Figure 40).

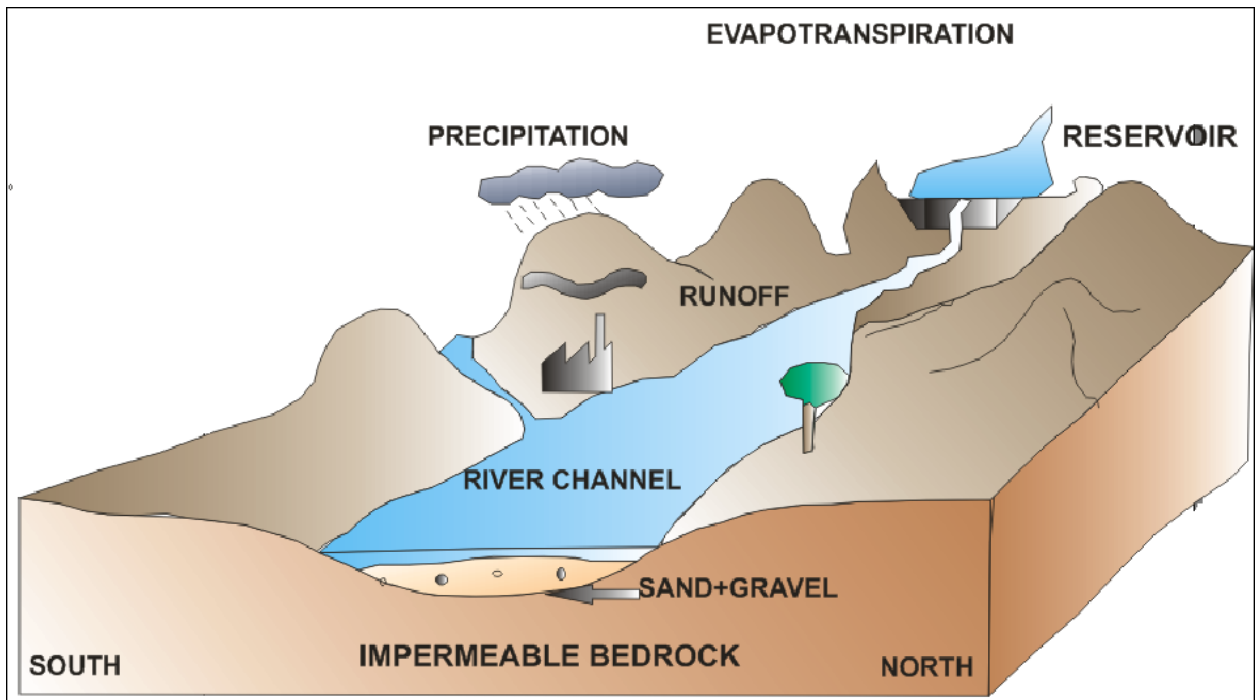


Figure 40: Pictorial representation of the hydrologic system of Motloutse river basin.

The chosen scale for the sand river basin allowed for analysis of groundwater development scenarios ranging from local-scale, multiple-well abstractions to increasing storage. The saturated aquifer thickness was derived from GPR results as this parameter is important to aquifer yield estimates. From the geology of the study area, ground-truthing executions and GPR, the alluvium-bedrock contact was derived and the granitic gneiss is the basement. The alluvium is gravelly sand with minor clay and silt lenses as depicted from grain size analyses and GPR. Based on the geologic and geophysical data the model domain was conceptualised as a single layer system. This productive aquifer of sand is variable ranging in thickness from 4.8 to 6.4m with an average thickness of 6m. The conceptual model is shown in Figure 41 .

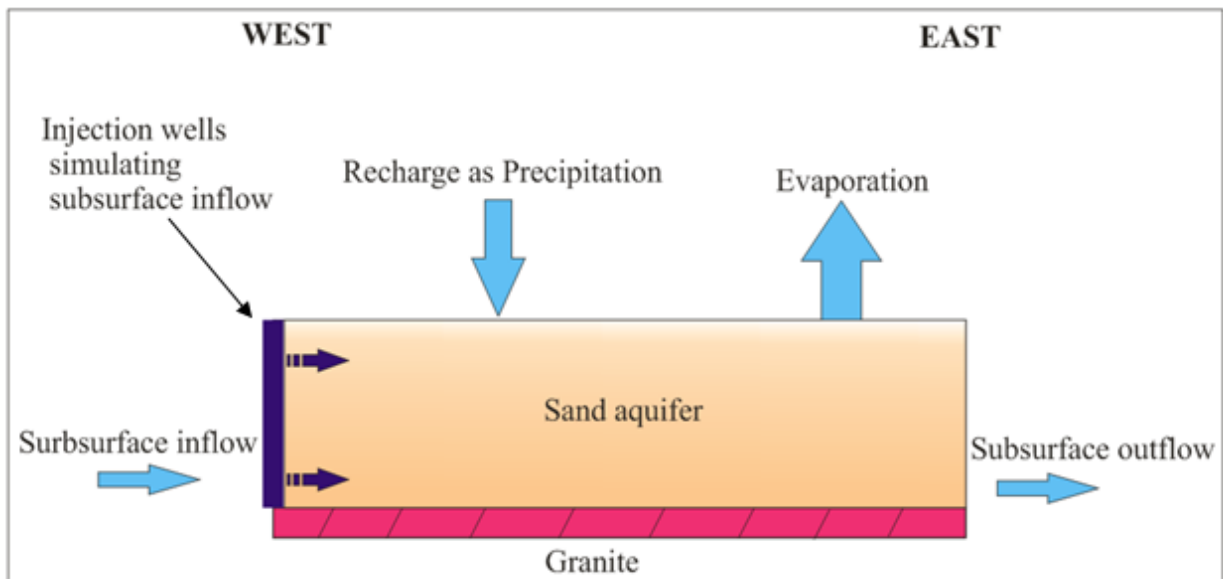


Figure 41: Conceptual model of Motloutse alluvial aquifer cross section.

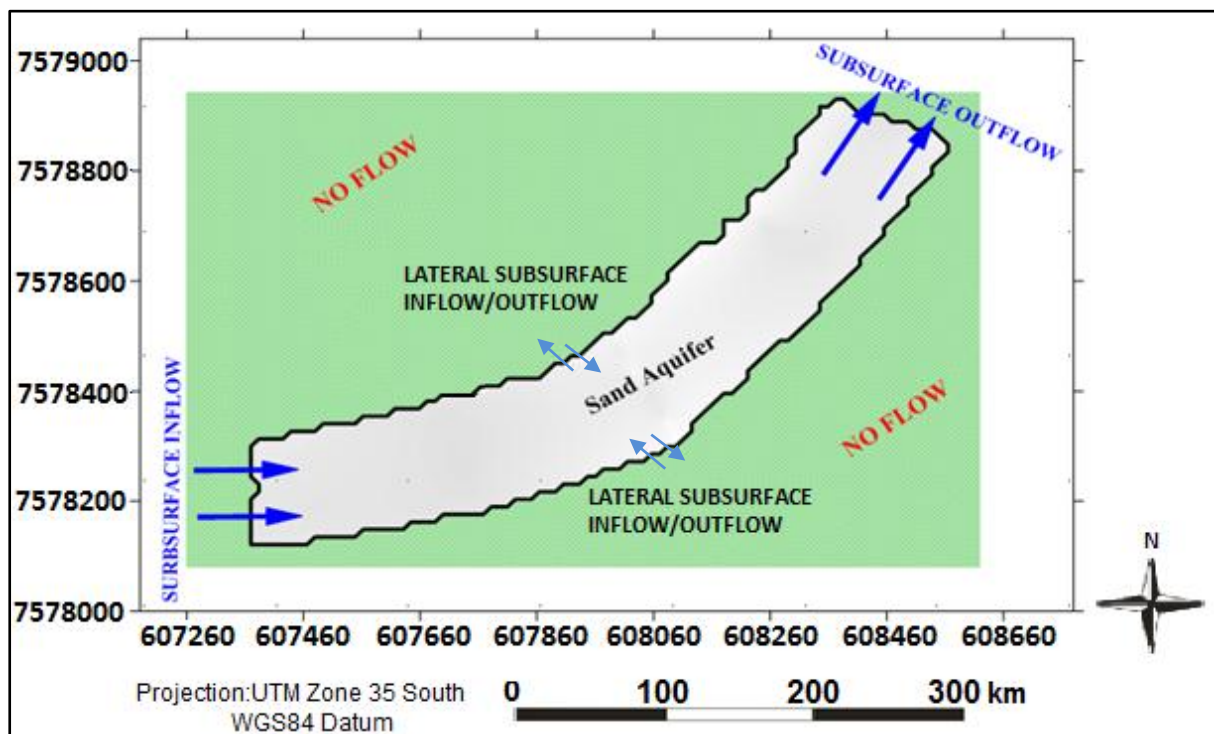


Figure 42: Conceptual model-Plan view

5.4.1.2 Model Discretisation

In a finite difference model the aquifer is represented by rectangular cell blocks with each cell assigned a permeability, specific yield, specific storage, thickness and recharge parameter. A single layer model with 54 rows and 50 columns was developed for Motloutse

river aquifer from digitised profile of the modelled area map. To effectively define the resource the river boundaries were defined as accurately as possible and aquifer geometry is governed by top and bottom elevations incorporated from geophysics survey.

Hydraulic heads in each cell and groundwater flow between cells and across boundaries is calculated simultaneously using finite difference mathematics until a finite solution is found within set convergence parameters.

5.4.1.3 Boundary Conditions and Assumptions

Groundwater model boundaries effectively dictate the flow direction and influence the water balance of a numerical model hence the type of boundary used depend on the modelling scope and model purpose. Active areas of the model bounded by no flow cells as in Figure 43.

The most part of the river channel boundaries were designated as no flow boundaries because of the contrasting difference in hydraulic conductivity. This is usually done to justify a difference in hydraulic conductivity of two orders of magnitude or greater between the adjacent units of the riverbed and the riverbank which is reflected in section 5.2; this causes refraction of flow lines such that flow in another unit is essentially horizontal and vertical on the other (Anderson and Woessner, 1992; Neuman and Witherspoon, 1969). General head boundary nodes were placed just interior to a no flow- boundary representing lateral subsurface flow which is anticipated for such an ephemeral river. This will consequently allow groundwater flow inside or outside of model domain as baseflow proportional to head differences.

GHB's are set by assigning a head and sediment conductance (K) to a selected group of cells. This allows water to move out of the aquifer when the water rises above the specified head in the wet season and in the in the reverse direction in the dry season as baseflow (Anderson and

Woessner, 1992). Riverbank sampling locations (Figure 17) yielded generally poor K values as presented in section 5.2 so the GHB nodes coincided with better or higher K values when compared to others.

Unnatural boundaries were allocated to the west and eastern boundaries for the purpose of modelling. The western boundary is located at the contact between Gneiss Formations and conceptualised as a specified flux boundary and this upstream section was lined up with injection wells to simulate groundwater flow into the model while the east is a general head boundary. General Head Boundary elevations were set to match available water level data. The water table is not fixed at this boundary and may change by some stresses in basin hence General Hydraulic Boundary (GHB) was selected.

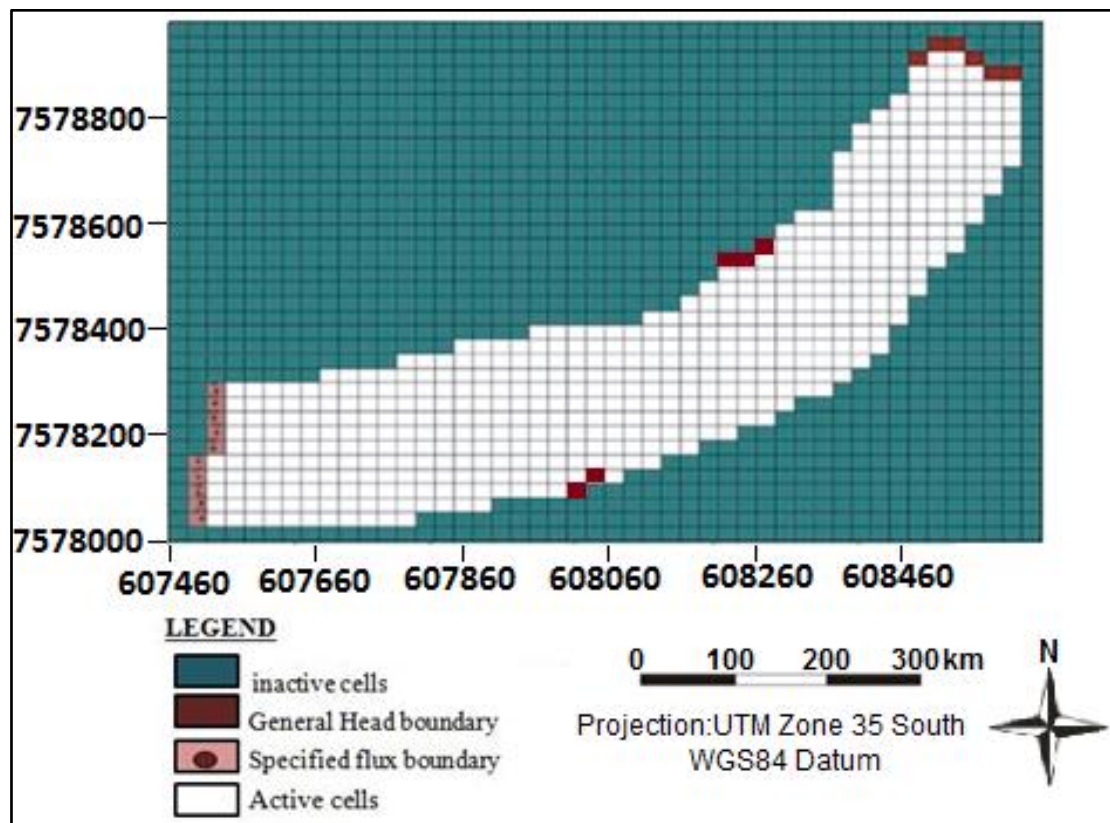


Figure 43: Model boundary conditions

The alluvial aquifer has been assumed as homogenous, isotropic and unconfined aquifer resting on a horizontal impermeable base. The bottom of the aquifer is simulated as a no-flow

boundary because data are insufficient for subsurface leakage into underlying aquifers if any therefore a single layer model has been used. This is also because the contact between river sand and granite basement have differing conductivities and natural earth materials are never completely impermeable and for modelling purposes may be taken as effectively impermeable when the hydraulic conductivities of neighbouring mediums differ by several orders of magnitude (Franke et al, 1987).

5.4.1.4.1 Recharge and Discharge

Rainfall-The Motloutse alluvial aquifer is an unconfined aquifer that contains fresh groundwater of recent age, recharged through precipitation almost annually by the episodic flowing of the Motloutse River. The precipitation was derived from meteorological data for each month that there has rainfall. The higher conductivity and storativity of the Motloutse river aquifer unit allows it to be readily and rapidly saturated in the ‘wet’ months. Recharge was spatially applied to the model domain or simulated using MODFLOW’s recharge package as 115mm/yr. This estimated value is a quarter of the long-term mean annual precipitation of the area representing the expected recharge on the model area for 2014 wet season of which the water levels were used on calibration.

River Inflow-Hydraulic gradients are low within the aquifer (Nord, 1985), resulting in low groundwater velocities and subsurface thorough-flow through the aquifer. As already mentioned this inflow was simulated by flux through injection wells. Darcy’s law was used to estimate the pumping rate of the injection wells expressed as

$$Q_{cs}=AKdh/dl=Kdw \quad (27)$$

Where Q_{cs} = cell surbsurface inflow

A =cross sectional area

K =hydraulic conductivity already derived in chapter 5 from grainsize analysis as 160m/day

$i = dh/dl$ = hydraulic gradient, hereby taken as the gradient of the river at the modelled section which yields 0.0016.

d = average saturated depth, taken as 6m which is the assumed maximum saturated thickness of the aquifer or the individual cell

w = cell width taken as 13.5m

The estimated total pumping rate of each injection wells is 21 cubic metres per day apparently resulting in $210\text{m}^3/\text{day}$ for the ten injecting wells as per the number of cells in the western boundary.

River Outflow-subsurface outflow at the downstream section has been represented by a general head boundary of which its hydraulic head will rise and fall according to the aquifer conditions in and out of model domain.

Evaporation-After a river flow event or flood the aquifer is discharged when the sand becomes unsaturated locally due to falling groundwater levels mainly due to subsurface evaporation. Evapotranspiration presents another potential loss by the sparse riverine vegetation but as there are no visible deep rooted plant growing within the channel, an effective extinction depth taken as 1m (Nord 1985; Wikner 1984) below which direct evaporation becomes insignificant.

MODFLOW's inbuilt evapotranspiration (ET) package incorporates and simulates the effects of direct evaporation in removing water from the saturated groundwater regime (McDonald & Harbaugh, 1988). This package requires 3 components; a maximum rate of evapotranspiration (ET) (L/T) is specified for each surface cell, ET surface elevation (L) and an 'extinction depth (L). When the water table depth is at or above the ET surface, evapotranspiration occurs at the maximum specified rate decreasing linearly with a decline in water table. When the water table lies below the extinction depth, zero evaporation occurs.

Evaporation rates are at maximum when the water table is at the sand surface therefore an estimated starting value of 635 mm/year from the MacDonald open water evaporation rates (Table 23) have been applied. Measured pan evaporation is useful for estimating potential ET when the water table is near land surface but actual maximum ET rates may be overestimated or underestimated. ET surface was taken as the average sand elevation of 778 mamsl.

Table 23: Monthly Open water Evaporation estimates (MacDonald, 1990) *all figures in mm.

Nov	Dec	Jan	Feb	Mar	Apr	May	Jun	Jul	Aug	Sep	Oct
209	211	215	185	183	145	118	93	105	139	180	217

Abstraction-Another obvious potential loss is abstraction by hand dug wells within the sand river from which unknown quantities are harvested but on the modelled area there was no evidence of this and quantification of such is beyond the scope of this dissertation.

5.4.1.4 Aquifer Parameters

In a numerical model the hydraulic characteristics such as thickness, hydraulic conductivity, and specific storage of the aquifer must be specified for each model cell.

A hydraulic conductivity value of 160m/day for gravelly sand was used and assumed isotropic in all directions. This K zone 1 value is derived from the grain-size analysis method of determining hydraulic conductivity. The Alyamani-Sen formula, which is one of the grain-size analysis method of determining hydraulic conductivity was chosen because the equation considers both sediment grain sizes as well as the sorting characteristics as explained in chapter 4.

Isotropic assumption was deemed reasonable for simplification as the aquifer mainly comprises of sand. Due to the fact that the riverbanks have low conductivity material (silt and clay) and on the contrast the riverbed has high K values, the model area had K distributed

spatially into two zones (Figure 44). K zone 2 (26m/day) of riverbank samples were derived from slug-tests because they are done on insitu samples whereby the sediment structure is preserved. This yielded very low K values as expected from silt and clay rich material. Also derived from aquifer material analysis is porosity value of 40 per cent obtained from insitu GPR method and 0.12 for specific yield.

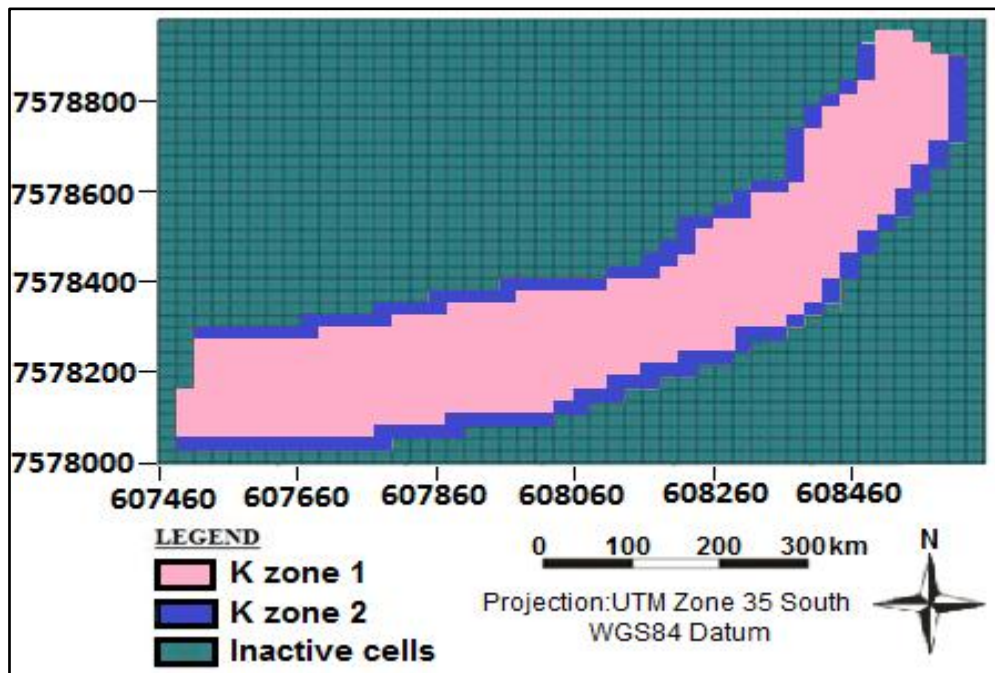


Figure 44: Spatial distribution of Hydraulic Conductivity on model domain

Specific storage (Ss) is the volume of water that a unit volume of aquifer (or aquitard) releases from storage under a unit decline in head by the expansion of water and compression of the soil or rock skeleton (Todd 1980).

For unconfined aquifers it ranges between 0.02-0.30 so in this regard an initial value of 0.30 was used in the model. All these time independent parameters have been applied over the entire model domain. The groundwater table occurs at a depth of 0.3 to 0.8 m; + or -0.2m below ground level in the sand river during the wet season.

In summary, the aquifer is modelled as;

- ❖ Unconfined and possess uniform aquifer properties
- ❖ Has an impermeable base
- ❖ Recharged during rainy season and discharged during the dry season, that is recharge is zero during dry season.
- ❖ It slopes and gravity is the driving force

5.4.2 Calibration

Initial estimates of recharge, hydraulic parameters, and boundary conditions used in the model were based on values determined in preceding chapters. Most of these values were adjusted accordingly within the range that would be expected in the Motloutse for similar conditions or materials. The model is repeatedly run until the computed solution matches field-observed values within an acceptable level of accuracy by trial and error.

The steady-state Motloutse river sand aquifer groundwater-flow model was calibrated to 2014/2015 wet season conditions. This period represents slightly wet conditions as the area received an above-average precipitation (Figure 3) during the year 2014. However most parameters employed were average and conservative therefore all results and alternatives derived from the model simulations are an average representation of the system. Oftentimes steady state calibration is performed to water levels that represent steady state conditions such as mean annual water levels, or mean seasonal water levels for a certain season (Anderson & Woessner, 1992). On this dissertation mean water levels for the 2014/2015 wet season were used for calibration.

The primary reason for choosing the 2014 wet conditions is because calibration to the latest available groundwater level measurements in groundwater model area as long-term water-level data are scarce. Since no systematic, long term water level data has been undertaken early documented data (appendix D) reveals groundwater declines are relatively small when

compared to the range of water-level elevations across the model area (728.20-740.57 mamsl), so use of this data allowed a rough calibration of the model, providing reasonable estimates of parameters for use in the model taking into account that this study model fundamentally seeks to show an understanding of groundwater flow in the Motloutse sand river aquifer. The hydraulic-head data used for calibration consisted primarily of water-level measurements in 9 hand dug wells between November 2014 and January 2015. These wells were dug along the GPR Profiles where sand elevations have been measured. Water levels measured weekly and due to the undulating nature of river sand surface the measured depth to water levels had to be recorded as absolute levels to the elevation datum (mamsl). Absolute water table depths were established as the difference between measured water levels and the average sand elevation for each profile.

Throughout the calibration process, no adjustments were made that conflicted with the general understanding of the geology and hydrology. A plot of modelled against observed heads is presented in Figure 45 with the data points representing hydraulic heads. The 45° line is the reference line, with points lying exactly on this line depicting a perfect fit. Data points above the line reflects that the model is over predicting the hydraulic heads in the system while those below the line reflects that the model is under predicting the hydraulic heads in the system.

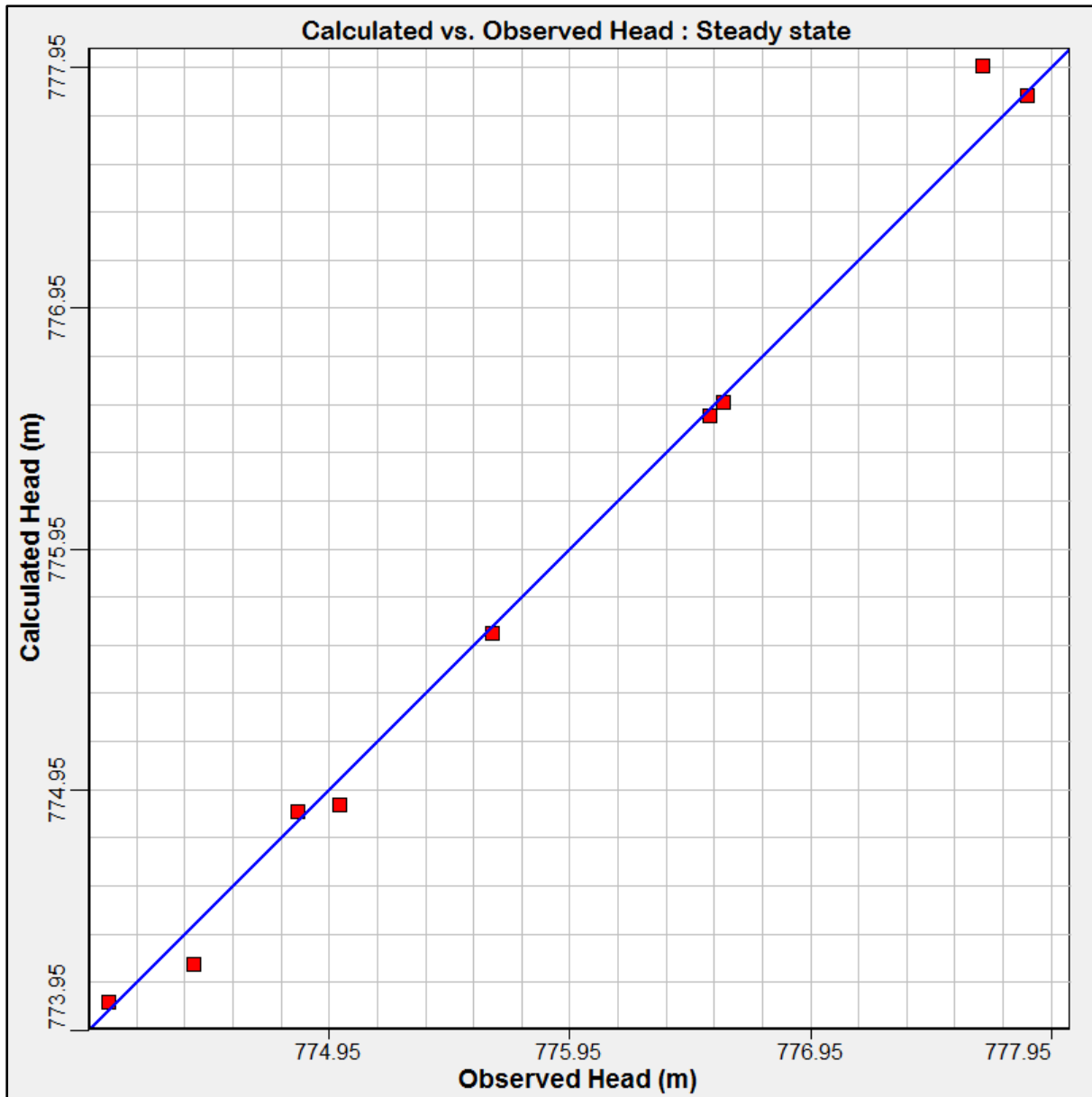


Figure 45: Comparison of Observed vs Simulated heads (at 9 observation wells).

The calibrated model fit the data reasonably well, implying that the conceptual model of flow and the representation of hydrogeology in the groundwater flow simulation model are reasonable. However, the overall result of the model was comparable with the measured well data, and few observations as in Figure 45 have poor convergence being a bit further from the 45 degree line. This can be attributed to errors in water level data collection, or that the model does not reflect well the geology and hydrogeology in that particular location and

finally this can also be due to the small model scale. The output statistical parameters derived from the calibration are shown in Table 24 below.

Table 24: Errors of the calibrated Model.

Error (m)			
Mean error	Mean Absolute error	Root Mean Square Error	Correlation coefficient
-0.008	0.089	0.126	0.997

The evaluation of the calibrated model result shows that: Water balance discrepancy was almost zero (Table 25). The overall results of the groundwater model are comparable with the measured well data and in agreement with the conceptual model.

Figure 46 shows output contour map of the hydraulic heads and the expected flow paths direction along the sand river aquifer. The general hydraulic gradient in the Motloutse follows the surface topography and the gradient is west-east which is in agreement with the conceptual model of the area. Figure 47 shows the location of hand dug observation wells.

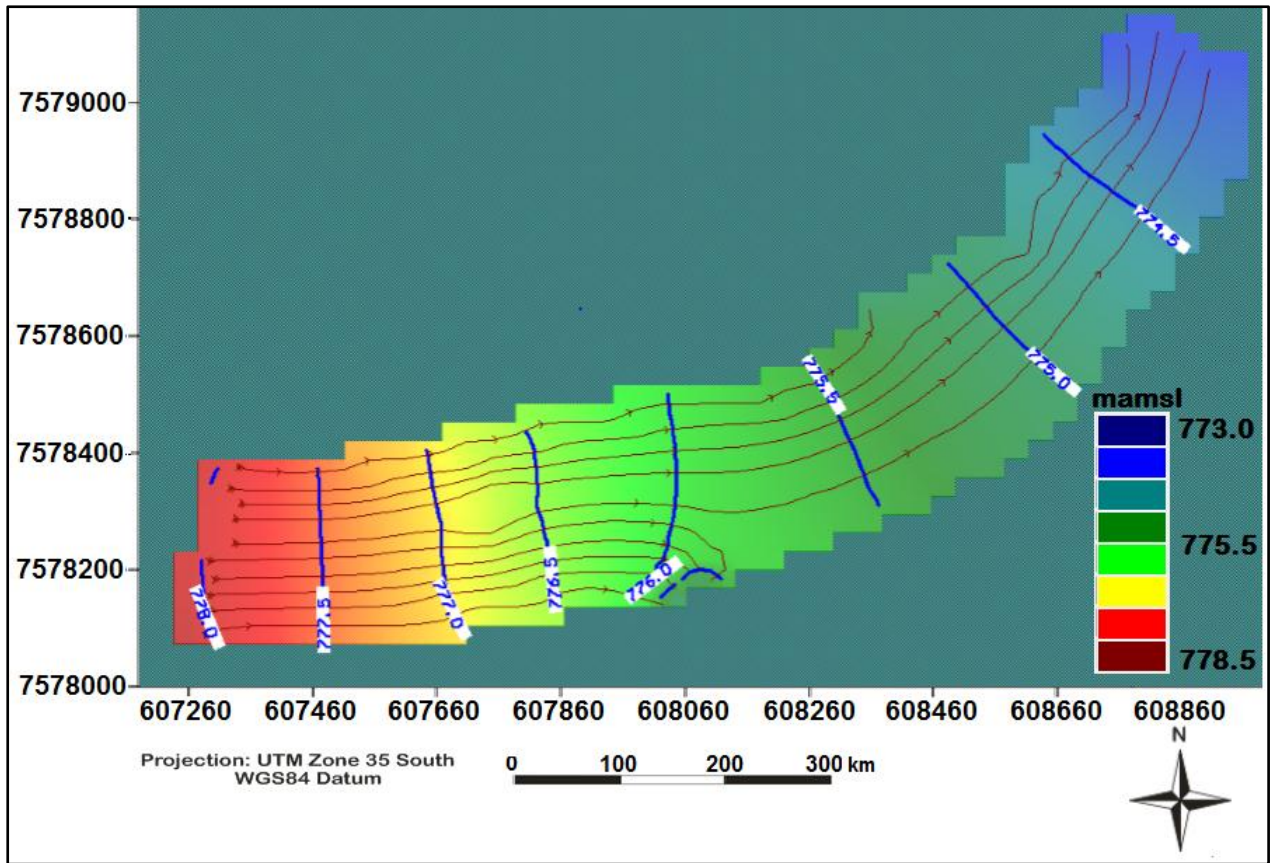


Figure 46: Simulated head distribution and flow direction and paths.

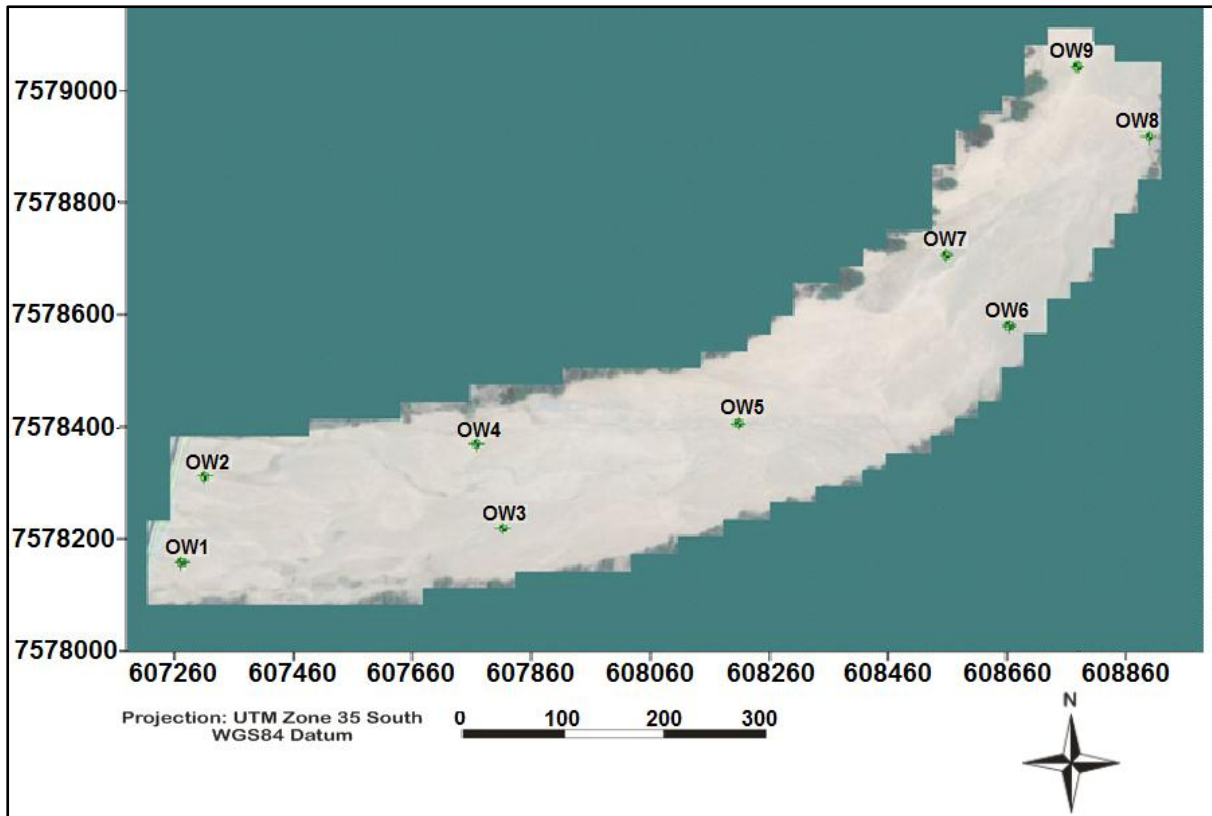


Figure 47: Location of Observation wells.

5.4.3 Water balance

The groundwater budget can be quantified on the basis of the calibrated model output and balancing of inputs and outputs is expected for any accurate groundwater flow model. Comparison of inflow and outflow components of the Motloutse alluvial aquifer groundwater flow system is shown in Table 25. Calibrated net aerial recharge and evaporation of the Motloutse alluvial aquifer is 172mm/year and 120mm respectively. Calibrated flux through western boundary is 60 m³/day for each of the ten injection wells, calibrated K values are 145m/day and 11m/day for the riverbed and riverbanks respectively.

Table 25: Wet season water budget.

Flow term	IN (m³/day)	OUT (m³/day)
Recharge	102.29	
Flow through specified flux boundary	540	
Evaporation		70.15
Head dependent flow through eastern boundary		571.85
Total	641.995	642.29
Per cent discrepancy	0.05%	

5.4.4 Sensitivity Analysis

A sensitivity analysis enables an assessment of the overall model performance by quantifying the sensitivity of the model simulations in the calibrated model caused by uncertainty in the estimates of aquifer parameters, stress and boundary conditions (Anderson and Woessner,1992). The system's response to variation in the calibrated recharge, hydraulic conductivity zones and evaporation was evaluated. The parameters were varied by a factor of 0.25 and the resulting heads were used to compute the mean error (ME), mean average error (MAE) and the root mean square error (RMSE) for each factor. These were compared against the calibrated and the departures plotted in Figure 48 , Figure 49, Figure 50 and Figure 51.

Figure 48 shows high hydraulic head errors when the hydraulic conductivity of zone 1 of the calibrated model is decreased showing that it is highly sensitive to decrease in hydraulic conductivity than its increment. For K zone 2, the same response is repeated with mean error decreasing with K increment (Figure 49).Figure 50 shows the model is sensitive to increase and decrease in recharge and generally generates a non-linear sensitivity response. However, this response is sharp near the calibrated value within a single factor of 0.25 and steadier as recharge is adjusted further from the calibrated value. The calibrated model is sensitive to evaporation (Figure 51) increment than its decrease. It can be concluded that the model is

most sensitive to decrease and increase in recharge than adjustments in both hydraulic conductivity and evaporation.

The model's sensitivity to the applied boundary conditions was also tested. The general head boundary was replaced with a constant head boundary and from the computed water budget there was a negligible change of 0.5% showing that the model is insensitive to general head boundary or constant head boundary.

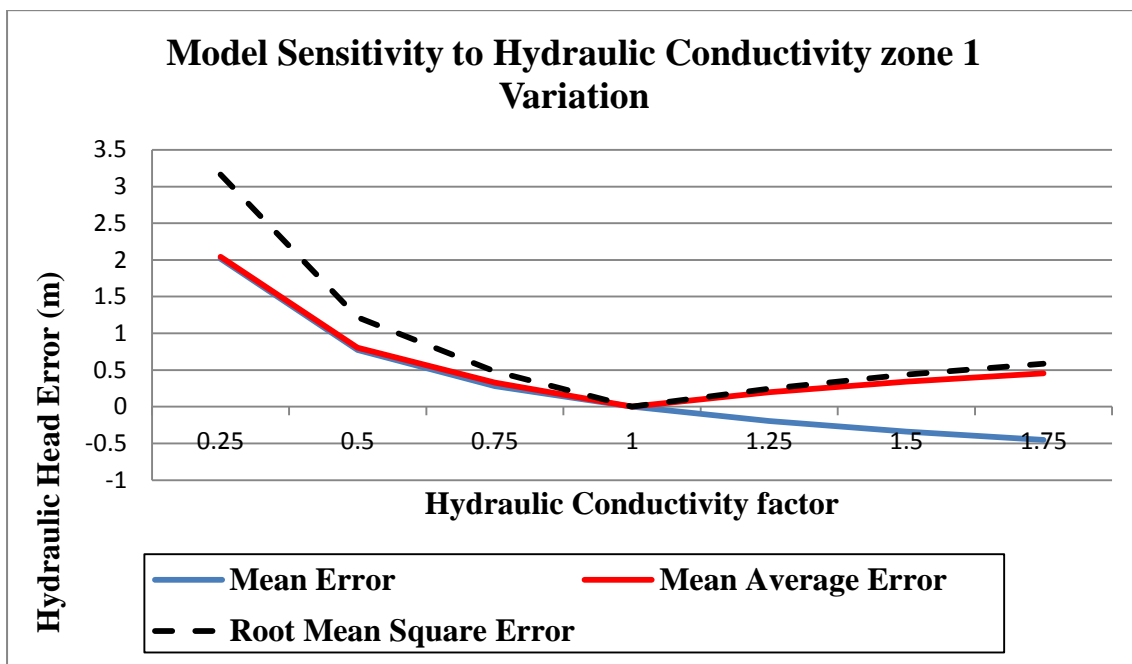


Figure 48: Sensitivity plot of calibrated model with respect to K zone 1.

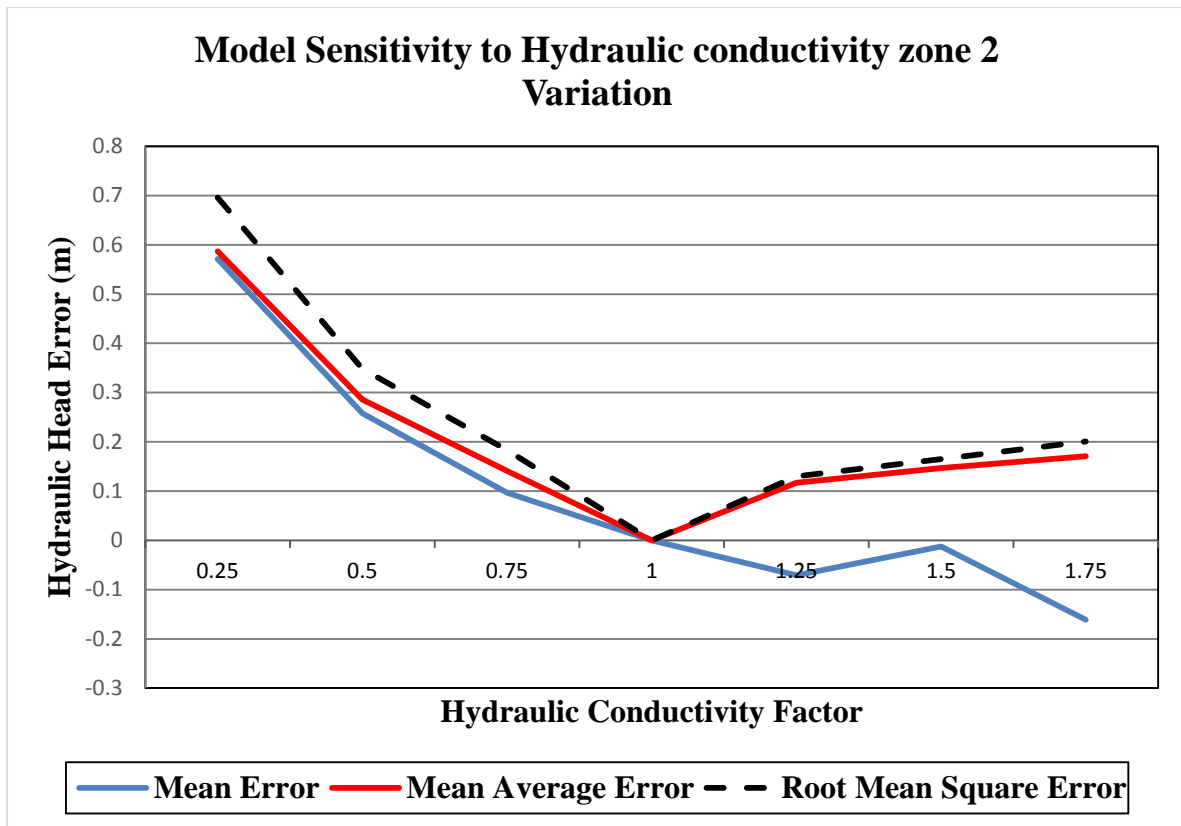


Figure 49: Model sensitivity to K zone 2

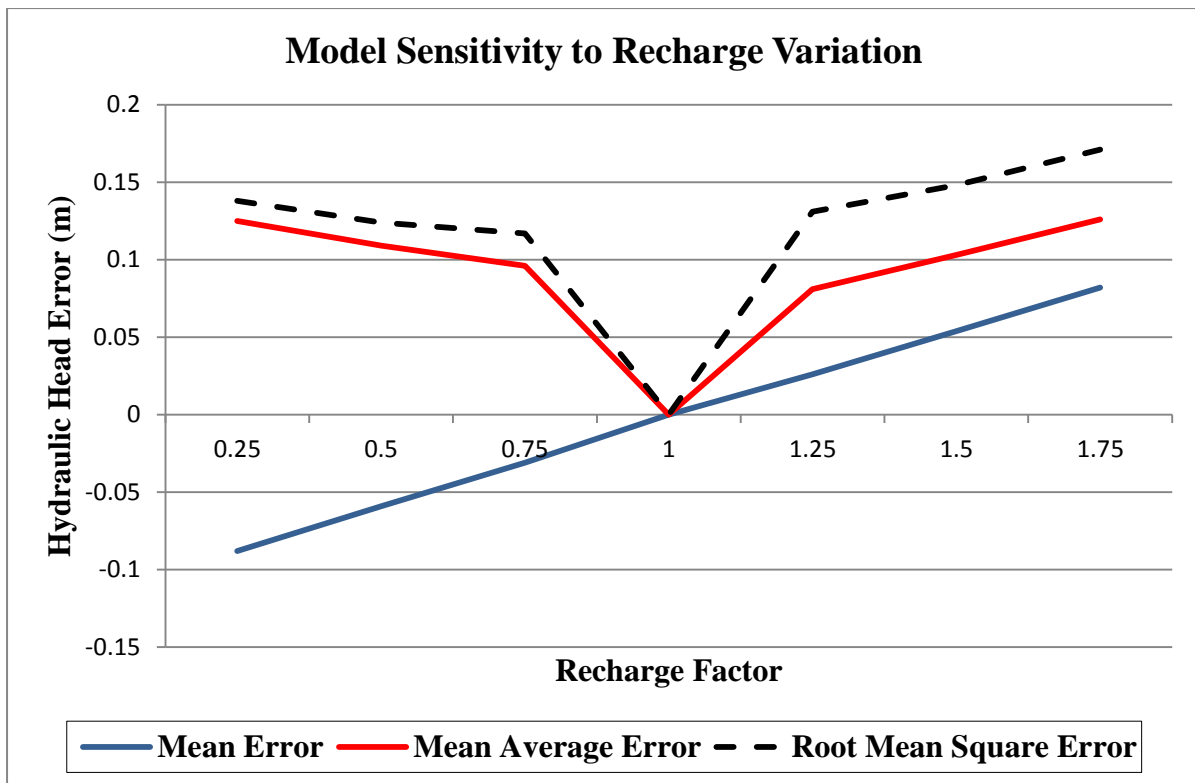


Figure 50 : Plot of model sensitivity to recharge.

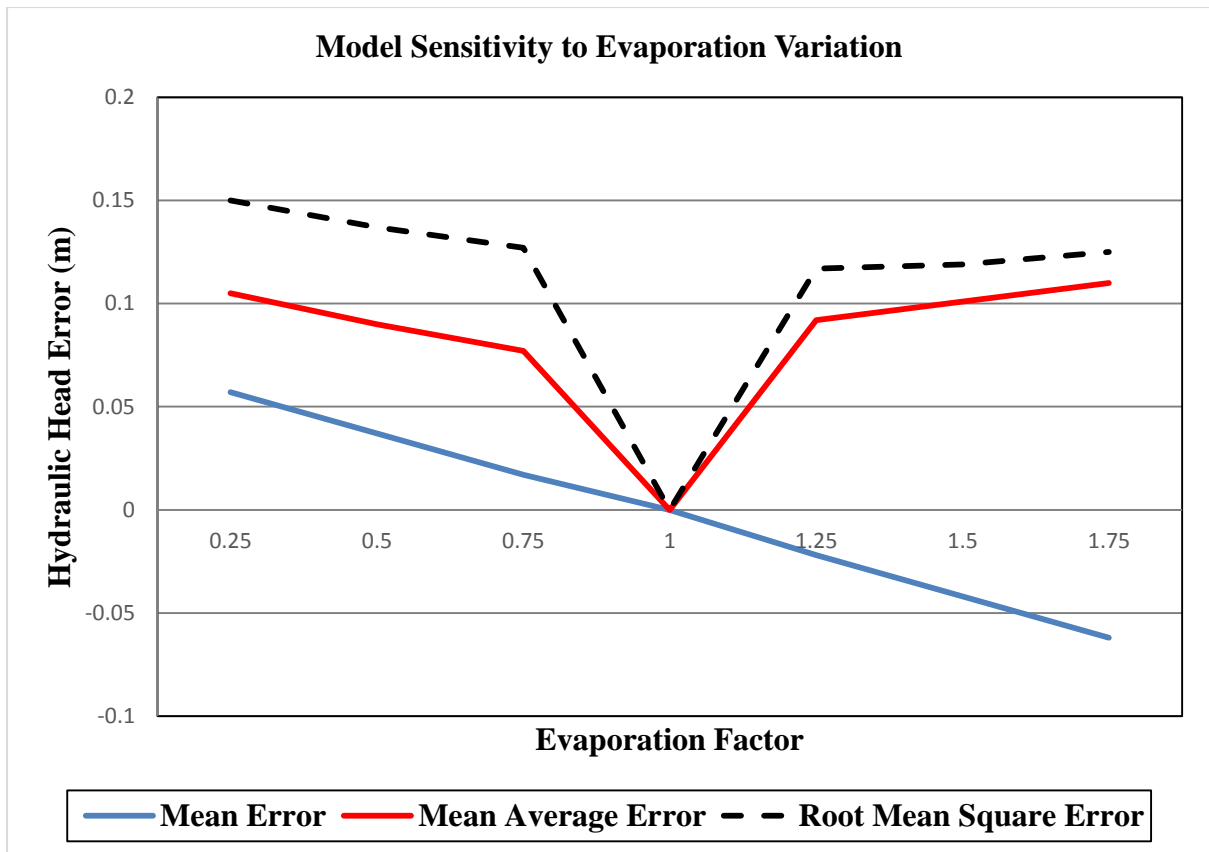


Figure 51: Sensitivity plot of evaporation

Sensitivity analysis on the modelled recharge indicates similar response when increasing or decreasing the recharge value. This is expected since equally distributed recharge is applied over the entire model domain and so the heads in the model respond linearly to increase or decrease in the recharge

5.4.5 Scenario Simulations

Model runs were made to simulate the following scenarios;

- ✓ Sand storage dam potential
- ✓ Optimum pumping rate and Well field spacing
- ✓ Potential irrigation area

It must be noted that all these scenarios were modelled under dry season conditions when the recharge has been turned off and calibrated evaporation value decreased by 20% to 100mm as

is the case in the dry season months as displayed in Figure 4 (chapter 2). Table 26 shows the resulting computed water budget for this dry season conditions.

Table 26: Dry season water budget.

Flow term	IN (m³/day)	OUT (m³/day)
Recharge	0	
Flow through specified flux boundary	600	
Evaporation		67.222
Head dependent flow through eastern boundary	131.34	665.15
Total	731.34	732.37
Per cent discrepancy	-0.14%	

5.4.5.1 Sand storage dam potential

A Sand dam is a wall built across a seasonal sandy riverbed that store water under sand protecting it from contamination and evaporation.

The natural storage capacity of the riverbed aquifer is envisaged to be increased by the sand storage dam in the following way: as the aquifer is fully replenished after rainfall events during the wet season, the river starts flowing of course but the groundwater flow is held back by the subsurface dam hence creating an extra storage. This stored water can be tapped throughout the dry season due to lower evaporation and increased storage capacity.

Model runs were initiated to simulate this scenario by assigning very low hydraulic conductivity value to the proposed sand dam location. The applied K of 0.1 m/day is equal to average building material usually used for such dams such as masonry, soil bricks and cement. The proposed site is where the alluvium is thicker for increased storage deduced from Figure 30, chapter 5. This simulation resulted in very significant increase in potentiometric heads upstream of the proposed dam site as in Figure 52. Clearly the model demonstrated well this scenario culminating in increased storage for the resource.

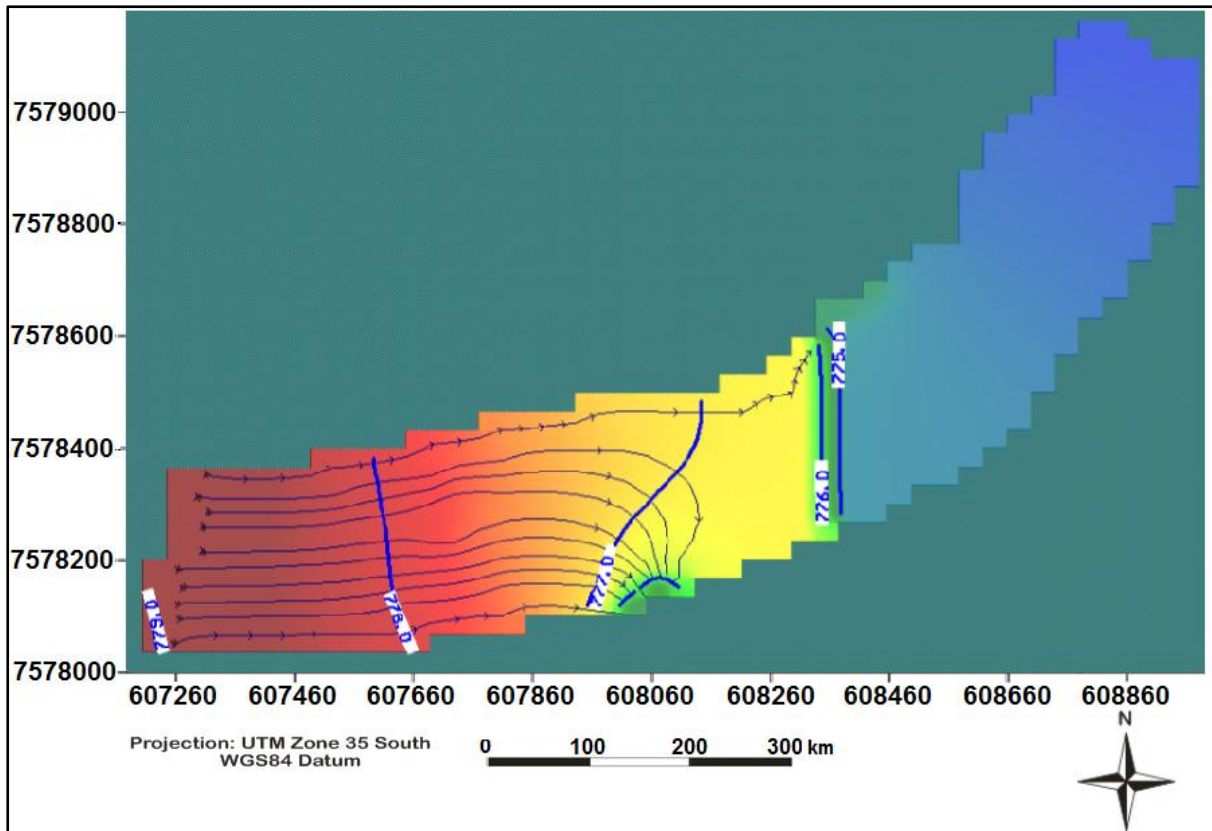


Figure 52: SSD scenario contours

5.4.5.2 Well Optimisation

Using Modflow well package in conjunction with MODPATH package, pumping wells were introduced to simulate abstraction scenario in order to estimate maximum sustainable rates, layout and optimal spacing between wells. This are shown in Table 27 below, with the 8 wells terminating in fresh granitic gneiss bedrock located along the river length in the middle of the river in areas of thicker alluvium and separation of about 100m. These figures were found through numerous runs taking the maximum possible pumping rate for the dry season that does not dewater the aquifer significantly by monitoring water levels and drawdowns. Analysis particle pathlines was also used in determining each well's area of influence. The maximum sustainable yield value of $200\text{m}^3/\text{day}$ translates into about 2l/s using a Honda pump. However these values can be improved by pumping at very smaller rates.

Table 27: Summary of Well Optimisation Parameters.

Max sustainable rate (m ³ /day)	Irrigable area (hectares)	Recommended no. of sources	Rate per source (m ³ /day)
120	4	8	15

5.4.5.3 Potential irrigation area

Crop water requirements for irrigation depend on the crop type and soil type of the area to be cultivated. Gross crop water requirements for suitable cropping patterns for the study area have been estimated by MacDonald, (1990). He estimated a crop water requirement ranging from 43m³/day/ha to 50m³/day/ha. However it must be noted that these volumes are a guideline as in practise significantly little water may be utilised. From the maximum sustainable rate of 120m³/day the potential irrigable area is up to 2.4 hectares.

The overall result of the calibrated steady-state groundwater flow model developed for the area is realistic as the deviation of the simulated heads from the observed heads is reasonable. The model calculated inflow and outflow terms are balancing, and groundwater flow direction simulated by the model is reasonable and in agreement with the flow direction defined in the conceptual model. Lastly modelled scenarios are reasonable and practical.

Nevertheless, there are a number of limitations and uncertainties in the steady-state groundwater flow model developed here.

5.4.6 Model Limitations

In groundwater modelling, some part of the data is used for model calibration and the remaining part is used for model Validation .It is often impossible to validate a model because usually too short set of observed data is available which is already required for calibration, therefore model validation was not accomplished here.

Numerical models of groundwater flow are limited in their representation of the physical system because they contain simplifications and assumptions that may or may not be valid. Results from groundwater flow models have a degree of uncertainty mainly because of uncertainties in many model input parameters and boundary conditions applied. The main constraints in the modelling process were data gaps and poor quality of the available data. The available records of the water level measurements are not continuous or long term and mostly are only single measurements.

Another area of uncertainty is resulting from defining the boundary conditions of the model domain. The boundary conditions were defined based on geological features such as impervious geology and formation contacts. The area is conceptualized as a single layer but in reality the separating layer may be partially impervious due to localized fractures and connected to aquifers below hence additional uncertainty may be introduced as a result of this assumption.

The model assumed that water could be abstracted from the wells until the water level reaches the base of the aquifer which will not happen in reality as there would be a residue of water that cannot be abstracted.

Finally the calibration of a groundwater model does not ensure that it is an accurate representation of the system. However an appropriate conceptual hydrogeological model is typically more important and consequently, the application of the model should be constrained by the limitations inherent in the underlying conceptual model.

5.5 RESOURCE QUANTIFICATION

The estimated sustainable extractable volume for the Motloutse 1km river stretch is 29400 m³. This figure has been derived by multiplying the daily sustainable rate by the 245 dry season period. Nord (1985) and Department of Lands (1998) have calculated the groundwater

resources of Motloutse sand river aquifer on the basis of total volume of groundwater per kilometre length of river. They found 29 000 and 38500m³ respectively, which compare well to the value derived in this dissertation.

Crop water requirements yielded a total area of 2.4 hectares as the irrigable area, which can benefit from water exploitation of Motloutse watercourse (as calculated in section 5.4.5.3). As part of integrated water resources management, water saving practises should be practised such as drip irrigation, sprinkler irrigation. Motloutse water resource must be developed in a way that balances social and economic needs ensuring the protection of ecosystems for future generations. Irrigation schemes should be managed with right institutional committees and community organisations, arrangements should be made to manage irrigation in an efficient manner.

6.0 CONCLUSIONS AND RECOMMENDATIONS

6.1 CONCLUSIONS

The groundwater potential of Motloutse water course has been determined successfully. Geophysics methods have been applied to resolve depth to granite bedrock successfully using GPR to an average depth of 6m and provided reasonable estimates of aquifer volume for resource modelling. Laboratory analysis of aquifer material has produced estimates of hydraulic conductivities for the main riverbed and for the riverbanks. These values are considered realistic for a gravelly sand aquifer with the calibrated groundwater model producing K values of 145 and 11m/day respectively. Porosity values and specific yield has been calculated as 0.4 and 0.12 percent respectively. Calibrated recharge and evaporation as 172mm/yr and 120mm respectively. The Motloutse alluvial aquifer yields a safe yield of 29400m³ for a kilometre river stretch.

Concerning hydrogeochemistry, data analyses demonstrated that 3 water types exist in the Motloutse alluvial aquifer dominated by Ca-Na-SO₄-Cl water class. The BCL Mine has an impact on the general hydrochemistry of Motloutse aquifer material which is typified by consistent trend of water quality deterioration near the mine and decreasing with distance away from mine. However the water is portable with regular monitoring emphasized and with respect to irrigation water quality the water suites irrigation well with concerns of the water quality depreciating due to the mine. Small scale irrigation is feasible considering the large area of low suitability soils and shallow depth to bedrock in the study area.

The conceptual model for Motloutse alluvial aquifer incorporating the previously interpreted data has been developed and so deemed appropriate and reasonable by but in no way proving

it is accurate. The steady state modelling has demonstrated that it can be used as a tool to improve our understanding of the groundwater flow system and aquifer properties. From the overall groundwater evaluation carried out by integration of geological, hydrogeological and groundwater modelling it is concluded that areal recharge, evaporation, subsurface inflow and outflow are the main processes that define the water balance components of the sand river bed aquifer. In addition it has been shown that direct rainfall is likely to fully recharge the aquifer during a wet season.

The groundwater potential estimated in this study is the minimum water available per km stretch of the river at Tobane, more water is expected from the riverbed. The ability of alluvial aquifers to store water to be utilised in drier periods has been demonstrated with the advantage that evaporation water losses are less as compared to surface evaporation water.

6.2 RECOMMENDATIONS

The steady state model can be further developed with additional data to cover a larger area including river and/or flood plains.

Drilling through the basement should be done when funds are available to identify the potential presence of underlying aquifer. The interaction of these deeper aquifer system studied here and in relation to regional groundwater flow system should be studied. In addition interaction between river plain hydrogeological system and the sand river system should be investigated as well.

To improve model boundary uncertainties the model area can be expanded to locate and investigate compartmentalised zones or isolated basins within the riverbed for modelling. After an improved steady state modelling providing initial heads, transient simulation should follow suit for an improved understanding of abstraction effects and aquifer properties.

Pumping tests must be conducted to estimate aquifer parameters for comparison with those derived in this dissertation.

For a better calibration of the model, long-term, continuous and systematic groundwater levels data collection should be commenced and databases set up with frequent monitoring by Department of water affairs, Botswana. In addition sand mining from the riverbed must be monitored very closely because it reduces the aquifer resource potential.

Chemical water quality for the Motloutse should also be monitored as well as the effluent from the BCL Mine. Bacteriological analysis of Motloutse alluvial aquifer must be conducted.

7.0 REFERENCES

- Aerts J, Lasarge R, Beets W, de Moel H, Mutiso G, de Vries A. 2007. Robustness of sand storage dams under climate change. *Vadose Zone Journal* 6: 572–580.
- Aldiss, D T. 1983a. The geology of the Tsetsebjwe area. *Bulletin Geological Survey of Botswana*, 24, 86pp.
- Aldiss, D T. 1983b. The geology of the Semolale area. *Bulletin Geological Survey of Botswana*, 25, 64 pp.
- Allan JD, Castillo MM. 2007. *Stream Ecology: Structure and Function of Running Waters* Springer: Berlin; 436
- Alyamani, M.S., and Sen, Z. 1993. Determination of Hydraulic Conductivity from Grain-Size Distribution Curves. *Ground Water*, 31, 551-555.
- Anderson, M.P., and Woessner. 1992. *Applied groundwater modelling-simulation of flow and advective transport*. San Diego: Academic Press. Inc.
- Anderson, N.J., 1997. *Modelling the Sustainable Yield of Groundwater Resource in Riverbed Aquifers in Arid and Semi-arid Areas*. MPhil to PhD Transfer Report. Department of Civil Engineering, University of London. London, England.
- Annan, A.P. 1999 *Practical Processing of GPR Data*. Proceedings of the Second Government Workshop on Ground Penetrating Radar.
- Annan, A.P. 2009 *Electromagnetic Principles of Ground Penetrating Radar*. In *Ground Penetrating Radar: Theory and Applications*, edited by Harry M. Jol, pp. 3-40. Elsevier, Amsterdam.

Barker, R., and Molle, F., 2004. Evolution of irrigation in South and Southeast Asia. Comprehensive Assessment Research Report 4, International Water Management Institute, Colombo, 39p.

Bennett, J D. 1971. Geological map of the Magothate area (QDS 2128C) (1:125000), with brief explanation. *Geological Survey of Botswana*

Bentley, L.R., Trenholm, N.M., 2002. The accuracy of water table elevation estimates determined from ground penetrating radar data. *Journal of Engineering and Environmental Geophysics* 7, 37– 53.

Beyer, W. 1964. Zur Bestimmung der Wasserdurchlässigkeit von Kies und Sand aus der Kornverteilung [On the determination of hydraulic conductivity of gravel and sand from grain-size distribution]. *Wasserwirtschaft Wassertechnik* 14: 165–169.

BNWMP, Botswana National Water Master Plan, 1991 Study. Volume 5. Hydrogeology., SMEC, WLP, SGI AB Consultants for Department of Water Affairs.

BNWMP, Botswana National Water Master Plan Review, 2006. Volume 4 Groundwater Resources., SMEC/EHES Consultants., AB for Department of Water Affairs

BOBS, 2009. Water Quality – Drinking Water Specifications, Botswana Bureau of Standards (BOS 32:200).

Bornette H, Heiler G. 1994. Environmental and biological responses of former channels to river incision: a diachronic study on the upper Rhône River. *Regulated Rivers: Research and Management* 9: 79–92. DOI:10.1002/rrr.3450090202

Bouwer, H. and Jackson, R.D., 1974. Determining Soil Properties. In: Jan Van Schilf gaarde (Editor), *Drainage for Agriculture*. Am. Soc. Agron. No. 17, Madison, WI, pp. 611-672.

Bridge, J., Collier, R. and Alexander, J. (1998). Large-scale structure of Calamus River deposits (Nebraska, USA) revealed using ground-penetrating radar. *Sedimentology*, 45(6), pp.977--986.

Bristow, C. and Jol, H. (2003). *Ground penetrating radar in sediments*. 1st ed. London: Geological Society.

Burval working Group, 2006. Groundwater resources in buried valleys. Leibniz Institute for Applied Geosciences (GGA-Institut) Hannover. Technical handbook chpt4.7 ground penetrating radar

California Department of Transportation. Method of test for Permeability of soils. 1st ed. California: State of California— business, transportation and housing agency, 1998. web. 24 nov. 2014. www.dot.ca.gov/hq/esc/ctms/pdf/CT_220.pdf

Carman, P.C. 1937. Fluid Flow through Granular Beds. *Trans.Inst.Chem.Eng.*, 15,150.

Carman, P.C. 1956. *Flow of Gases through Porous Media*. Butterworths Scientific Publications, London.

Carney, J N, Aldiss, D T, and Lock, N P. 1994. The Geology of Botswana. *Bulletin Geological Survey of Botswana*, 37, 113 pp.

Carrier, W.D. 2003. Goodbye, Hazen; Hello, Kozeny-Carman. *Journal of Geotechnical and Geoenvironmental Engineering*.1054.

Chen, X.H., 2000. Measurement of streambed hydraulic conductivity and its anisotropy. *Environmental Geology* 39, 1317–1324.

Cobbing JE, Hobbs PJ, Meyer R, Davies J. 2008. A critical overview of trans boundary aquifers shared by South Africa. *Hydrogeology Journal* 16: 1207–1214.

Conyers, Lawrence B. 2004 *Ground-Penetrating Radar for Archaeology*. AltaMira Press, Lanham.

Coward, MP. 1976. Archaean deformation patterns in Southern Africa. *Transactions of the Royal Philosophical Society of London*, A283. 313-331.

Daniels, D.J., 2004. *Ground Penetrating Radar*, 2nd edition. The Institute of Electrical Engineers, London, UK.

Darcy, H. (1856). *Les Fontaines Publiques de la Ville de Dijon*, Dalmont, Paris

Davis, J.L., Annan, A.P., 1989. Ground penetrating radar for high resolution mapping of soil and rock stratigraphy. *Geophysical Prospecting* 37, 531–551.

De Hamer W, Love D, Owen RJS, Booij MJ, Hoekstra A. 2008. Potential water supply of a small reservoir and alluvial aquifer system in southern Zimbabwe. *Physics and Chemistry of the Earth* 33: 633–639.

Department of Lands, 1998 Motloutse Sand River Storage Feasibility Study Final Report Wellfield Consulting Services

Department of Meteorological Services Botswana, August 1984. *Climatological Summaries for Botswana*, Ministry of Environment, Wildlife and Tourism.

Dojack, L. (2012). *Ground Penetrating Radar Theory, Data Collection, Processing, and Interpretation: A Guide for Archaeologists*.

Domenico, P. A, and F. W Schwartz. *Physical And Chemical Hydrogeology*. New York: Wiley, 1998. Print.

Doolittle, James A., B. Jenkinson, D. Hopkins, M. Ulmer, W. Tuttle. 2006. Hydrogeological investigations with ground-penetrating radar (GPR): Estimating water-table depths and local ground-waterflow pattern in areas of coarse-textured soils. *Journal of Science* 37:941-949.

Environmentek, CSIR (Council of Scientific and Industrial Research). 2003. Protection and Strategic Uses of Groundwater Resources in Drought Prone Areas of the SADC Region. Groundwater Situation Analysis of the Limpopo River Basin, Summary Report. Prepared for SADC. CSIR Environmentek Report No. ENV-PC 2003-047.

Ermanovics I F, (1980). The Geology of the Mokgware Hills area, Botswana Geological Survey Bulletin, 13.

FAO, 2004, Drought impact mitigation and prevention in the Limpopo River Basin, Land and Water Discussion Paper <http://www.fao.org/docrep/008/y5744e/y5744e00.htm>

Fetter, C.W., 1994. Applied Hydrogeology, third ed. Prentice-Hall, Inc., Upper Saddle River, New Jersey. 691 p.

Fetter, C.W., 2001. Applied Hydrogeology (4th ed.), Prentice-Hall, Upper Saddle River, New Jersey, 598p.

Fisher, E., McMechan, G.A., Annan, A.P., 1992. Acquisition and processing of wide-aperture ground-penetrating radar data. *Geophysics* 57 (3), 495–504.

Franke, O. Lehn, Thomas E Reilly, and Gordon D Bennett, 1987, Definition Of Boundary And Initial Conditions In The Analysis Of Saturated Ground-Water Flow Systems. Washington: an introduction, Dept. of the Interior, U.S. Geological Survey, Techniques of Water-Resources Investigations 03-B5, 4p.

Freeze, R.A., and Cherry, J. A. 1979. Groundwater. Prentice Hall Inc., Englewood Cliffs, New Jersey.

Freeze, R.A., and Cherry, J.A., 1979, Groundwater: Englewood Cliffs, NJ, Prentice-Hall, 604 p.

Galagedara, L., Parkin, G., Redman, J., Von Bertoldi, P. and Endres, A. (2005). Field studies of the GPR ground wave method for estimating soil water content during irrigation and drainage. *Journal of Hydrology*, 301(1), pp.182--197.

Gibbs Sir Alexander & Partners.1969 1970 & 1971, Temporary Water Supply for SelibePhikwe Development

Halcrow., Sir William and Partners.,1982. North – west Somalia refugee water supply consultancy, Oxfam project report.

Harari, Z., 1996. Ground-penetrating radar (GPR) for imaging stratigraphic features and groundwater in sand dunes.*Journal of Applied Geophysics* 36, 43– 52.

Harbaugh,A.W., 2005. A16: MODFLOW-2005, the US Geological Survey modular ground-water module – the Groundwater flow process. *Techniques of Water Resources Investigations of the United States Geological Survey Book 6, Modeling Techniques, Section A: Ground Water*. US Geological Survey. Washington, DC.

Hazen, A. 1892.Some Physical Properties of Sands and Gravels, with Special Reference to their Use in Filtration. 24th Annual Report, Massachusetts State Board of Health, Pub.Doc. No.34, 539-556

Hem, John David. Study And Interpretation Of The Chemical Characteristics Of Natural Water. Dept. of the Interior, U.S. Geological Survey, 1985. Print.

Herbert R, Barker J , Davies J, Katai O,1997.Exploiting Ground Water from Sand Rivers in Botswana using Collector Wells. Proc. 30th /International Geology Congress., Vo/.22, pp. 235-257

Hiscock, K. M. *Hydrogeology*. Malden, MA: Blackwell Pub., 2005. Print.

Holtz,R.D and Kovacs ,W.D. An Introduction to Geotechnical Engineering .Prentice-Hall civil engineering and engineering mechanics series. Prentice Hall.

Hughes DA, Kapangaziwiri E, Baker K. 2010. Initial evaluation of a simple coupled surface and ground water hydrological model to assess sustainable ground water abstractions at the regional scale. Hydrology Research 41: 1–12.irrigation development, in techniques for environmentally sound water resources development. Wooldridge R., (ed) Pentech Press, London. ISBN 0-7273-2107-2.

Huisman, J.A., Sperl, C., Bouten, W., Verstraten, J.M., 2001. Soil water content measurements at different scales: accuracy of time domain reflectometry and ground-penetrating radar. Journal of Hydrology 245, 48– 58.

Jol HM, Bristow CS (2003): GPR in sediments: advice on data collection, basic processing and interpretation, a good practice guide. – In Bristow C S, Jol H M (eds.) Ground penetrating radar in sediments. Geological Society.

Karant, K. R., 1987. Groundwater assessment, development and management. Tata McGRAW – HILL PUBLISHING CO. LTD, pp. 59.

Kasenow, M., 2002.Determination of Hydraulic Conductivity from Grain Size Analysis.Water Resources Publications, Littleton, Colorado.

Kearey, P. and Brooks, M. (1991). *An introduction to geophysical exploration*. 1st ed. Oxford: Blackwell Scientific Publications.

Key R.M, Litherland, M & Hepworth, J.V. 1976. The evolution of the Archaean crust of northeastern Botswana. *Precambrian Research*, 3, 275-413.

King J, Brown C Sabet H. 2003. A scenario-based approach to environmental flow assessments for rivers. *River Research and Applications* 19:619–639. DOI: 10.1002/rra.709

Kondolf GM, Swanson ML. 1993. Channel adjustments to reservoir construction and gravel extraction along Stony Creek, California. *Environmental Geology* 21: 256–269.

Kozeny, J. 1927. Über Kapillare Leitung Des Wassers in Boden. *Sitzungsber Akad. Wiss. Wien Math. Naturwiss. Kl., Abt. 2a*, 136, 271-306 (In German).

Landon, M.K., Rus, D.L., Harvey, F.E., 2001. Comparison of instream methods for measuring hydraulic conductivity in sandy streambeds. *Ground Water* 39 (6), 870–885.

Lasage R, Aerts J, Mutiso G-CM, de Vries A. 2007. Potential for community based adaptation to droughts: sand dams in Kitui, Kenya. *Physics and Chemistry of the Earth* 33: 67–73.

Leckebusch, Jürg 2003 Ground-penetrating Radar: A Modern Three-dimensional Prospection Method. *Archaeological Prospection* 10:213-240.

Liner, C. and Liner, J. (1995). Ground-penetrating radar: a near-face experience from Washington County, Arkansas. *The Leading Edge*, 14(1), pp.17--21.

Love D, Walsh KL. 2009. Geological evidence does not support suggestions of mining in the Nyanga upland culture. *Prehistory Society of Zimbabwe Newsletter* 140: 1–6. Love D,

Uhlenbrook S, Twomlow S, van der Zaag P. 2010. Changing rainfall and discharge patterns in the northern Limpopo Basin, Zimbabwe. *Water SA*. 36.

Love, D., Hamer, W. de, Owen, R., Booij, M., Uhlenbrook, S., Hoekstra, A. and Zaag, P. van der. 2007. Case studies of groundwater: Surface water interactions and scale relationships in small alluvial aquifers. Paper presented at the 8th Water Net/WARFSA/GWP-SA Annual Symposium, Lusaka, Zambia, 31 October -2 November 2007. Amsterdam, Netherlands: Water Net.

Lunt, I., Hubbard, S. and Rubin, Y. (2005). Soil moisture content estimation using ground-penetrating radar reflection data. *Journal of Hydrology*, 307(1), pp.254--269.

McDonald, M.G., and Harbaugh, A.W., 1988, A modular three-dimensional finite-difference ground-water flow model: Techniques of Water-Resources Investigations of the United States Geological Survey, Book 6, Chapter A1, 586 p.

MacDonald, M and Partners, (1990). Motloutse Dam feasibility/preliminary design study. Volume 5: Annex B, F.

Mansell, M.G., Hussey, S., 2005. An investigation of flows and losses within the alluvial sands of ephemeral rivers in Zimbabwe. *Journal of Hydrology* 314, 192 – 203.

Masvopo, T.; Love, D.; Makurira, H. 2008. Evaluation of the groundwater potential of the Malala Alluvial Aquifer, Lower Mzingwane River, Zimbabwe. In, *Abstract Volume, 9th WaterNet/WARFSA/GWP-SA Symposium, Johannesburg, South Africa, October 2008*, p7

Meinzer, O. E. (1923), The occurrence of groundwater in the United States, with a discussion of principles, U.S. Geol. Surv. Water Supply Pap., 489.

Moyce, W., Mangeya, P., Owen, R., and Love, D., 2006. Alluvial aquifers in the Mzingwane Catchment: their distribution, properties, current usage and potential expansion. *Physics and Chemistry of the Earth*, 31, 988-994.

Neal A 2004 Ground-penetrating radar and its use in sedimentology: principles, problems and progress; *Earth Sci.Rev.* **66** 261–330.

Neubauer, W., A. Eder-Hinterleitner, S. Seren, and Melichar P.2002 Georadar in the Roman Civil Town Carnuntum, Austria: An Approach for Archaeological Interpretation of GPR Data. *Archaeological Prospection* 9:135-156.

Neuman, S.P. and P.A. Witherspoon, 1969. Theory of flow in a confined two aquifer system, *Water Resources Research*, vol. 5, no. 4, pp. 803-816.

Nord, M., 1985. Sand rivers of Botswana, Phase 2. Department of Water Affairs, Government of Botswana.

Odong, J., 2007. Evaluation of empirical formulae for determination of hydraulic conductivity based on grain-size analysis. *Journal of American Science* 3 (3), 54–60.

Oosterbaan, R.J. & Nijland, H.J. 1994. Determining the saturated hydraulic conductivity. In H.P. Ritzema, ed. *Drainage principles and applications*, pp. 435–475. 2nd edition. ILRI Publication 16. Wageningen, The Netherlands, ILRI.

Owen RJS and Rydzewski JR., 1991. Shallow groundwater as a resource for small-scale

Owen RJS. (1994) Water resources for small scale irrigation from shallow alluvial aquifers in the communal lands of Zimbabwe. MPhil thesis, Department of Civil Engineering, University of Zimbabwe.

Owen, R., and Dahlin T., 2005. Alluvial aquifers at geological boundaries: geophysical investigations and groundwater resources. In: Bocanegra E, Hernandez M. and Usunoff E. (Eds.) Groundwater and Human Development, AA Balkema Publishers, Rotterdam, pp233-246.

Owen, R.J.S., 2000. Conceptual Models for the Evolution of Groundwater Flow Paths in Shallow Aquifers in Zimbabwe. Unpublished DPhil Thesis. University of Zimbabwe.

Owen R (2012) Groundwater needs assessment. Limpopo Basin Commission, LIMCOM. http://www.splash-era.net/downloads/groundwater/2_LIMCOM_final_report.pdf. Accessed 16 April 2015.

Pallett, J. (ed.): 1997: Sharing water in southern Africa, Desert Research Foundation of Namibia, Windhoek.

Paya B.K, 1996, The Geology of Bobonong Area, An explanation of the Geology of that part of Quarter degree sheet 2128C within Botswana. Bulletin 40, Botswana Geological Services, Lobatse Botswana.

Reeves, C V 1978. A failed Gondwana spreading axis in southern Africa. *Nature*, 273, 222

Reynolds, J.M., 1997. An Introduction to Applied and Environmental Geophysics. Wiley, New York.

Sawunyama T. MSc. Thesis IWRM estimation of small reservoir storage capacities in Limpopo river basin using geographical information systems (gis) and remotely sensed surface areas, (unpublished)

Sawyer Clair Nathan, and Perry Lee Maccarty. Chemistry For Sanitary Engineers [By] Clair N. Sawyer [And] Perry L. Mccarty. 2D Ed. New York: McGraw-Hill, 1967. Print.

Schenk, C.J., Gautier, D.L., Olhoeft, G.R., Lucius, J.E., 1993. Internal structure of an eolian dune using ground-penetrating radar. *Special Publications International Association of Sedimentology* 16, 61–69.

Schicht, R.J., and Walton, W.C., 1961, Hydrologic budgets for three small watersheds in Illinois: Illinois State Water Survey, Report of Investigation 40, 40 p

Schmalz, B. and Lennartz, B. (2002). Analyses of soil water content variations and GPR attribute distributions. *Journal of Hydrology*, 267(3), pp.217--226.

Sensors & Software 2003 *EKKO_View Enhanced & EKKO_View Deluxe User's Guide*. Sensors & Software, Mississauga.

Shields FD Jr, Simon A, Steffen LJ. 2000. Reservoir effects on downstream river channel migration. *Environmental Conservation* 27: 54–66.

Skinner, A C. 1978a. The geology of the Mahalapye area. *Bulletin Geological Survey of Botswana*, 9, 60pp.

Smith, M.C., Vellidis, G., Thomas, D.L., Breve, M.A., 1992. Measurement of water table fluctuations in a sandy soil using ground penetrating radar. *Transactions of the American Society of Agricultural Engineers* 35, 1161– 1166.

Song J, Chen XH, Cheng C, Wang D, Lackey S, Xu Z (2009) Feasibility of grain-size analysis methods for determination of vertical hydraulic conductivity of streambeds. *J Hydrol* 375(3-4):428–437

Todd, D.K. (1988). *Ground water hydrology*. John Wiley & Sons, New York, 535pp

Todd, D.K., 1980, Ground-water hydrology (Second Edition): John Wiley and Sons, New York, 535 p

Todd,D.K., and Mays, L.W. 2005.Groundwater Hydrology. John Wiley & Sons, New York.

Topp, G.C., Davis, J.L., Annan, A.P., 1980. Electromagnetic determination of soil water content.Measurements in coaxial transmission lines. *Water Resour. Research* 16, 572–582.

Townley, L.R., 1998. Shallow groundwater systems. In: Dillon, P. and Simmers, I. (Eds.) *International Contributions to Hydrogeology 18: Shallow Groundwater Systems*. Balkema, Rotterdam, pp3-12.

Turesson, A. (2006). Water content and porosity estimated from ground-penetrating radar and resistivity. *Journal of Applied Geophysics*, 58(2), pp.99--111.

Uhlenbrook, S., Roser, S., Tilch, N., 2004. Hydrological process representation at themeso-scale: the potential of a distributed, conceptual catchment model. *Journal of Hydrology*, 291: 278-296.

Uma,K.O.,Egboka,B.C.E., and Onuoha,K.M.1989. New Statistical Grain-Size Method for Evaluating the Hydraulic Conductivity of Sandy Aquifers. *Journal of Hydrology*, Amsterdam,108,367-386. 16

Van Dam, R. and Schlager, W. (2000).Identifying causes of ground-penetrating radar reflections using time-domain reflectometry and sedimentological analyses.*Sedimentology*, 47(2), pp.435--449.

Van der Zaag P, Gupta J. 2008. Scale issues in the governance of waterstorage projects. *Water Resources Research* 44: W10417. DOI: 10.1029/2007WR006364

vanOvermeeren, R.A., 1998. GPR and wetlands of The Netherlands. In: Plumb, R.G. (Ed.), Proceedings of the Seventh International Conference on Ground-Penetrating Radar, May 27 to 30, 1998, Lawrence, Kansas. Radar Systems and Remote Sensing Laboratory, University of Kansas, pp. 251–258.

Vukovic, M., and Soro, A. 1992. Determination of Hydraulic Conductivity of Porous Media from Grain-Size Composition. Water Resources Publications, Littleton, Colorado

Wakefield J. 1977. The structural and metamorphic history of the Phikwe area—evidence for post-Great dyke deformation in the Limpopo mobile belt. 141-156 in Ermanovics IF, Key RM & McEwen G (editors). The proceedings of a seminar pertaining to the Limpopo Mobile belt. Botswana Geological survey Bulletin, 12.

Ward JV, Stanford JA. 1995. Ecological connectivity in alluvial river ecosystems and its disruption by flow regulation. Regulated Rivers: Research and Management 11: 105–119
DOI: 10.1002/rrr.345011010

Wikner, T., 1980. Sand rivers of Botswana, Phase 1. Department of Water Affairs, Government of Botswana.

Wipplinger, O., 1958. Storage of Water in Sand. South West Africa Administration Water Affairs Branch, Windhoek, Namibia.

Woodward, J., Ashworth, P., Best, J., Smith, G. and Simpson, C. (2003). The use and application of GPR in sandy fluvial environments: methodological considerations. *Geological Society, London, Special Publications*, 211(1), pp.127--142.

World Health Organization., 1993. Guideline for drinking water quality, recommendations. Second Edition, Geneva.

WSB, 2007. Bobonong Groundwater Investigation and Development Project. Tender Number PR 10/3/3/07 II. Prepared by Water Surveys Botswana for Geological Survey Dept, Govt. Botswana.

Zheng, Chunmiao, and G.D, Bennete. 1995. Applied contaminate transport modelling. New York : VanNostrand Reinhold, 440 pages.

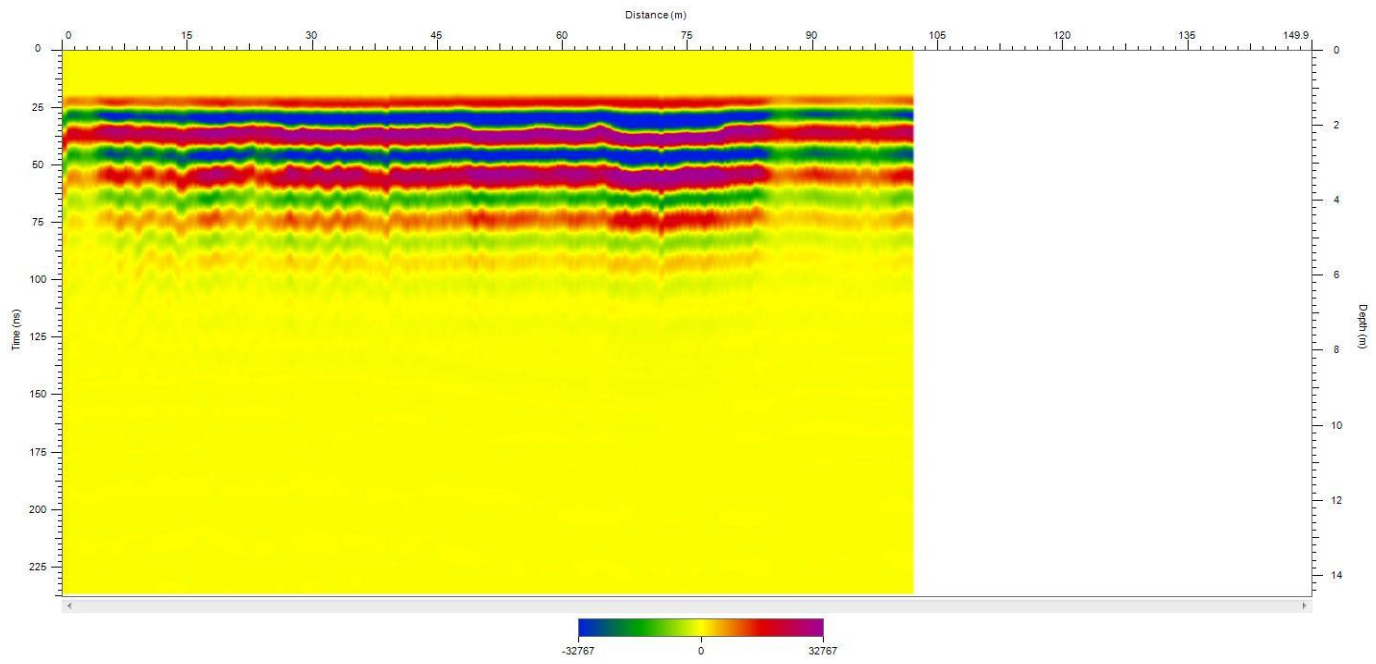
APPENDICES APPENDIX A

GPR RADARGRAMS

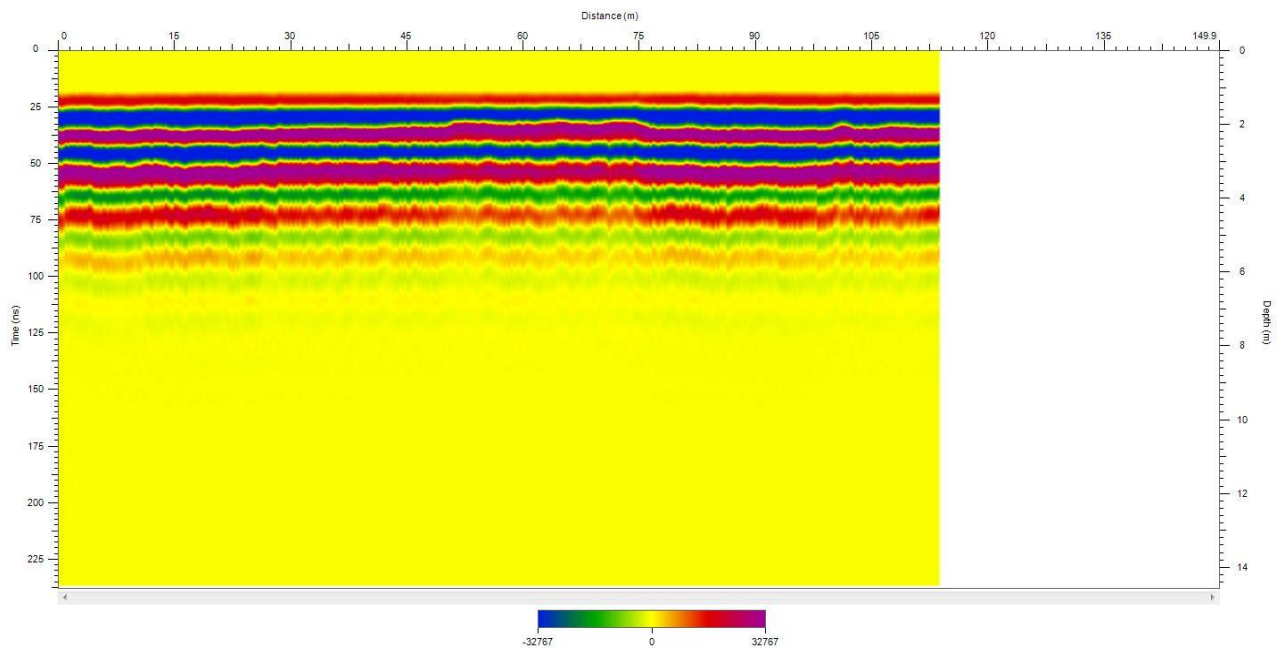
A1

Viewer software

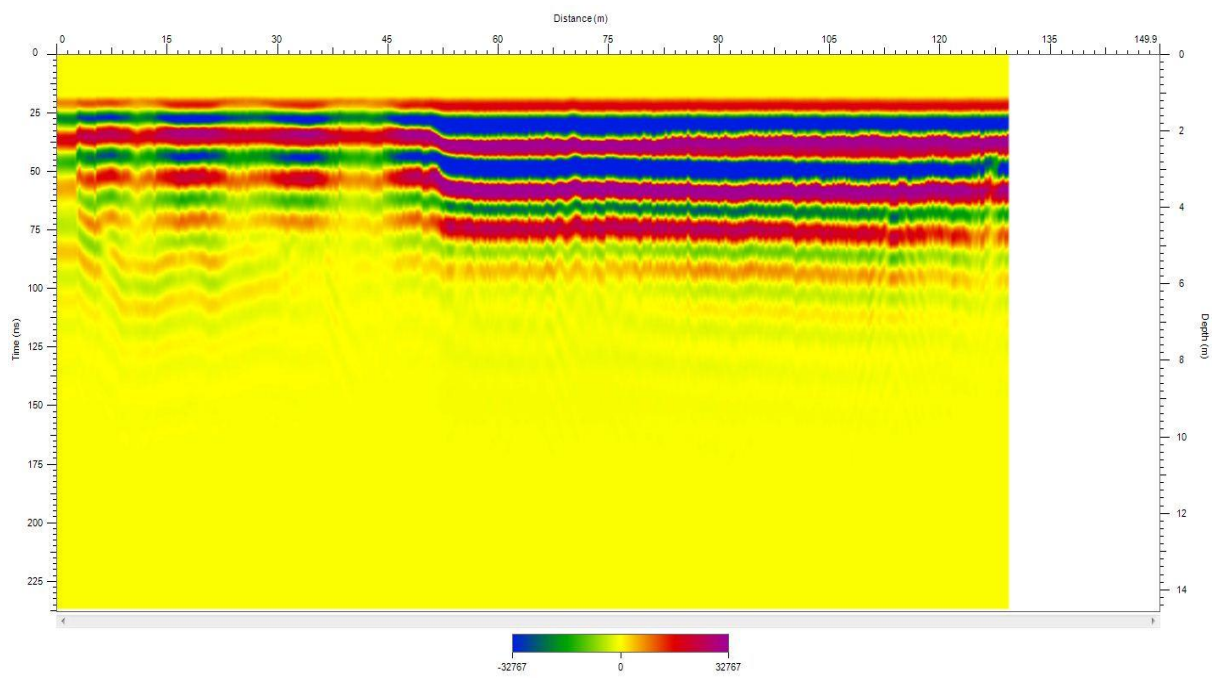
File number:0142



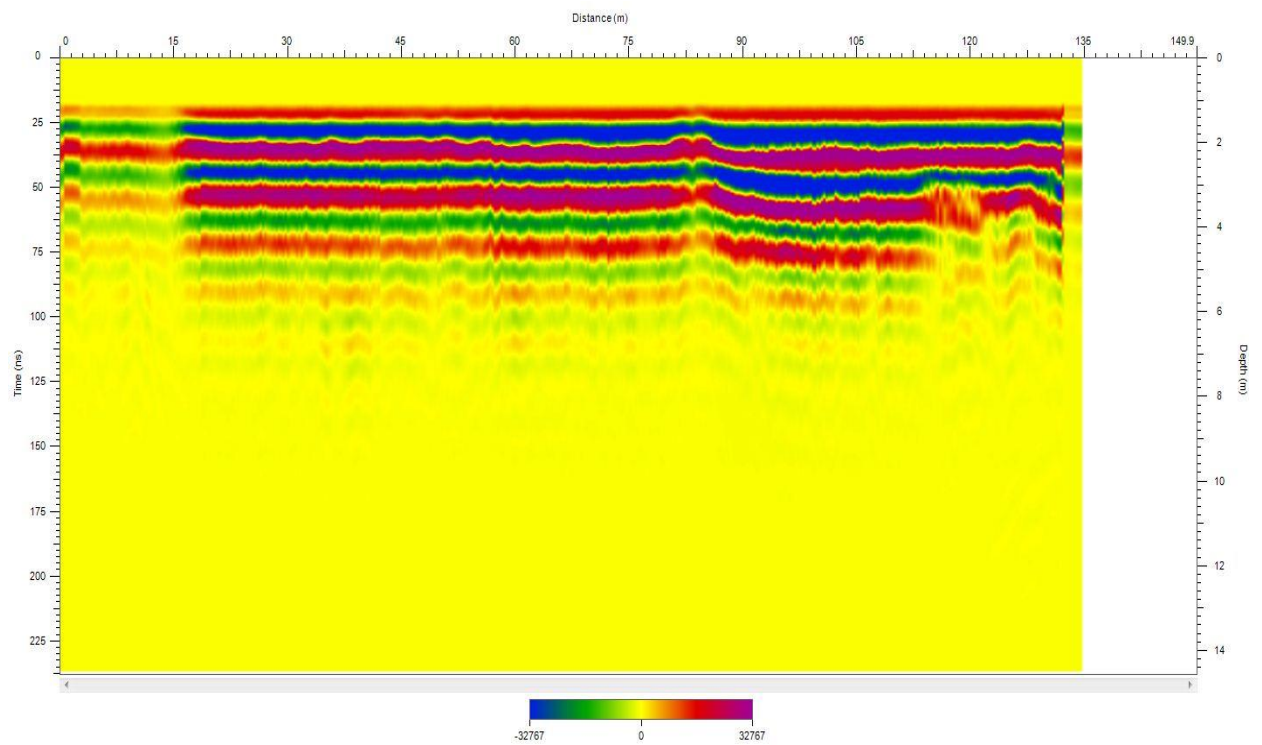
File number:0143



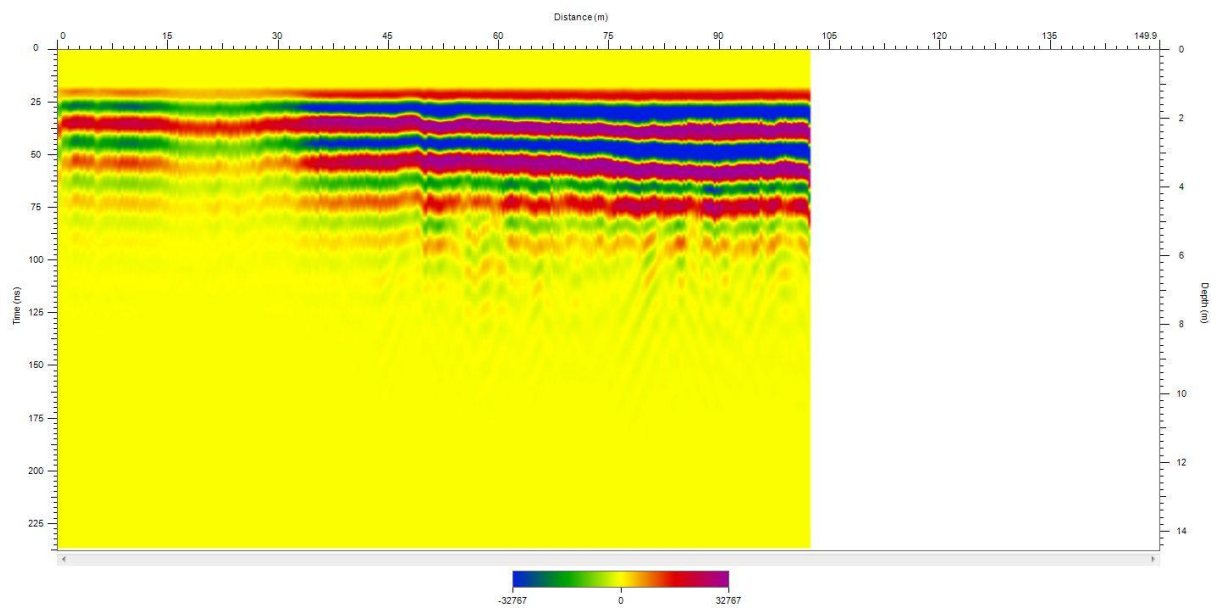
File number:0144



File number:0145



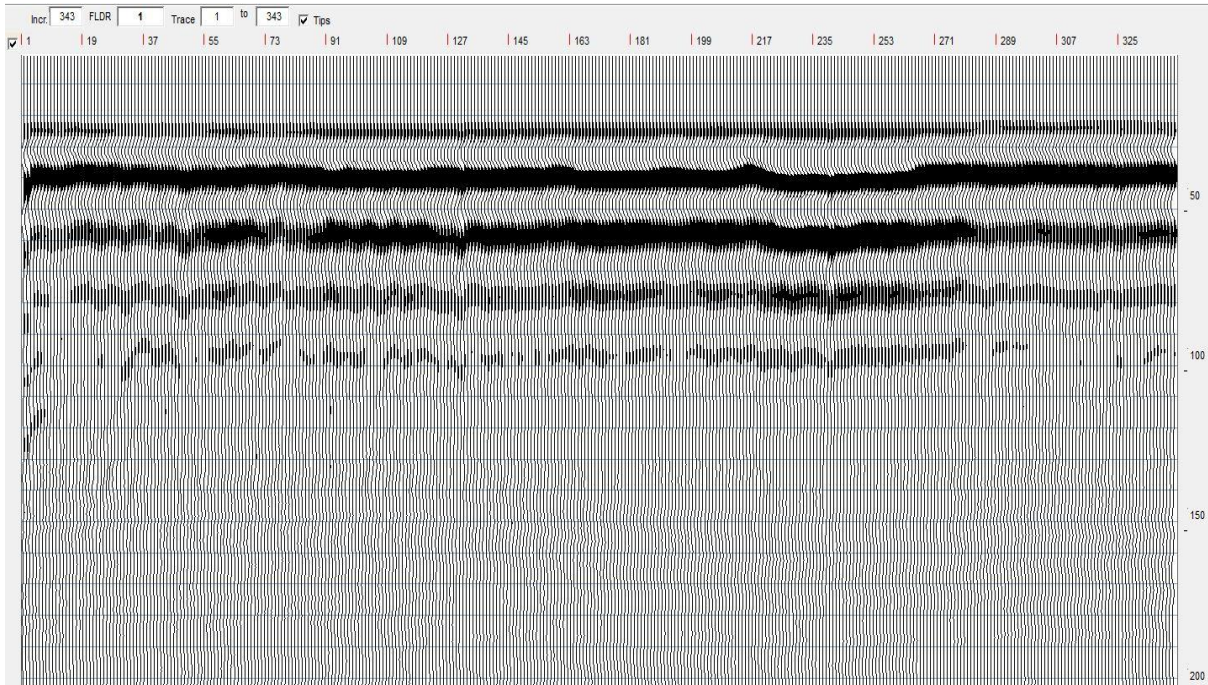
File number:0146



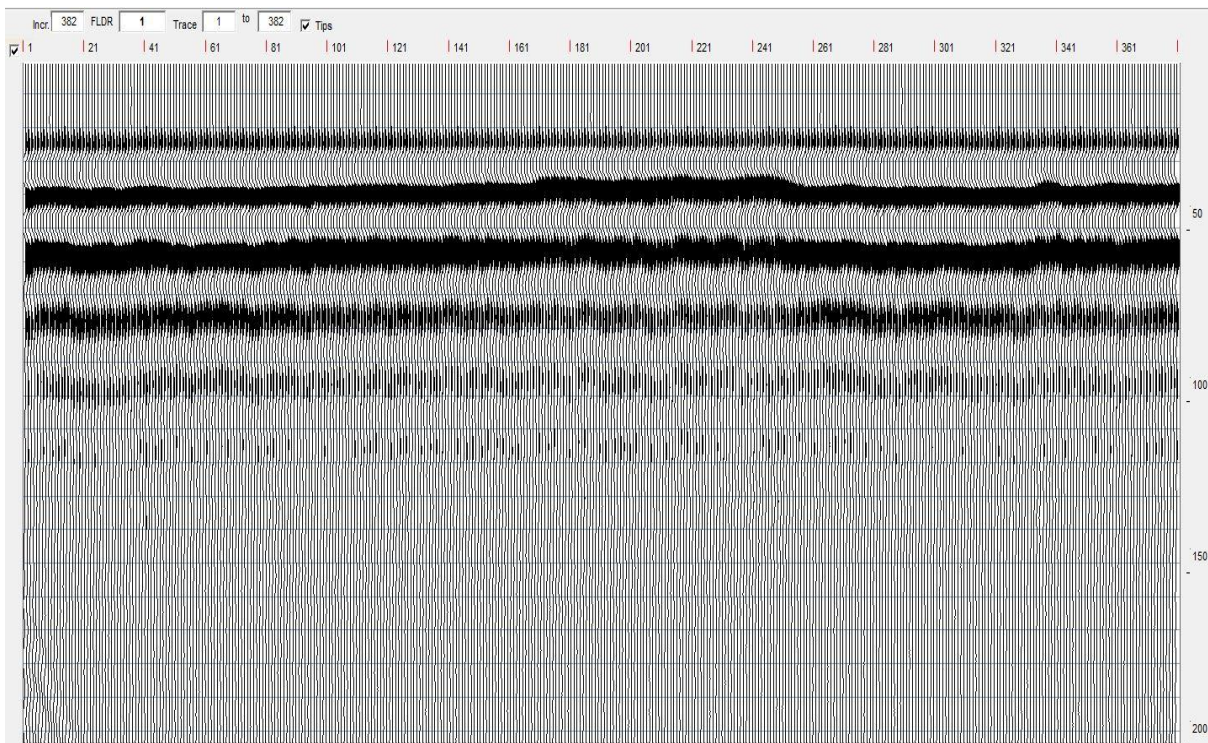
A2

SUNT Radargrams

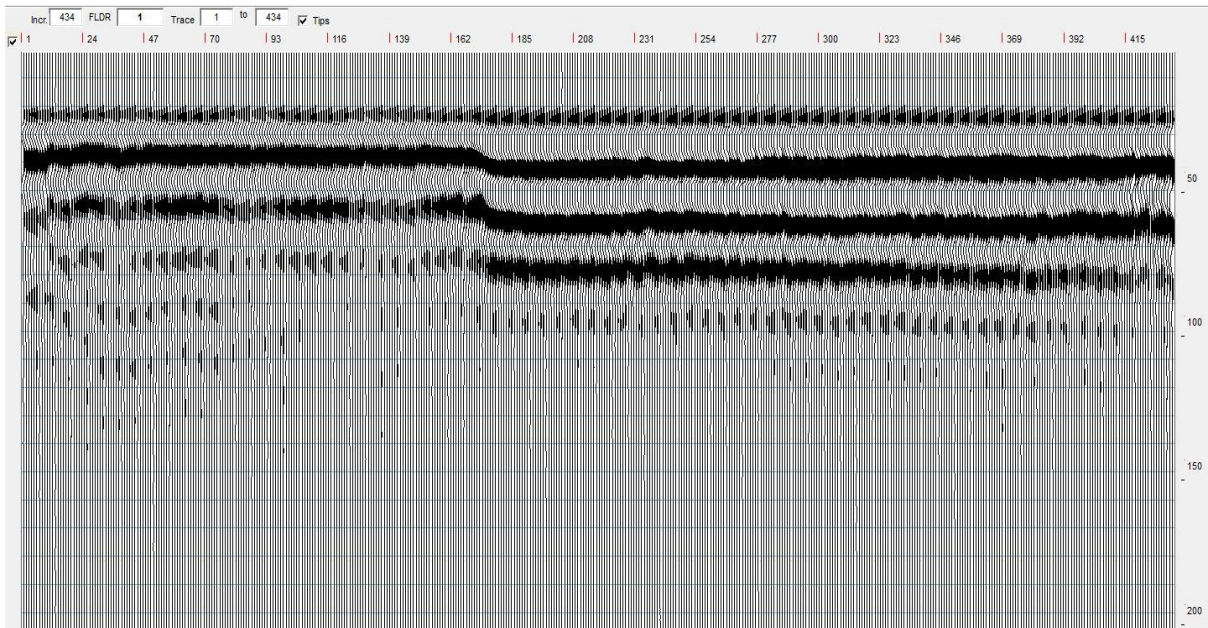
File number:0142



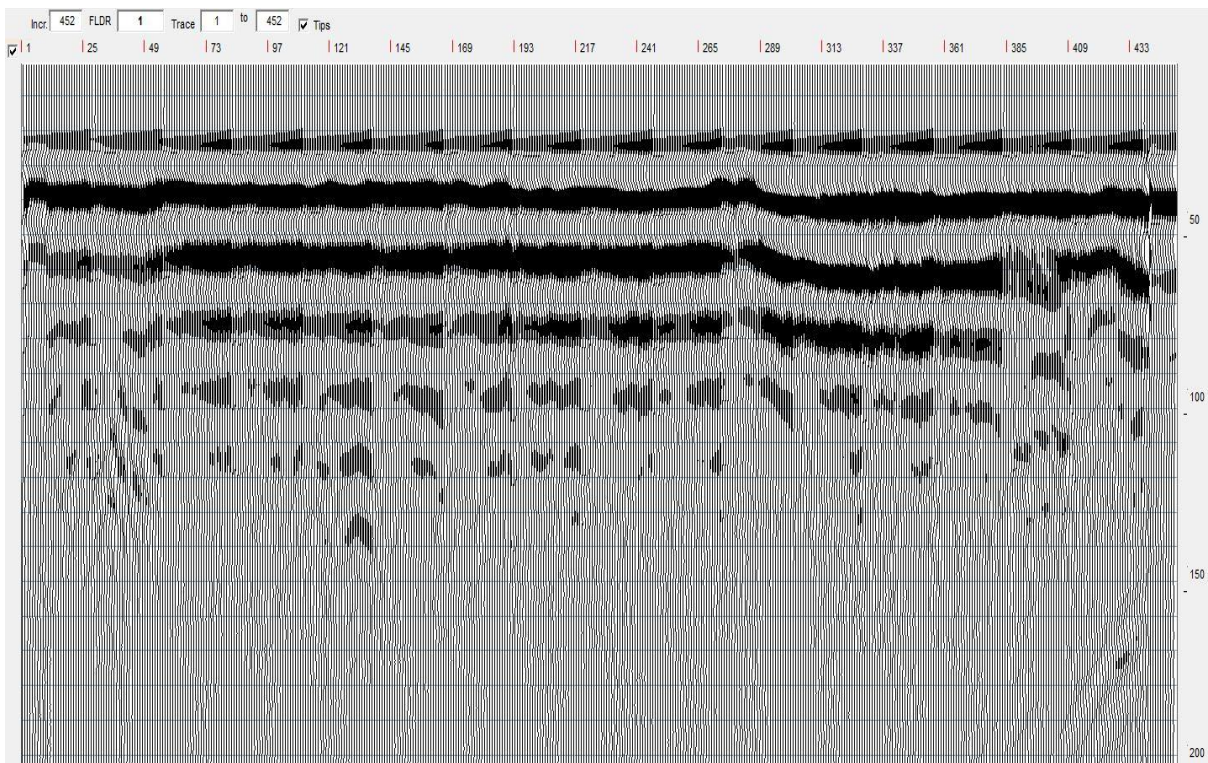
File number:0143



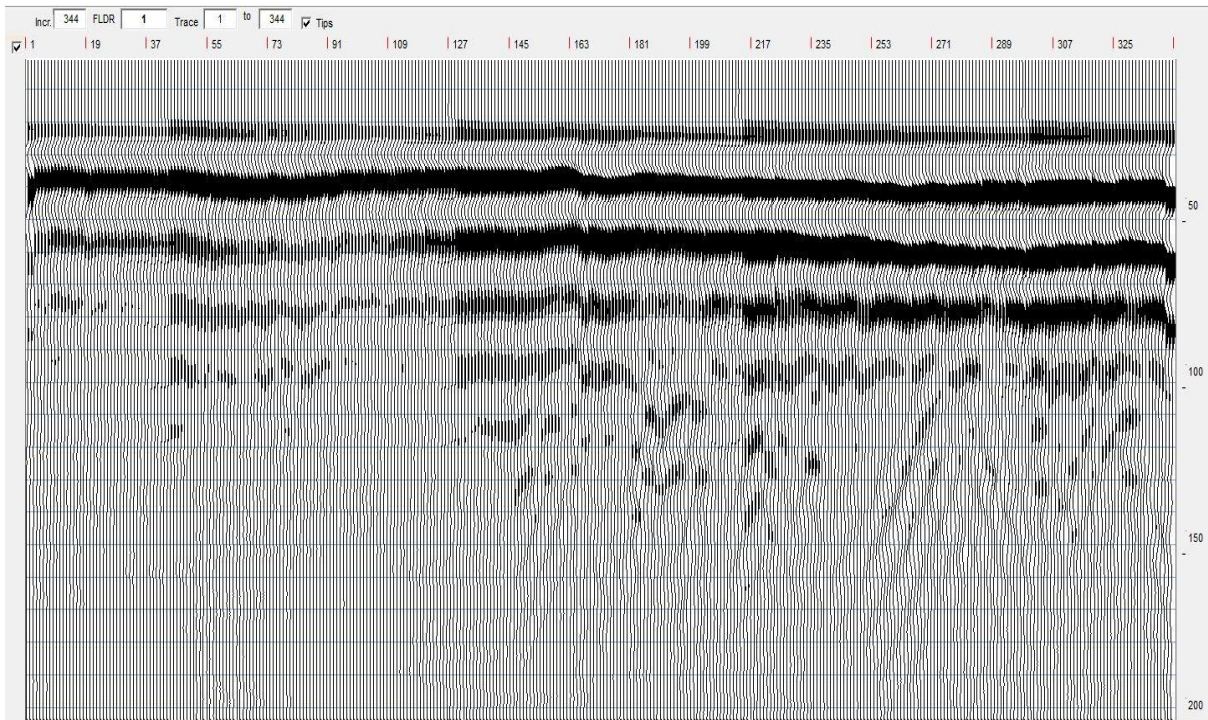
File number:0144



File number:0145

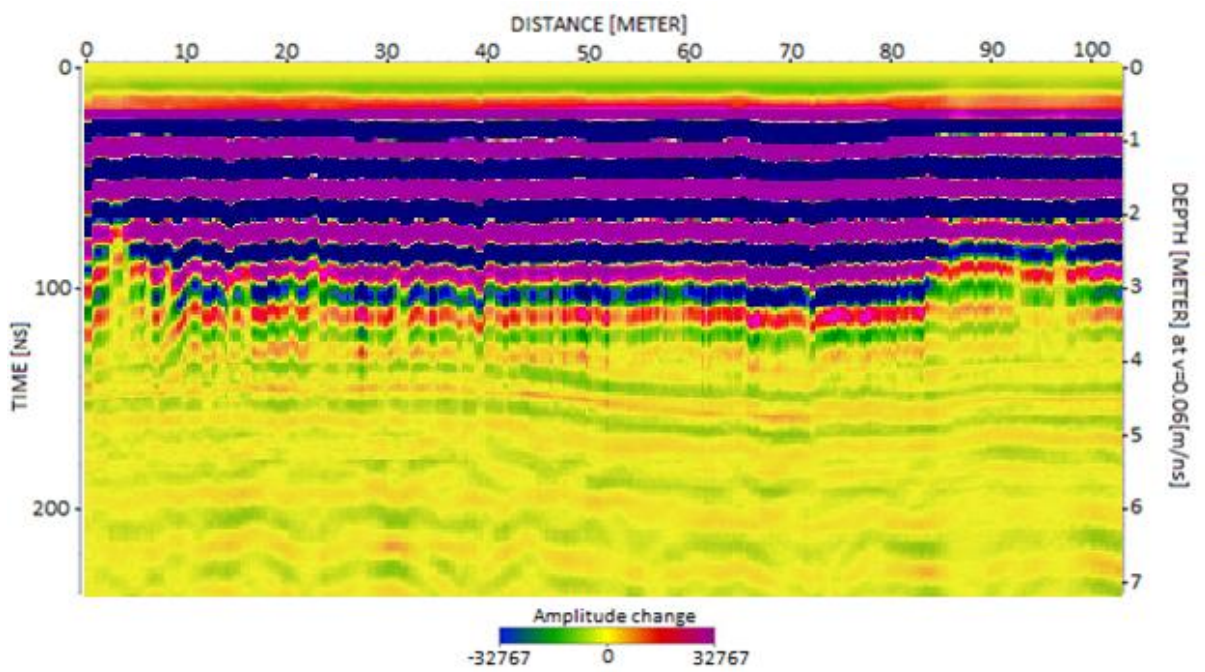
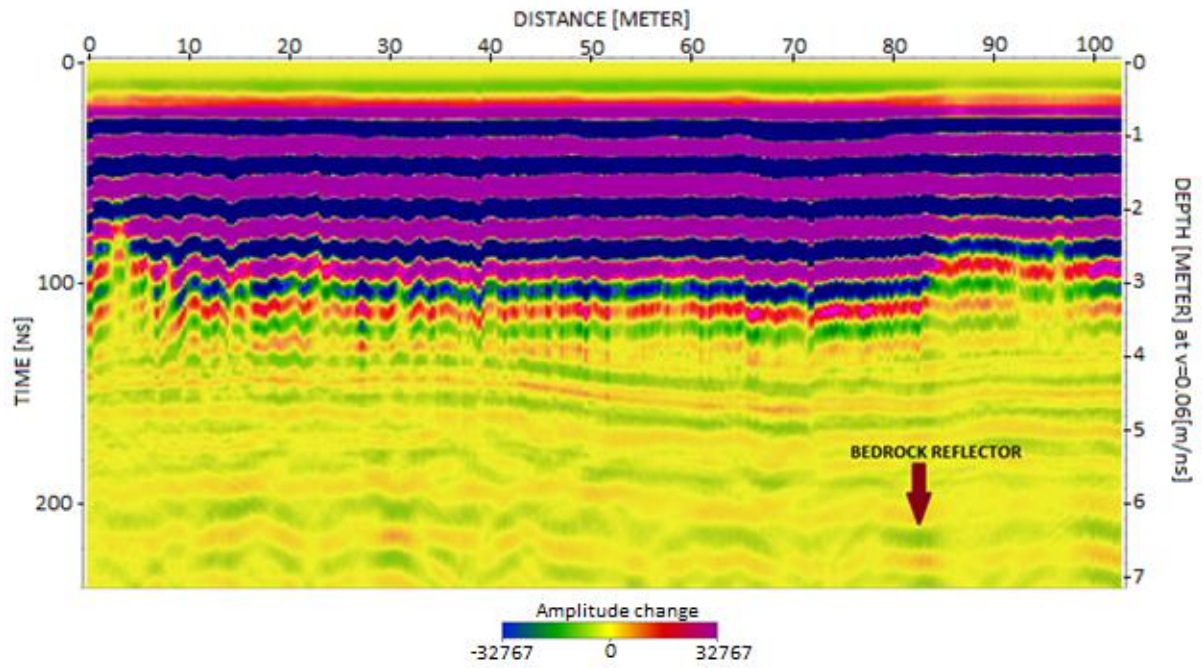


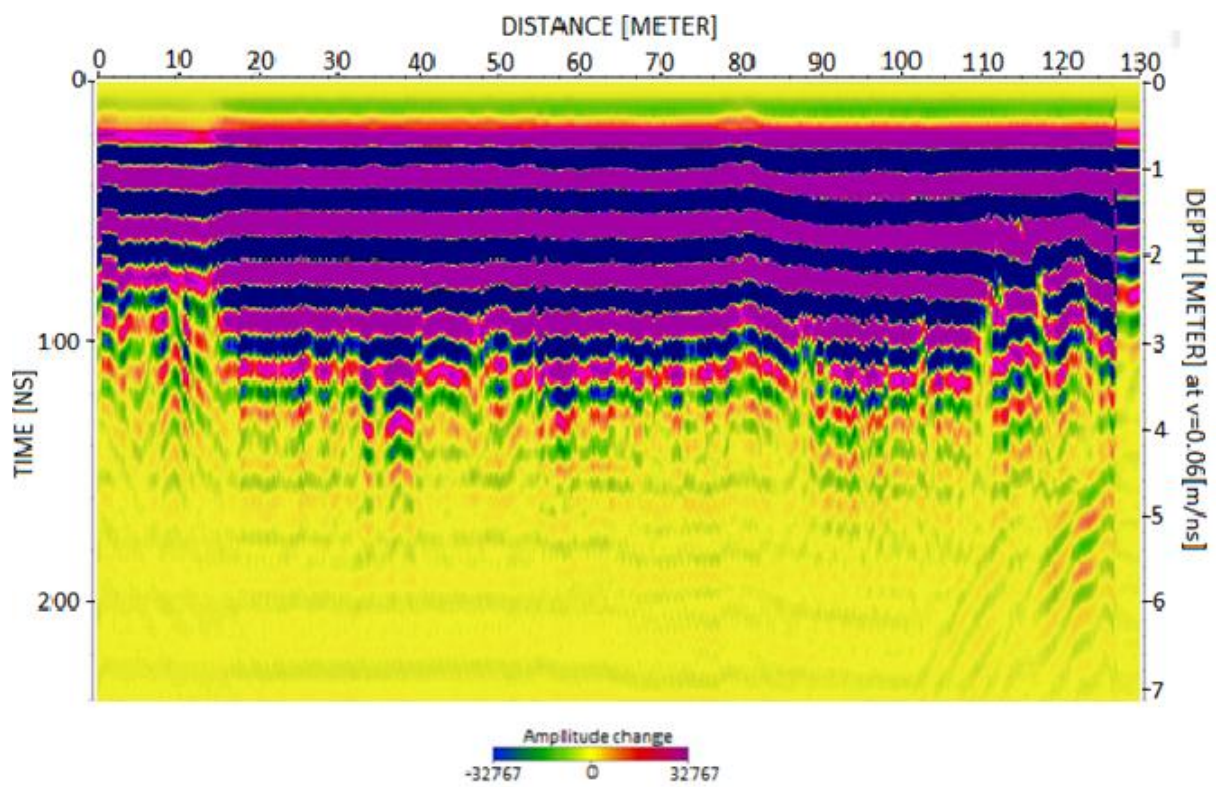
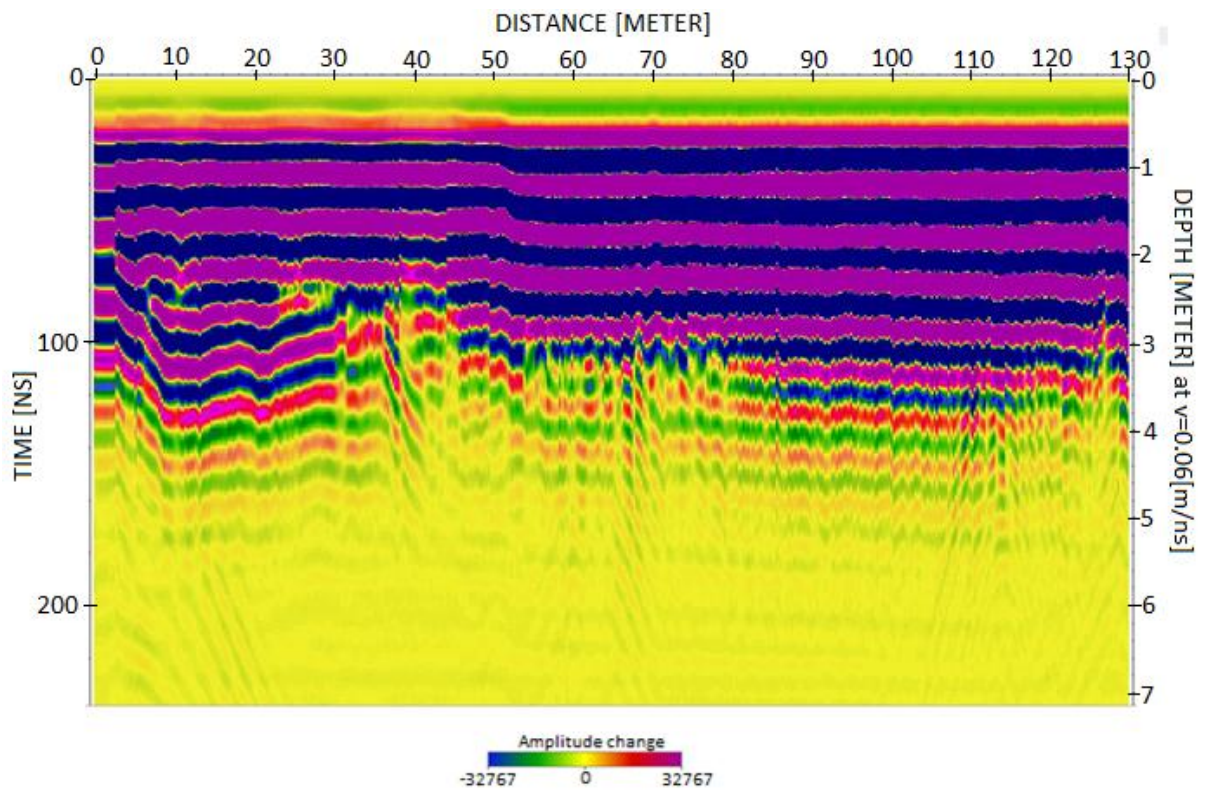
File number:0146

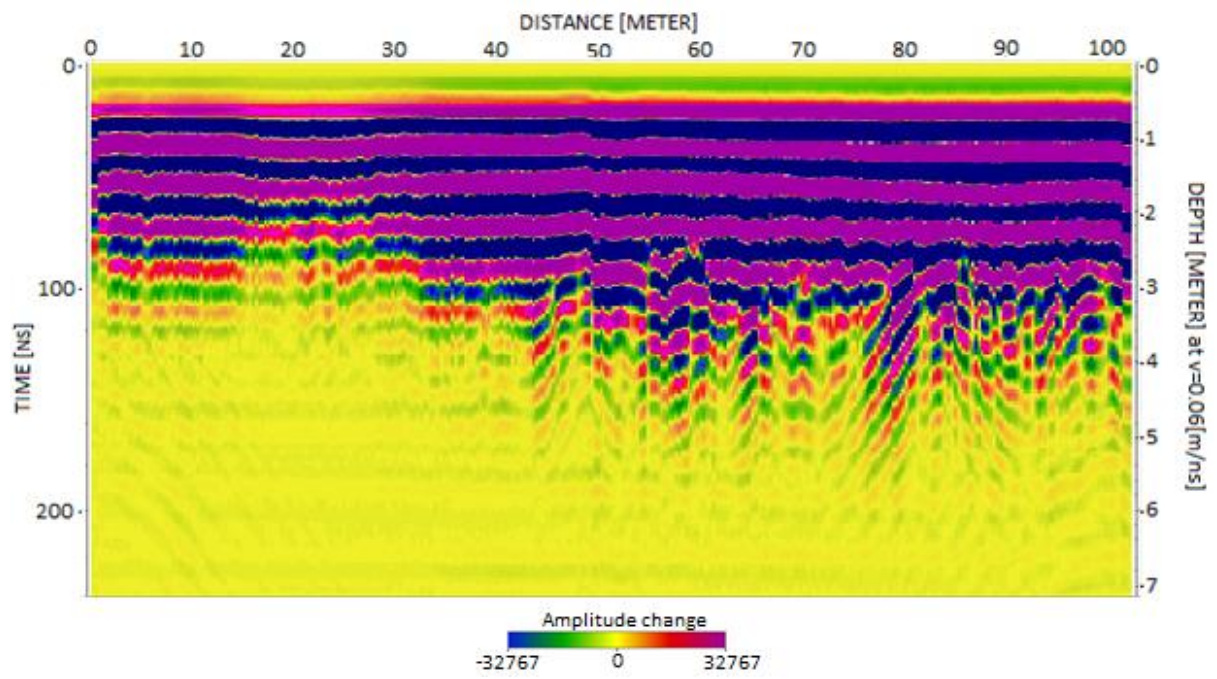


A3

Processed Radargrams







APPENDIX B

SIEVE DATA SHEETS AND SLUG TESTS

Project Information:

Project: Motloutse Alluvial Aquifer

Sample ID: S1-1

Test Date: 2/09/2016

Sieve Data:

Wet Sample & Pan Wt.(g): 0.00

Dry Sample & Pan Wt.(g): 1697.00

Pan Weight(g): 250.00

Dry Sample Wt.(g): 1447.00

Percent Moisture: -117.28

Split Sample: No

Split Sieve Size:

Sieve Size Data

Sieve	Size (mm)	Weight Retained	Cumulative Weight	Specs	% Passing
3"	75	0	0		
2.5"	63.5	0	0		
2"	50.8	0	0		
1.5"	37.5	0	0		
1"	25	0	0		
3/4"	19	0	0		
1/2"	12.7	0	0		
3/8"	9.5	17	17		98.83
1/4"	6.3	23	40		97.24
#4	4.75	21	61		95.78
#8	2.36	130	191		86.80
#10	2	0	0		
#16	1.18	377	568		60.75
#20	0.85	0	0		
#30	0.6	544	1112		23.15
#40	0.425	0	0		
#50	0.3	245	1357		6.22
#60	0.25	0	0		
#100	0.15	51	1408		2.70
#200	0.075	37	1445		0.14
Pan		2.00			

Project Information:

Project: Motloutse Alluvial Aquifer

Sample ID: S1-2

Test Date: 2/09/2016

Sieve Data:

Wet Sample & Pan Wt.(g): 0.00

Dry Sample & Pan Wt.(g): 1721.00

Pan Weight(g): 250.00

Dry Sample Wt.(g): 1471.00

Percent Moisture: -117.00

Sieve Size Data

Sieve	Size (mm)	Weight Retained	Cumulative Weight	Specs	% Passing
3"	75	0	0		
2.5"	63.5	0	0		
2"	50.8	0	0		
1.5"	37.5	0	0		
1"	25	0	0		
3/4"	19	0	0		
1/2"	12.7	0	0		
3/8"	9.5	156	156		89.39
1/4"	6.3	60	216		85.32
#4	4.75	54	270		81.65
#8	2.36	227	497		66.21
#10	2	0	0		
#16	1.18	377	874		40.58
#20	0.85	0	0		
#30	0.6	352	1226		16.66
#40	0.425	0	0		
#50	0.3	208	1434		2.52
#60	0.25	0	0		
#100	0.15	31	1465		0.41
#200	0.075	5	1470		0.07
Pan		1.00			

Project Information:

Project: Motloutse Alluvial Aquifer

Sample ID: S1-3

Test Date: 2/09/2016

Sieve Data:

Wet Sample & Pan Wt.(g): 0.00

Dry Sample & Pan Wt.(g): 1684.00

Pan Weight(g): 250.00

Dry Sample Wt.(g): 1434.00

Percent Moisture: -117.43

Sieve Size Data

Sieve	Size (mm)	Weight Retained	Cumulative Weight	Specs	% Passing
3"	75	0	0		
2.5"	63.5	0	0		
2"	50.8	0	0		
1.5"	37.5	0	0		
1"	25	0	0		
3/4"	19	0	0		
1/2"	12.7	0	0		
3/8"	9.5	67	67		95.33
1/4"	6.3	95	162		88.70
#4	4.75	143	305		78.73
#8	2.36	501	806		43.79
#10	2	0	0		
#16	1.18	301	1107		22.80
#20	0.85	0	0		
#30	0.6	240	1347		6.07
#40	0.425	0	0		
#50	0.3	68	1415		1.32
#60	0.25	0	0		
#100	0.15	14	1429		0.35
#200	0.075	4	1433		0.07
Pan		1.00			

Project Information:

Project: Motloutse Alluvial Aquifer

Sample ID: S1-4

Test Date: 2/09/2016

Sieve Data:

Wet Sample & Pan Wt.(g): 0.00

Dry Sample & Pan Wt.(g): 1621.00

Pan Weight(g): 250.00

Dry Sample Wt.(g): 1371.00

Percent Moisture: -118.23

Sieve Size Data

Sieve	Size (mm)	Weight Retained	Cumulative Weight	Specs	% Passing
3"	75	0	0		
2.5"	63.5	0	0		
2"	50.8	0	0		
1.5"	37.5	0	0		
1"	25	0	0		
3/4"	19	0	0		
1/2"	12.7	0	0		
3/8"	9.5	0	0		
1/4"	6.3	15	15		98.91
#4	4.75	20	35		97.45
#8	2.36	125	160		88.33
#10	2	0	0		
#16	1.18	229	389		71.63
#20	0.85	0	0		
#30	0.6	470	859		37.35
#40	0.425	0	0		
#50	0.3	384	1243		9.34
#60	0.25	0	0		
#100	0.15	89	1332		2.84
#200	0.075	34	1366		0.36
Pan		5.00			

Project Information:

Project: Motloutse Alluvial Aquifer

Sample ID: S1-5

Test Date: 2/09/2016

Sieve Data:

Wet Sample & Pan Wt.(g): 0.00

Dry Sample & Pan Wt.(g): 1751.00

Pan Weight(g): 250.00

Dry Sample Wt.(g): 1501.00

Percent Moisture: -118.23

Sieve	Size (mm)	Weight Retained	Cumulative Weight	Specs	% Passing
3"	75	0	0		
2.5"	63.5	0	0		
2"	50.8	0	0		
1.5"	37.5	0	0		
1"	25	0	0		
3/4"	19	0	0		
1/2"	12.7	7	7		99.53
3/8"	9.5	168	175		88.34
1/4"	6.35	65	240		84.01
#4	4.75	47	287		80.88
#8	2.36	231	518		65.49
#10	2	0	0		
#16	1.18	385	903		39.84
#20	0.85	0	850		
#30	0.6	374	1277		14.92
#40	0.425	0	1152		
#50	0.3	201	1478		1.53
#60	0.25	0	1294		
#100	0.15	18	1496		0.33
#200	0.075	2	1498		0.20
Pan		3.00			

S1-1	volume(l)	time trial 1	time trial 2	time trial 3	time trial 4	avg t	K in m/s	K in m/day	corrected k
	1	66	52	49	51	54.5	0.001523	131.58333	114.3985483
	2	137	115	111	114	119.25	0.001392	120.27323	104.5655494
	3	199	172	171	171	178.25	0.001397	120.69495	104.9321888
	4	263	232	229	231	238.75	0.001391	120.14729	104.4560567
	5	309	295	290	293	296.75	0.001399	120.83052	105.050057
							a mean	122.70587	106.6804801
							g mean	122.62808	106.6128511

	volume(l)	time trial 1	time trial 2	time trial 3	time trial 4	avg t	K in m/s	K in m/day	corrected k
S1-2	1	65	50	48	50	53.25	0.001559	134.67214	117.0839603
	2	135	116	108	110	117.25	0.001416	122.3248	106.3491835
	3	200	170	165	160	173.75	0.001433	123.82086	107.649857
	4	265	230	228	228	237.75	0.001396	120.65264	104.8954092
	5	310	296	290	290	296.5	0.0014	120.9324	105.1386321
							a mean	124.48057	108.2234084
							g mean	124.37501	108.1316338

	volume(l)	time trial 1	time trial 2	time trial 3	time trial 4	avg t	K in m/s	K in m/day	corrected k
S1-3	1	48	52	50	45	48.75	0.001703	147.10342	127.8917105
	2	106	105	103	104	104.5	0.001589	137.2496	119.3248016
	3	171	155	164	165	163.75	0.001521	131.38244	114.2238941
	4	244	229	230	232	233.75	0.00142	122.71729	106.6904109
	5	283	279	284	282	282	0.001472	127.15056	110.5446965
							a mean	133.12066	115.7351027
							g mean	132.85535	115.5044391

	volume(l)	time trial 1	time trial 2	time trial 3	time trial 4	avg t	K in m/s	K in m/day	corrected k
S1-4	1	60	52	58	61	57.75	0.001437	124.1782	107.9605348
	2	115	114	110	113	113	0.001469	126.9255	110.3490422
	3	181	192	186	185	186	0.001339	115.666	100.5600143
	4	245	240	245	248	244.5	0.001358	117.3217	101.9995237
	5	300	281	298	305	296	0.001402	121.1367	105.3162312
							a mean	121.0456	105.2370692
							g mean	120.9737	105.1745045

	volume(l)	time trial 1	time trial 2	time trial 3	time trial 4	avg t	K in m/s	K in m/day	corrected k
S1-5	1	55	49	48	52	51	0.001627	140.61356	122.2494291
	2	134	100	105	106	111.25	0.001492	128.9221	112.0848698
	3	178	154	157	158	161.75	0.001539	133.00695	115.6362452
	4	251	220	224	221	229	0.00145	125.26273	108.9034216
	5	287	265	267	270	272.25	0.001524	131.70416	114.5035975
							a mean	131.9019	114.6755126
							g mean	131.80445	114.5907848

	volume(l)	time trial 1	time trial 2	time trial 3	time trial 4	avg t	K in m/s	K in m/day	corrected k
S2-1	1	78	74	68	75	73.75	0.001125	97.23785	84.53858826
	2	131	122	124	123	125	0.001328	114.7407	99.75553415
	3	190	188	192	191	190.25	0.001309	113.0821	98.31360133
	4	254	256	253	248	252.75	0.001314	113.4923	98.67016237
	5	311	305	309	310	308.75	0.001344	116.1343	100.9671398
							a mean	110.9374	96.44900519
							g mean	110.7069	96.24857277

	volume(l)	time trial 1	time trial 2	time trial 3	time trial 4	avg t	K in m/s	K in m/day	corrected k
S2-2	1	100	98	93	95	96.5	0.00086	74.3139	64.60850657
	2	152	154	149	149	151	0.001099	94.98399	82.57908456
	3	215	223	225	219	220.5	0.001129	97.56859	84.82613448
	4	270	261	274	273	269.5	0.001232	106.4385	92.53760125
	5	332	301	321	327	320.25	0.001296	111.964	97.3414658
							a mean	97.05378	84.37855853
							g mean	96.12613	83.57206099

	volume(l)	time	time	time	time	avg t	K in m/s	K in	corrected k
--	-----------	------	------	------	------	-------	----------	------	-------------

		trial 1	trial 2	trial 3	trial 4			m/day	
S2-3	1	153	134	152	151	147.5	0.000563	48.61893	42.26929413
	2	176	163	172	165	169	0.000982	84.86736	73.78367911
	3	261	246	245	249	250.25	0.000995	85.96953	74.7419087
	4	305	289	294	295	295.75	0.001123	96.99126	84.32420469
	5	386	384	384	387	385.25	0.001077	93.07322	80.91785703
							a mean	81.90406	71.20738873
							g mean	79.63236	69.23237379

	volume(l)	time trial 1	time trial 2	time trial 3	time trial 4	avg t	K in m/s	K in m/day	corrected k
S2-4	1	170	174	169	172	171.25	0.000485	41.87616	36.40712925
	2	200	193	185	184	190.5	0.000871	75.28915	65.45638724
	3	299	296	297	294	296.5	0.00084	72.55944	63.08317927
	4	335	332	338	335	335	0.000991	85.62736	74.44442847
	5	402	407	405	406	405	0.001025	88.53446	76.97186277
							a mean	72.77731	63.2725974
							g mean	70.44069	61.24113731

APPENDIX C

HYDROGEOCHEMICAL DATA

Station ID	Lab ph	Field ph	Lab EC	Field EC	Na ⁺	K ⁺	Ca ²⁺	Mg ²⁺	Cl	HCO ₃ ²⁻	SO ₄ ²⁻	F ⁻	Br ⁻	NO ₃ ⁻	NO ₂ ⁻	TDS
			µs/cm	µs/cm	mg/l	mg/l	mg/l	mg/l	mg/l	mg/l	mg/l	mg/l	mg/l	mg/l	mg/l	mg/l
WS1	6.27	7.96	840	0.8	63.2	10.2	68.4	13	127.088	165.92	55.7	0.15	0	2.15	1.96	529
WS2	6.73	8.24	5913	5.05	502	118	639	170	609.912	63.44	2501	0.5	0	0.47	2.46	3725
WS3	6.75	8	3864	3.46	339	70	381	102	387.223	131.76	1451	0.67	0	5	3.27	2434
WS4	6.78	7.8	1559	1.51	106	24	162	32	140.705	63.44	492	0.2	0	0.22	2.18	982
WS5	7.06	7.9	1081	0.53	54.5	14.8	115	31.6	120.28	366	91.7	0.25	0.35	0.91	3.26	681
BOS 32:2009 Compliance Standard Class II	5-10	5-10	3100	3100	400	50	200	100	200		400	1		50	3	2000

APPENDIX D

HISTORIC WATER LEVEL DATASETS

	Tobane(Stn B1)	
Date	sand level	water level
02/03/79	739.8	739.47
18/04/79	739.82	738.94
15/06/79	741.093	740.143
17/07/79	739.85	739.37
01/09/79	741.188	740.213
79-10-09	739.85	739.37
08/01/80	741.195	740.915
17/02/80	739.371	739.311
12/05/80	739.484	738.795
13/06/80	739.156	738.336
25/07/80	739.532	738.436
03/09/80	739.5	738.307
15/05/81	739.583	728.2
12/06/81	739.645	739.049
17/07/81	741.005	740.565
19/08/81	739.22	739.19
16/09/81	739.578	739.178
08/10/81	739.576	739.149
07/12/81	739.443	739.217
04/01/82	739.785	739.625
02/02/82	739.362	737.032
10/03/82	739.33	738.6
05/04/82	739.38	738.38
19/05/82	739.433	739.056
01/07/82	739.465	738.576

05/08/82	739.503	738.031
25/08/82	739.494	738.197
07/09/82	739.419	738.129

Tobane

date	water level	sand level	depth to water
Jun-90	738.5	739	0.5
Jul-90	738.1	739	0.9
Aug-90	737	739	2
Sep-90	737.9	739.4	1.5
Oct-90	736.9	738.5	1.6
Nov-90	738.8	739	0.2
Dec-90			
Jan-91	739	739.1	0.1
Feb-91			
Mar-91	739	739.4	0.4
Apr-91			
May-91	738.6	739.2	0.6
Jun-91	738	738.5	0.5
Jul-91	738.1	739.5	1.4
Aug-91	737.8	739.5	1.7
Sep-91	737.7	739.5	1.8
Oct-91	737	739.5	2.5
Nov-91	736.4	739.5	3.1
Dec-91	737.6	739.5	1.9
Jan-92	738.8	739.8	1
Feb-92	738.5	739.9	1.4
Mar-92	738	739.9	1.9
Apr-92	738	739.9	1.9
May-92	737.4	739.9	2.5
Jun-92	737	739.9	2.9
Jul-92	736.9	739.9	3
Aug-92	736.9	739.9	3

Sep-92			
Oct-92			
Nov-92			
Dec-92			
Jan-93			
Feb-93	739	739.9	0.9
Mar-93			
Apr-93			
May-93	738	739.9	1.9
Jun-93	737.9	739.9	2
Jul-93	736.9	740	3.1
Aug-93	737.3	740	2.7
Sep-93	738	740	2
Oct-93	737.5	740	2.5
Nov-93			
Dec-93			
Jan-94	739	739.8	0.8
Feb-94	739	739.8	0.8
Mar-94	738.5	739.8	1.3
Apr-94	738.2	739.8	1.6
May-94	738	739.8	1.8
Jun-94	737.5	739.8	2.3
Jul-94	737	739.8	2.8
Aug-94	736.9	739.8	2.9
Sep-94	736.4	739.8	3.4
Oct-94	736.3	739.8	3.5
Nov-94	739.5	739.8	0.3
Dec-94	739.2	739.8	0.6
Jan-95	739.2	739.9	0.7

Feb-95	739.1	739.9	0.8
Mar-95	739	739.7	0.7
Apr-95	738.2	739.7	1.5
May-95	738.2	739.7	1.5
Jun-95	738.4	739.7	1.3
Jul-95	738	739.7	1.7
Aug-95	738	739.5	1.5

OBSERVATION WELL DATA

date										
	OB1 WL	Abs WL	OB2 WL	Abs WL	OB3 WL	Abs WL	OB4 WL	Abs WL	OB5 WL	Abs WL
08/11/14	0.41	777.579	0.34	777.649	0.73	777.376	0.72	777.386	0.44	776.291
15/11/14	0.37	777.619	0.31	777.679	0.69	777.416	0.65	777.456	0.43	776.301
23/11/14	0.42	777.569	0.34	777.649	0.74	777.366	0.76	777.346	0.4	776.331
29/11/14	0.4	777.589	0.36	777.629	0.54	777.566	0.55	777.556	0.36	776.371
05/12/15		777.989		777.989	0.62	777.486	0.63	777.476	0.43	776.301
13/12/15	0.36	777.629	0.35	777.639	0.74	777.366	0.76	777.346	0.34	776.391
20/12/15	0.4	777.589	0.35	777.639	0.64	777.466	0.65	777.456	0.42	776.311
03/01/15		777.989		777.989	0.7	777.406	0.74	777.366	0.43	776.301
10/01/15	0.41	777.579	0.32	777.669	0.72	777.386	0.71	777.396	0.39	776.341
17/01/15	0.37	777.619	0.39	777.599	0.74	777.366	0.75	777.356	0.38	776.351

date								
	OB6 WL	Abs WL	OB7 WL	Abs WL	OB8 WL	Abs WL	OB9 WL	Abs WL
08/11/14	0.69	776.153	0.71	776.133	0.72	775.150	0.59	775.280
15/11/14	0.68	776.163	0.78	776.063	0.69	775.180	0.66	775.210
23/11/14	0.65	776.193	0.75	776.093	0.73	775.140	0.66	775.210
29/11/14	0.67	776.173	0.57	776.273	0.7	775.170	0.55	775.320
05/12/15	0.73	776.113	0.62	776.223	0.65	775.220	0.63	775.240
13/12/15	0.65	776.193	0.75	776.093	0.67	775.200	0.65	775.220
20/12/15	0.72	776.123	0.64	776.203	0.65	775.220	0.65	775.220
03/01/15	0.65	776.193	0.71	776.133	0.64	775.230	0.72	775.150
10/01/15	0.71	776.133	0.71	776.133	0.72	775.150	0.61	775.260
17/01/15	0.72	776.123	0.72	776.123	0.73	775.140	0.61	775.260

APPENDIX E

COORDINATES,DEPTH TO BEDROCK AND SAND ELEVATIONS

Latitude (dms)	Longitude (dms)	depth to bedrock (m)	sand surface elevation (mamsl)
Profile 1			
215345.9	280228.1	5.7	777.386
215345.6	280228.1	5.8	776.974
215345.1	280228.1	5.8	776.887
215344.7	280228	5.7	776.762
215344.3	280228	5.7	776.694
215343.9	280228	6	776.677
215343.5	280228	6	776.878
215343.1	280227.9	6	776.975
215343.9	280227.9	5.9	776.983
215342.7	280227.9	5.9	777.258
215342.3	280227.9	5.8	777.291
		Average	776.979
Profile 2			
215345.9	280237.5	5.7	777.115
215345.3	280237.3	5.8	777.075
215344.7	280237.1	5.6	777.013
215344.2	280237	5.6	777.145
215343.7	280236.9	5.4	777.089
215343.4	280236.8	5.5	777.199
215342.9	280236.7	5.6	777.199
215342.3	280236.5	5.6	777.093
215341.8	280236.4	5.6	777.021

215341.2	280236.2	5.6	777.051
215340.8	280236.2	5.6	777.166
		Average	777.106

Profile 3

215342.4	280246.2	6.8	775.941
215341.8	280245.8	6.8	775.895
215341.5	280245.6	6.8	775.795
215341	280245.3	5.8	775.755
215340.6	280245.1	5.8	774.978
215340.2	280244.8	5.9	774.773
215339.7	280244.6	5.9	774.783
215339.2	280244.3	6.6	775.958
215338.7	280244.1	6.4	775.654
215338.3	280243.8	6	775.848
215338	280243.4	6	776.957
215337.9	280243.6	6.4	775.973
215337.6	280243.3	6.6	775.993
215337.2	280243.1	6.6	775.933
		Average	775.731

Profile 4

215335.3	280253.7	6	774.306
215335	280253.2	6.2	774.157
215334.6	280252.7	6.1	774.086
215334.3	280252.3	5.8	774.033
215334.1	280252	5.8	774.539
215333.8	280251.6	5.8	775.418
215333.4	280251.1	5.8	775.709

215333.1	280250.7	5.8	776.657
215332.9	280250.3	5.8	776.655
215332.5	280249.8	5.7	776.593
215332.3	280249.7	5.7	777.021
215332.1	280249.5	6.4	777.413
215331.8	280249.3	6.7	777.587
215331.5	280249	6.8	777.624
		Average	775.843

Profile 5

215328.1	280257	6.4	776.098
215327.9	280256.5	6.6	774.099
215327.7	280256	4.8	775.423
215327.5	280255.6	5.4	775.117
215327.3	280255.2	5.6	774.642
215327.2	280254.8	5.8	774.87
215327.1	280254.4	6	774.647
215326.9	280254.1	6.2	774.433
215326.8	280253.6	6.2	774.08
215326.6	280253.2	6.2	775.018
215326.4	280252.8	6.2	775.145
		Average	774.870